Identification and Characterization of Two Isoforms of Human Megakaryoblastic Leukemia-1 and Their Specific Regulation in Myofibroblast Differentiation

Inauguraldissertation

zur

Erlangung der Würde eines Doktors der Philosophie

vorgelegt der

Philosophisch-Naturwissenschaftlichen Fakultät

der Universität Basel

von

Matthias Scharenberg

aus Haan (Rheinland), Deutschland

Basel, 2013

Genehmigt von der Philosophisch-Naturwissenschaftlichen Fakultät
auf Antrag von Prof. Dr. Ruth Chiquet-Ehrismann und Prof. Dr. Gerhard Christofori.

Basel, den 18.06.2013

Prof. Dr. Jörg Schibler

(Dekan)

creative commons

Namensnennung-Keine kommerzielle Nutzung-Keine Bearbeitung 2.5 Schweiz

---

Sie dürfen:

das Werk vervielfältigen, verbreiten und öffentlich zugänglich machen

Zu den folgenden Bedingungen:

Namensnennung. Sie müssen den Namen des Autors/Rechteinhabers in der von ihm festgelegten Weise nennen (wodurch aber nicht der Eindruck entstehen darf, Sie oder die Nutzung des Werkes durch Sie würden entlohnt).

Keine kommerzielle Nutzung. Dieses Werk darf nicht für kommerzielle Zwecke verwendet werden.

Keine Bearbeitung. Dieses Werk darf nicht bearbeitet oder in anderer Weise verändert werden.

- Im Falle einer Verbreitung müssen Sie anderen die Lizenzbedingungen, unter welche dieses Werk fällt, mitteilen. Am Einfachsten ist es, einen Link auf diese Seite einzubinden.
- Jede der vorgenannten Bedingungen kann aufgehoben werden, sofern Sie die Einwilligung des Rechteinhabers dazu erhalten.
- Diese Lizenz lässt die Urheberpersönlichkeitsrechte unberührt.

Quelle: http://creativecommons.org/licenses/by-nc-nd/2.5/ch/ Datum: 3.4.2009

Table of Contents

Abbreviations

ATP/GTP	Adenosine/guanosine triphosphate
CAF	Cancer (carcinoma)-associated fibroblasts
ECM	Extracellular matrix
EMT	Epithelial-to-mesenchymal transition
EMyT	Epithelial-to-myofibroblast transition
EndMT	Endothelial-to-mesenchymal transition
FCS	Fetal calf serum
GEF	Guanine nucleotide exchange factor
GPCR	G protein-coupled receptor
hASC	Human adipose tissue-derived mesenchymal stem/stromal cell
HEK293	Human embryonic kidney cell line 293
LC-MS	Liquid chromatography-mass spectrometry
LPA	Lysophosphatidic acid
MAPK	Mitogen-activated protein kinase
MKL1	Megakaryoblastic leukemia-1
MMP	Matrix metalloproteinase
MRTF	Myocardin-related transcription factor
MSC	Multipotent stromal cell/mesenchymal stem cell
PKM1/2	Pyruvate kinase isozyme M1/M2
RTK	Receptor tyrosine kinase
SBE	Smad-binding element
SILAC	Stable isotope labeling with amino acids in cell culture
SMA	Smooth muscle α-actin
SMC	Smooth muscle cell
SPC	Sphingosylphosphorylcholine
SRF	Serum response factor
TAD	Transcriptional activation domain
TCF	Ternary complex factor
TGF-β	Transforming growth factor-β
VSMC	Vascular smooth muscle cell

Summary

Summary

The reversible differentiation of various precursor cell types into myofibroblasts/cancer-associated fibroblasts (CAFs) is an important physiological as well as pathological process. Recently, the Rho-actin-MKL1-SRF pathway has been shown to regulate this process. MKL1 activity has emerged as the crucial relay adjusting the status of the actin cytoskeleton and the transcription of a substantial part of SRF target genes, including smooth muscle-specific genes. To investigate the role of MKL1 in more detail, we analyzed the exact molecular structure of the human MKL1 protein, its gene architecture, and its regulation of expression. For the first time, we describe the existence of a second human MKL1 isoform, MKL1_S, that is transcribed from an alternative promoter. In contrast to the published isoform MKL1_L, expression of this novel isoform varies strongly between different cell types and tissues. Furthermore, we identified an upstream GTG translation start of MKL1_L, resulting in a long N-terminal tail that is not present in MKL1_S. Using human adipose tissue-derived stem cells (ASCs) as a differentiation model, we were able to show that only the shorter isoform MKL1_S is strongly up-regulated within the first 24 h of TGF-β-induced myofibroblast/CAF differentiation. TGF-β constitutes the major physiological trigger of the myofibroblast/CAF differentiation program. By applying other stimuli that were reported to drive differentiation of MSCs/ASCs into the smooth muscle direction, we found that induction of MKL1_S is specific for TGF-β. To assess the mechanistic role of specific MKL1_S up-regulation, we over-expressed MKL1_S and MKL1_L in HEK293 cells and analyzed target gene expression after stimulation of the Rho-actin-MKL1 pathway. We found that MKL1_S shares the majority of its target genes with MKL1_L, including α-smooth muscle actin. However, we identified several genes that were significantly more strongly induced by MKL1_S, coding for extracellular proteins, such as MMP-16 and SPOCK-3. This MKL1_S-specific activity was mediated by a functional motif in the MKL1_S-specific N-terminal sequence. We postulate that the specific up-regulation of MKL1_S in the initial phase of TGF-β-induced myofibroblast/CAF differentiation contributes to the progression to the advanced phase, which is characterized by enhanced contractility, extracellular matrix deposition and modification, and the down-regulation of cellular migration.

Moreover, using a proteomics approach to identify MKL_1 binding proteins, we identified pyruvate kinase (PK) M1/M2 as a novel interaction partner of MKL1. PKM1/2 is an enzyme that mediates the last, rate-limiting step of glycolysis, and thereby controls the channeling of pyruvate either into the highly efficient cellular respiration process or into the less efficient lactic acid fermentation. The latter was found to be strongly increased in tumor cells, a phenomenon known as Warburg effect. The novel interaction between PKM1/2 and MKL1 might reveal a so far unknown link between tumor metabolism and MKL1-mediated cellular motility or differentiation into myofibroblasts/CAFs.

Introduction

Introduction

1. Signal transduction - from changes in the extracellular microenvironment to altered gene expression.

Cells in multicellular organisms do not function autonomously. They actively sense their microenvironment and adapt to occurring changes (for general reviews see Alberts et al., 2010; Bryant and Mostov, 2008; Jones and Wagers, 2008). These changes may be of biochemical nature, e.g., when hormones, cytokines, growth factors, survival factors, or death factors are released, or when cells communicate directly by interactions of their cell surface receptors. In the case of circulating cells, these biochemical cues constitute the main route of communication between a cell and its environment. However, in the case of non-circulating cells within tissues, changes in the physical and mechanical properties of the microenvironment play an equally important role. These may cause the formation or the break down of cell-cell contacts, which are a crucial prerequisite for the integrity of many tissues, especially the epithelium and the endothelium (reviewed in Kalluri and Weinberg, 2009). In connective tissues, a major regulator of cell fate and cell behaviour is the extracellular matrix (ECM), in which the cells are embedded. The ECM is an assembly of large, fibrillar proteins that does not only provide structural support, but also transmits mechanical forces (reviewed in DuFort et al., 2011). These are directly sensed by integrin receptors on the cell surfaces. Notably, ECM components have also been shown to act as solid-phase presenters of soluble mediators. As such, they are able to create biochemical gradients across tissues and to integrate various components into complex biochemical signals (reviewed in Hynes, 2009). The interconnection between the biochemical and the mechanical environment of a cell allows for a plethora of possible messages to the cell. Immediate and direct adaptation of the cell to these cues involves the rearrangement of its cytoskeleton, e.g., the formation or break down of stress fibers, protrusions, and focal adhesions, as well as changes in energy metabolism. In this way, the cell can provisionally adjust its morphology and its activity to the demands of the cellular microenvironment. However, an optimal and sustained adaptation often requires changes in gene expression, to utilize the RNAs and proteins to indirectly fine-tune the cellular response. Therefore, a complex machinery of cell surface receptors and intracellular signaling pathways translates the extracellular stimuli into alterations of gene expression. This enables the

cell to profoundly react to the extracellular needs, e.g., by migrating towards or retracting from a stimulus, going into proliferation or apoptosis, or differentiating into another cell type.

Biochemical factors from the cellular microenvironment may act as ligands for complementary, integral transmembrane receptors on the cell surface. These receptors integrate the signals and elicit appropriate intracellular responses. Two prominent families of extracellular receptors are the G protein-coupled receptors (GPCRs) and the receptor tyrosine kinases (RTKs) (for general reviews see Audet and Bouvier, 2012; Lemmon and Schlessinger, 2010). The activation of the receptor involves a conformational change, which often results in the exposure of an intrinsic enzymatic activity. In the case of GPCRs and RTKs, this is a guanine nucleotide exchange factor (GEF) activity and a tyrosine kinase activity, respectively. These activities allow the receptors to activate intracellular signaling components and adaptor proteins. For both receptor families, GPCRs and RTKs, the downstream signaling components belong to the family of G proteins, which bind guanosine triphosphate (GTP) nucleotides. GPCRs activate membrane-associated heterotrimeric G proteins, whereas RTKs activate cytosolic members of the Rho, Ras, and Raf families of small G proteins. Both classes of G proteins trigger downstream signaling cascades. These may propagate either via adaptor proteins that form signaling complexes, or via rapid transient modifications, e.g. phosphorylation, mediated by enzymes such as kinases and phosphatases. Signaling cascades constitute an important mechanism of amplifying and integrating signals. Eventually, these signaling cascades culminate in the activation of specialized transcription factors, which specifically recognize short DNA motifs in the promoters of their target genes. Binding of the transcription factor to the DNA recruits RNA polymerase II and elicits gene transcription. As a whole, these signal transduction processes ensure precise modification of the cellular gene expression as demanded by the cellular microenvironment. There are a number of different signaling pathways, some of which show rather tissue- or cell type-specific activity, whereas others show ubiquitous activities. The possible crosstalk between these pathways at all stages of the signal transduction process makes it a highly complex and accurate relay between the extracellular environment and cellular gene expression. However, owing to this complexity and the importance of this process, mutations or malfunctions of single

components within these cascades are enough to disturb the integrity of whole tissues. In many instances this leads to the development of disease, including different kinds of cancers.

The sophisticated mechanisms of communication between cells and between cells and the ECM establish the basis for the higher organization of cells in tissues. During the development of an organism, these communication processes enable stem or precursor cells to find the right path towards their destination and, once they have reached it, to differentiate into the required cell type. In this way, well-defined layers and compartments of specialized cell types enable tissue-specific functions and establish the basis for the formation of whole organs. Importantly, these processes are not only essential during the development of a tissue, but also for its maintenance. Communication between cells of the different compartments as well as with the ECM is essential for the integrity of tissues. In addition, most tissues undergo constant remodeling processes. This is necessary to substitute dead cells and maintain tissue homeostasis, even after injury of the tissue. Therefore, some cell types, such as multipotent stem/stromal cells (MSCs), keep their ability to differentiate into various cell types in the adult organism (for general reviews see Cook and Genever, 2013; Hinz et al., 2012; Nombela-Arrieta et al., 2011). The ECM of the tissue is also subject to continuous remodeling. The fibroblast, a specialized cell type that is the predominant cell type in connective tissues, secretes most ECM components, including collagens and fibronectin. Other classes of secreted proteins, e.g., the matrix metalloproteinases (MMPs), are responsible for activating and degrading ECM proteins by cleavage (reviewed in Lu et al., 2011). All these proteins are produced by the cells according to the requirements of their microenvironment.

In conclusion, the signal transduction process and the resulting alterations in gene expression enable a continuous adaptation of individual cells to biochemical and mechanical changes in their microenvironment. In non-circulating cells of multicellular organisms, this is the basis for higher-order organization of cells in tissues and organs, including the continuous maintenance of tissue homeostasis and the regeneration after injury.

2. The transcription factor SRF and its regulation by cofactors

The serum response factor (SRF) is a member of the ancient MADS (MCM1, Agamous, Deficiens, SRF) family of transcription factors. It is encoded by a single gene and contains a 57-amino acid MADS box domain that mediates its homodimerization, DNA binding, and association with cofactors. SRF is a ubiquitously expressed transcription factor that binds to an AT-rich, *cis*-regulatory DNA element ($CC(A/T)_6GG$), known as the CArG box (Schröter et al., 1987; Treisman, 1986; Treisman, 1987). This element has been identified in single or duplicate copies in the promoters of a wide range of hypothetical target genes, the so-called "CArGome" (Sun et al., 2006a). More than 150 genes have already been validated as SRF targets, but the full extent of the CArGome still needs to be explored (Selvaraj and Prywes, 2004; Sun et al., 2006a; Zhang et al., 2005). Genes that are regulated by SRF can be subdivided into two major classes. Class I comprises serum- and growth-responsive genes, such as *c-fos* and *egr-1* (Norman et al., 1988; Treisman, 1987). Class II comprises genes encoding muscle-specific, contractility-promoting proteins, such as smooth muscle α-actin (SMA) and SM22-α/transgelin, and genes encoding actin cytoskeletal components, such as β-actin, vinculin, and β1-integrin (reviewed in Olson and Nordheim, 2010). The fundamental biological importance of SRF-controlled processes became apparent when SRF knockout studies were performed in mice. Embryos failed to form mesoderm and died at the onset of gastrulation (Arsenian et al., 1998). Conditional knockouts and other studies further revealed that SRF is essential for cardiac development (Niu et al., 2005; Parlakian et al., 2004), differentiation into smooth muscle (Miano et al., 2004) and skeletal muscle cells (Boxer et al., 1989; Selvaraj and Prywes, 2003), and neuronal migration and plasticity (Alberti et al., 2005; Ramanan et al., 2005). $SRF^{-/-}$ embryonic stem (ES) cells were unable to differentiate into mesodermal cells and showed severe defects in the organization of the actin cytoskeleton. Embryoid bodies derived from the same cells lacked important myogenic proteins such as cardiac and smooth muscle α-actin (SMA) (Niu et al., 2005; Schratt et al., 2002; Weinhold et al., 2000).

Such broad biological activity as displayed by SRF requires highly tissue- and stimulus-specific regulation. This is mostly achieved by context-specific association with different families of transcriptional coactivators, a powerful way of generating a diversity of transcriptional outcomes with only a limited number of transcription factors (reviewed

in Posern and Treisman, 2006). In the last decade, our understanding of the complex regulation of SRF activity advanced greatly by the discovery of the family of myocardin-related transcription factors (MRTFs). These SRF cofactors are required for the expression of class II SRF target genes, and will be described in more detail in section 3. SRF controls the transcription of the class I targets of mitogen-responsive genes mainly via binding to members of the ternary complex factor (TCF) subclass of Ets-type cofactors. The interactions of SRF with TCF and MRTF cofactors are mutually exclusive (Wang et al., 2004; Zaromytidou et al., 2006). Several growth factor receptors activate the mitogen-activated protein kinase (MAPK) signaling pathway that amplifies transcriptional activity of TCF family members by phosphorylation. Activated members of this family, comprising Elk1, SAP-1, and Net, bind to specific Ets DNA recognition motifs on the DNA that are adjacent to SRF binding sites in target gene promoters. Binding of both types of transcription factors in close proximity on a promoter enables the formation of a ternary complex, thereby eliciting the transcription of the target gene (see figure 1) (reviewed in Posern and Treisman, 2006).

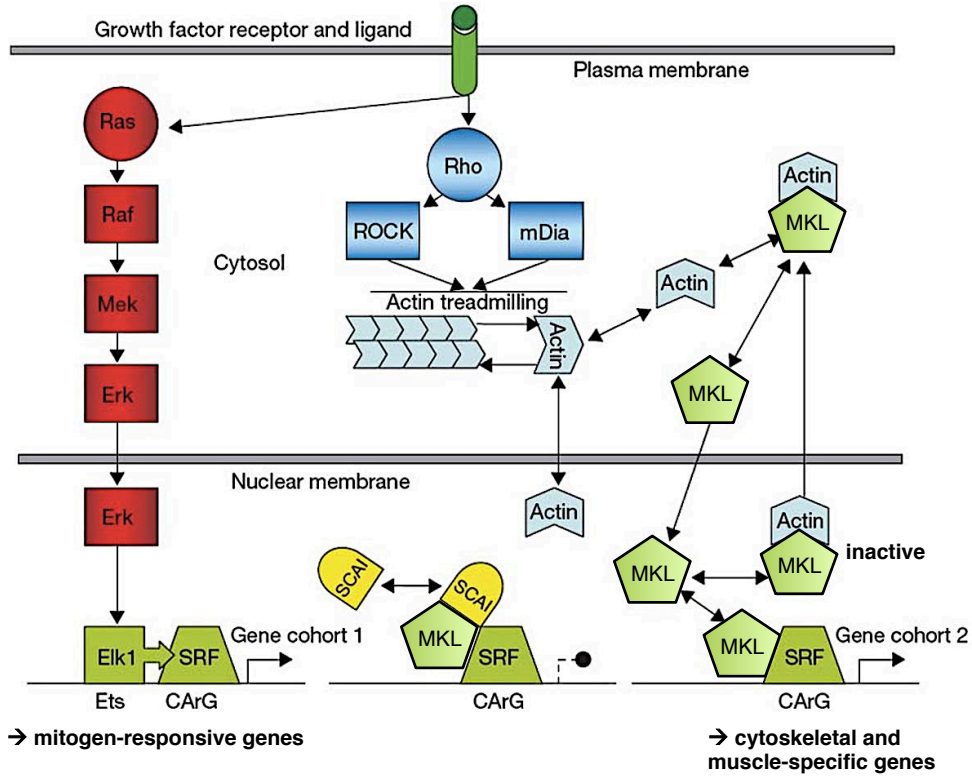

(Adapted from Juliano, 2009)

Figure 1: Major pathways regulating SRF activity.
The two pathways involve different transcriptional coactivators, which trigger transcription by forming active complexes with SRF on CArG box elements in the promoters of genes. Elk1 is a member of the ternary complex factor (TCF) subclass of Ets-type cofactors, and MKL is a member of the myocardin-related transcription factors (MRTFs). Interactions of each of the two types of coactivators with SRF are mutually exclusive (see section 3).

In addition to members of the TCF and MRTF families of transcriptional coactivators, several other factors have been described to regulate SRF activity. Brandt et al. (2009) discovered the protein SCAI (suppressor of cancer cell invasion) that specifically inhibits MRTF/SRF transcriptional activity by binding to the complex (see figure 1). SCAI suppressed the expression of several cytoskeleton-associated proteins and with it the process of invasive cancer cell migration. Similarly, FHL2, a transcriptional coactivator with strong expression in the heart and an SRF target gene itself, was reported to compete with MRTFs for SRF binding and thus prevent the expression of smooth muscle-specific genes in embryonic stem cells (Philippar et al., 2004). Positive

regulation of SRF-dependent transcription has been shown for members of the GATA family of zinc finger transcription factors and for the Nkx2-5 family of homeodomain proteins (Belaguli et al., 2000; Chen and Schwartz, 1996). Although many factors have been identified that regulate SRF activity, the MAPK-TCF and the Rho-actin-MRTF pathways emerged as the major pathways regulating SRF activity. However, based on multiple datasets of conditional and whole-body knockouts available today in *Mus musculus* (mouse), *Drosophila melanogaster*, *Caenorhabditis elegans*, and others species, it seems that the growth- and proliferation-regulating aspect of SRF biology is dispensable. SRF knockout animals, tissues or cells did not show impeded growth or proliferation indicating that SRF, when present, regulates these processes in a redundant manner. In contrast, knockout studies collectively found severe defects in cytoskeletal and contractile systems, attributing SRF the role of a "master regulator of the actin cytoskeleton and contractile apparatus" (reviewed in Miano et al., 2007).

3. The family of myocardin-related transcription factors (MRTF) - transcriptional coactivators of SRF

Rho/ROCK-dependent association of SRF with members of the myocardin-related transcription factor (MRTF) family has recently been described as a mechano- and growth factor-sensitive pathway that regulates the expression of class II SRF target genes, encoding cytoskeletal and contractility-promoting proteins (Wang et al., 2001; Wang et al., 2002), as well as ECM components (reviewed in Chiquet et al., 2009). Myocardin, the founding member of the MRTF family, shows highly restricted expression in cardiac and smooth muscle cells and is a powerful transactivator of genes that are specific for these types of muscles. Myocardin represents the earliest known marker for heart and smooth muscle during embryogenesis. Its forced expression in fibroblasts and ES cells induces expression of a whole range of SMC-specific genes and of several cardiac genes, but does not elicit the full cardiomyocyte differentiation program (reviewed in Parmacek, 2007). Myocardin$^{-/-}$ mice show normal heart development, but die at embryonic day E10.5 from a complete lack of vascular smooth muscle cells (VSMCs)(Li et al., 2003). Notably, two isoforms that differ in their N-terminal domains are generated from the myocardin gene by alternative splicing, the longer one being

mainly expressed in cardiac muscle and the shorter one in smooth muscles. The cardiac isoform was reported to harbor a specific motif for interacting with MEF2, the other member of the MADS family of transcription factors and the closest relative of SRF (Creemers et al., 2006b). In cardiomyocytes, a complex of this myocardin isoform with MEF2 regulates expression of MEF2 target genes, but also binds to an enhancer region of the myocardin gene itself to control its tissue-specific expression (Creemers et al., 2006a). The concept that two isoforms of a transcriptional coactivator of the MRTF family can associate with different members of the MADS box family to control target gene expression in a tissue-specific manner adds another twist to the complexity of the regulation of muscle-specific and cytoskeletal genes.

Shortly after the discovery of myocardin as a regulator of SRF-mediated transcription, two closely related SRF coactivators were identified, megakaryoblastic leukemia-1 (MKL1, also termed MAL/BSAC) and -2 (MKL2, also termed MAL16)(Sasazuki et al., 2002; Wang et al., 2002). To indicate their similarity to myocardin, these proteins are also known as the myocardin-related transcription factors (MRTFs), with MKL1 corresponding to MRTF-A and MKL2 to MRTF-B. In contrast to myocardin, both MKL1 and -2 show ubiquitous, but not fully overlapping expression patterns. MKL2 shows more lineage-restricted expression in the embryo than MKL1. All three MRTF family members contain a SAP domain (named after the related proteins SAF-A/B, Acinus and PIAS), which in other proteins has been shown to mediate interactions with DNA and to be involved in chromosomal organization (Aravind and Koonin, 2000). However, the exact function of this domain in MRTFs remains elusive. For a subgroup of SRF/MRTF target genes a dependency on the SAP domain has been shown (Asparuhova et al., 2011; Wang et al., 2001). The interactions of MRTFs with SRF are mediated by the basic B1 motif together with an adjacent glutamine (Q)-rich region (Wang et al., 2001; Zaromytidou et al., 2006). B1 shares homology with the SRF-binding B-box of ELK proteins from the family of TCF cofactors (Wang et al., 2004). Furthermore, a C-terminal transactivation domain is required to activate SRF-mediated target gene expression (Wang et al., 2002). MRTF proteins contain a leucine zipper-like domain that mediates homo-and heterodimerization (Miralles et al., 2003). Homodimerization was shown to be essential for MRTF function, since forced expression of constructs lacking the C-terminal transcriptional activation domain (TAD) suppresses activity of MRTFs in a

dominant-negative fashion (Cen et al., 2003; Miralles et al., 2003). However, the exact contribution of heterodimerization between co-expressed MRTF family members to important MRTF functions still needs to be elucidated.

Recently, a fourth member of the MRTF family with high expression in skeletal muscle has been described, which was termed MEF2-activating SAP transcriptional regulator (MASTR) (Creemers et al., 2006b). Although MASTR contains a SAP domain that is typical of MRTFs, otherwise this protein does not resemble the typical MRTF structure. It is clearly shorter than the other family members and lacks important parts such as the SRF-interacting domains and the dimerization domain. Instead, it contains the same N-terminal MEF2 interaction domain as the cardiac myocardin isoform and might regulate MEF2 transcriptional activity.

4. The Rho-actin-MKL1-SRF pathway - linking the actin cytoskeleton to gene expression

As described in the previous section, myocardin expression is restricted to cardiac and smooth muscle cells. However, MKL1/MRTF-A, like SRF, is found in all tissues and cell types, and is therefore of great interest for comprehensive studies of SRF-mediated processes. Thus, from now on I will focus mainly on MKL1-regulated processes. The MKL1 protein shares the general domain architecture with myocardin, including the SRF interacting domains and the dimerization domain. Interestingly, both coactivators differ in one important aspect of regulation, namely the inhibition of their activity by binding to globular (G-)actin. Although all three N-terminal actin-binding RPEL motifs (Arg-Pro-X-X-X-Glu-Leu) are conserved in both, the RPEL sequences in myocardin diverged to such a degree that G-actin binds only weakly (Guettler et al., 2008). In contrast, MKL1 stably binds up to 5 G-actin molecules, one to each RPEL motif and one to each stretch linking the motifs (Hirano and Matsuura, 2011; Mouilleron et al., 2011). In quiescent cells, binding to the full complement of G-actin renders MKL1 inactive, keeping it mainly in the cytosol. Rho GTPase-mediated rearrangement of the actin cytoskeleton in response to stimulation from the extracellular environment depletes G-actin and liberates MKL1, which can accumulate in the nucleus to activate SRF transcription (Miralles et al., 2003). Therefore, MKL1 activity is directly dependent on the

polymerization status of the actin cytoskeleton. However, myocardin barely binds to G-actin and, as consequence, remains in a constitutively nuclear and activated state (Guettler et al., 2008).

The discovery of the Rho-actin-MKL1-SRF pathway established a direct connection between the actin cytoskeleton and gene expression. It also explained for the first time how extracellular stimulation elicits both immediate cytoskeletal rearrangements and sustained adaption of cytoskeletal gene expression in a coordinated fashion.

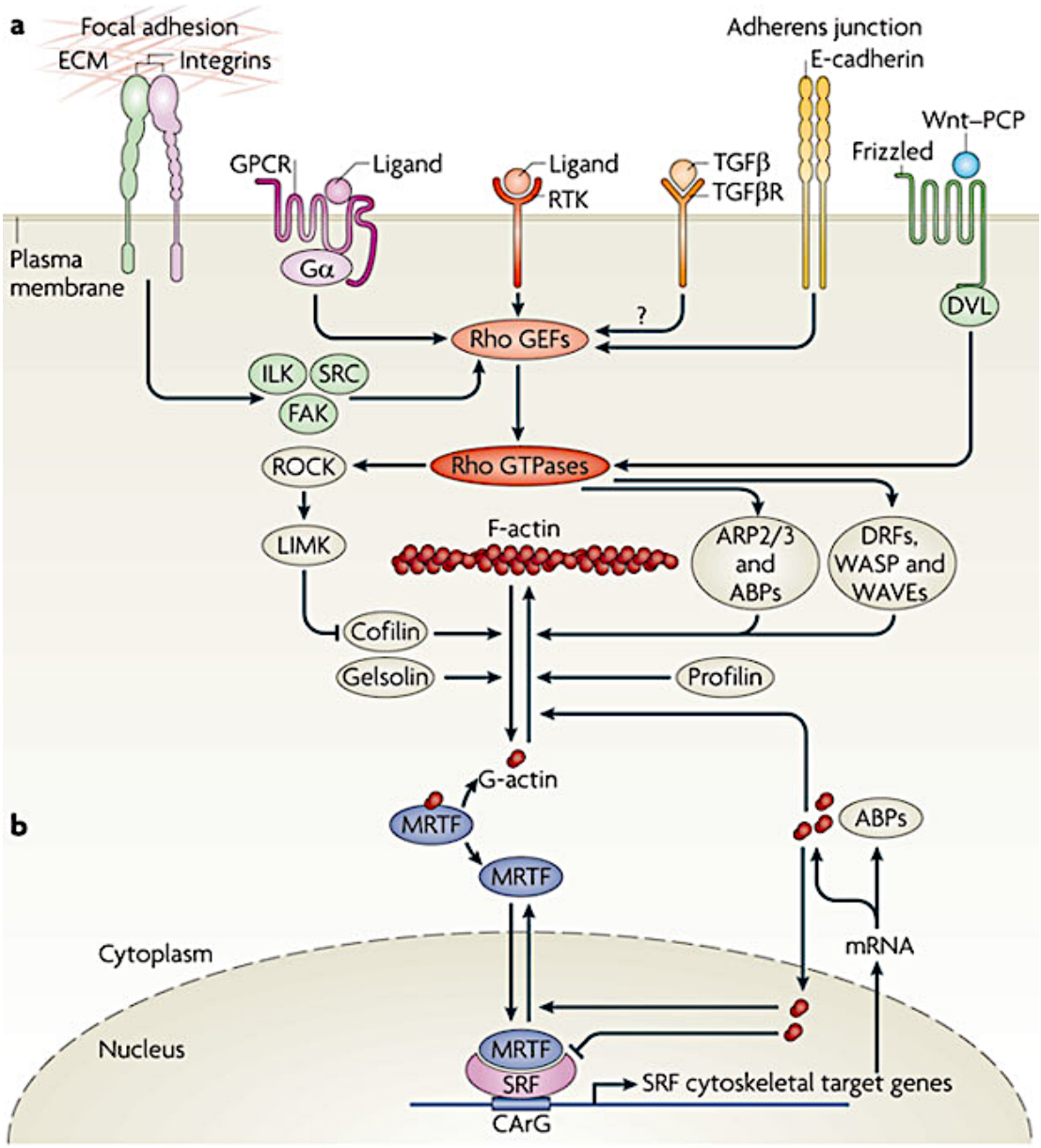

(From Olson and Nordheim, 2010)

Figure 2: Overview of the Rho-actin-MKL1-SRF pathway that translates stimuli from the extracellular environment into changes in gene expression.

a) Several classes of cell surface receptors have been shown to activate the family of Rho GTPases via guanine nucleotide exchange factor (GEFs). Rho GTPases in turn promote actin polymerization via actin-nucleating proteins, such as profilin, actin-related protein 2/3 (ARP2/3) complex, and formins (DRF = Diaphanous-related formin, mDia). Concomitantly, they promote the stabilization of F-actin polymers via Rho-associated kinase (ROCK)-LIM kinase (LIMK)-mediated inhibition of actin-severing proteins. **b)** MKL1/MRTF-A that is liberated from G-actin inhibition translocates to the nucleus and induces SRF-mediated transcription of muscle-specific genes and cytoskeletal components. ABP, actin-binding protein; DVL, Dishevelled; FAK,

focal adhesion kinase; ILK, integrin-linked protein kinase; PCP, non-canonical Wnt–planar cell polarity pathway; WASP, Wiskott–Aldrich syndrome protein; WAVEs, WASP-family verprolin homologues.

Activity of the Rho-actin-MKL1-SRF pathway can be triggered by different kinds of extracellular stimuli that impinge on Rho GTPase activation. These stimuli can use several classes of cell surface receptors, as depicted in Figure 2. "Classical" stimulation of the pathway involves growth factors, e.g., from serum, binding to RTKs, or bioactive lipids, such as lysophosphatidic acid (LPA), binding to GPCRs. However, as mentioned in section 1, not only biochemical, but also mechanical signals play an important role in tissue homeostasis and tissue repair. To convert forces into biochemical signals and eventually into changes in gene expression, mechanosensitive pathways are required. A few pathways with these specialized properties have been identified, including signaling via YAP/TAZ (Dupont et al., 2011), or the nuclear factor kappa-B (NFκB)(e.g., Kumar et al., 2003). Importantly, the Rho-actin-MKL1-SRF pathway is also able to act as a mechanosensor when activated by integrin receptors. Integrins can bind to components of the ECM as well as to other cells and transform mechanical stimuli into biochemical signals. At sites of force transfer, focal complexes form and components such as integrin-linked kinase (ILK) mediate the integrin-induced activation of Rho and the Rho-actin-MKL1-SRF pathway (Maier et al., 2008). Force application on fibroblasts triggers the nuclear accumulation of MKL1, but not MKL2, and induces α-smooth muscle actin (SMA) expression (Zhao et al., 2007). Therefore, MKL1 assumes a specific role within the MRTF family regarding the transduction of mechanical signals from the cellular microenvironment to alter gene expression.

Due to the diversity of stimuli that eventually activate Rho and impact on the actin cytoskeleton, it is not yet fully clear whether the Rho-actin-MKL1-SRF pathway triggers gene expression in a stimulus-specific manner, or rather in a way that reflects the current state of the actin cytoskeleton, independent of the underlying extracellular stimulus. Actin regulates MKL1 activity on multiple levels. MKL1 was reported to contain a bipartite nuclear localization signal (NLS) that is located within the N-terminal RPEL domain. The binding of up to five G-actin molecules to this domain masks the NLS motif and thus prevents nuclear import of MKL1 (Hirano and Matsuura, 2011;

Mouilleron et al., 2011; Pawłowski et al., 2010). However, MKL1 is not entirely cytosolic in all cell types when unstimulated, probably caused by incomplete binding of G-actin. When liberated from G-actin, MKL1 is actively imported into the nucleus by binding via its NLS to members of the importin-α/β family. However, G-actin can passively diffuse into the nucleus and inhibit the interaction of MKL1 with DNA-bound SRF. Recently it was discovered that the formin mDia induces actin polymerization even in the nucleus, indicating that the G- to F-actin equilibrium in both, cytosol and nucleus, regulates MKL1 activity (Baarlink et al., 2013). Lastly, G-actin contains a nuclear export signal that enables it to shuttle MKL1 out of the nucleus via the exportin Crm1 (Vartiainen et al., 2007). In addition to regulation by actin, MKL1 was reported to be phosphorylated at both tyrosine and serine/threonine residues (Miralles et al., 2003). Muehlich et al. (2008) found that the serum-inducible phosphorylation at serine 454 prevents nuclear import of MKL1 and is triggered by MAPK signaling. They also showed that phosphorylation of MKL1 is required for its binding to G-actin.

Another remarkable aspect of the Rho-actin-MKL1-SRF pathway is its feedback loop regulation. The class II SRF target genes that are regulated by MKL1 comprise many components and regulators of the actin cytoskeleton, including β-actin itself and the smooth-muscle specific α-actin (SMA) (Cen et al., 2004; Selvaraj and Prywes, 2004). In this way, MKL1-SRF-mediated transcription not only promotes sustained and fine-tuned changes of the actin cytoskeleton, but also controls its own activity via the availability of its inhibitor. In addition to direct regulation of gene transcription by MKL1-SRF, miRNA targets have been shown to play an important role in the biological effects of MKL1-SRF. For instance, SRF regulates transcription of a bicistronic miRNA cluster encoding miR-1 and miR-133 in cardiac and skeletal muscle cells (Liu et al., 2008; Zhao et al., 2005). These miRNAs target many mRNAs that are associated with the actin cytoskeleton and the Rho-actin-MKL1-SRF pathway. E.g., among the targets of miR-133 is the SRF transcript itself, allowing a precise feedback loop regulation of SRF activity. Similarly, SRF- and myocardin-mediated expression of miR-143 and miR-145 in cardiac and smooth muscle cells (Cordes et al., 2009) regulates many Rho-actin-MKL1/myocardin-SRF-connected mRNAs, including myocardin itself, kruppel-like factor 4 (KLF4), and ELK1. These miRNA-mediated mechanisms might therefore contribute to the coordination of activities of the different MRTF family members as well as of the

different families of SRF-regulating coactivators, including MRTFs and TCFs. The combination of direct target genes and indirect miRNA target genes that are controlled by the Rho-actin-MKL1-SRF pathway creates a whole array of regulatory feedback loops that fine-tunes adaptation of the actin cytoskeleton machinery to the extracellular demands (reviewed in Olson and Nordheim, 2010).

Obviously, a pathway that directly converts changes in the actin polymerization state into transcriptional changes of a large group of cytoskeletal genes assumes a crucial part in the control of actin-mediated cell motility and stress-responsiveness (reviewed in Olson and Nordheim, 2010). In the next sections I will discuss how the activity of the Rho-actin-MKL1-SRF pathway impacts on embryonic, physiological, and pathological processes.

5. The role of the Rho-actin-MKL1-SRF pathway in embryonic development

In the postnatal organism, MKL1/MRTF-A shows ubiquitous expression in all cell types and tissues. During embryonic development it was found to be enriched in mesenchymal, muscle, and epithelial cells (Pipes et al., 2006). Surprisingly with regard to its widespread expression and the fundamental defects in $SRF^{-/-}$ mice, about 65 % of $MKL1^{-/-}$ mice are viable and fertile. Only a subset of 35 % of the mice dies around embryonic day E10.5 due to myocardial cell necrosis (Li et al., 2006; Sun et al., 2006b). In contrast, $MKL2^{-/-}$ mice die at E13.5-E14.5 due to cardiac outflow tract defects. These defects are caused by an MKL2-specific differentiation defect of smooth muscle cells (SMCs) from the cardiac neural crest (Li et al., 2005; Oh et al., 2005). $Myocardin^{-/-}$ mice survive no longer than day E10.5 lacking differentiated SMCs, resulting in, among other defects, an underdeveloped aorta (Li et al., 2003). These knockout phenotypes of members of the MRTF family indicate that, whereas myocardin and MKL2 have at least some specific functions in the development of smooth muscle cells, MKL1 function during development seems dispensable and redundant with the other family members.

6. The role of the Rho-actin-MKL1-SRF pathway in physiology and disease

6.1 Involvement in normal mammary gland function and nursing

Interest in MKL1 as a transcriptional coactivator of SRF ceased after the reports that MKL1 was dispensable for embryogenesis (see section 5). However, in the past few years it became clear that MKL1 is of specific importance in stress-responsive physiological and pathological processes in a wide range of tissues. MKL1-specific functions, e.g., in response to mechanical stimuli (see section 4) or in response to TGF-β (see section 6.4), as well as its ubiquitous expression, make MKL1 the predestined SRF coactivator to mediate such stress-responsive physiological and pathological processes. It seems plausible that the partial embryonic lethal phenotype of $MKL1^{-/-}$ mice reflects impaired stress responses of the heart. Additionally, mammary glands in female $MKL1^{-/-}$ mice failed to prepare for pregnancy and developed an involution-like phenotype. This was linked to an impairment of hormone- and mechanical stress-induced differentiation of myoepithelial cells in these mice. This differentiation requires the expression of muscle-specific and contractility-promoting SRF target genes, such as SMA and calponin 1. Since contraction of myoepithelial cells in response to suckling is a prerequisite for milk ejection, $MKL1^{-/-}$ mothers failed to feed their offspring properly, such that pups died around postnatal day P14-P20 (Li et al., 2006; Sun et al., 2006b). The next sections will summarize more findings that implicate specific MKL1 functions in physiological and pathological processes. However, more conditional knockout models will need to be assessed under stress conditions to reveal further specific functions of MKL1 in normal tissue homeostasis, repair, and disease.

6.2 Involvement in megakaryocytic differentiation and leukemia

MKL1 was first identified as part of a fusion protein in acute megakaryoblastic leukemia (AMKL), and hence named megakaryoblastic leukemia-1. In patients with AMKL, a fusion protein with the RNA binding motif protein 15 (Rbm15 or OTT) results from a chromosomal translocation between chromosomes 1 and 22 (Ma et al., 2001; Mercher et al., 2001). AMKL represents a form of acute myeloid leukemia (AML) in infants that is associated with poor prognosis. About 70% of pediatric AMKL in the first year of life is caused by the t(1;22)(p13;q13) translocation that yields in the Rbm15-MKL1 fusion

protein, also termed OTT-MAL. Characteristics of AMKL are an expansion of megakaryoblasts in the bone marrow, myelofibrosis, and low platelet numbers in the blood (thrombocytopenia). The mechanisms by which expression of the fusion protein contributes to these phenotypes are not yet clear. However, it is assumed that the 5' Rbm15-MKL1 3' product is responsible, since, in contrast to the reciprocal fusion transcript that is also detected in AMKL, this former transcript harbors the majority of important domains from both proteins (Ma et al., 2001; Mercher et al., 2001). Rbm15 is a nuclear envelope protein that is required for efficient mRNA export from the nucleus (Zolotukhin et al., 2009). Descot et al. (2008) reported a deregulated SRF activation by the Rbm15-MKL1 fusion protein. They found accumulation of the fusion protein in the nucleus as well as constitutive SRF transcriptional activity, due to an inability to bind to G-actin. Thus, the fusion protein is independent of the MKL1 regulation by Rho and actin. The contribution of Rbm15 to the leukemic phenotype is still elusive. However, the connection between a deregulation of the Rho-actin-MKL1-SRF pathway and defects in megakaryopoiesis and platelet production increased the understanding of the normal megakaryocytic differentiation process. Blood cells need to be constantly replenished in enormous numbers, which is accomplished by differentiation from hematopoietic stem and progenitor cells. Cheng et al. (2009) examined the peripheral blood of $MKL1^{-/-}$ mice and found a reduced number of mature megakaryocytes, the platelet-producing cell type, with a concomitant reduction in cell ploidy. As an obvious consequence, platelet numbers in the knockout mice were lower than in wild-type mice. In addition, they found that MKL1 was up-regulated during the differentiation process, and overexpression of MKL1 increased the number as well as the ploidy of megakaryocytes in an SRF-dependent manner (Cheng et al., 2009). *In vitro* differentiation into megakaryocytes induced nuclear accumulation and transcriptional activity of MKL1 (Gilles et al., 2009; Smith et al., 2013). These data suggest that the Rho-actin-MKL1-SRF pathway plays a crucial role in regulating megakaryocytic differentiation, but an excessive activation seems to prevent terminal differentiation, which involves the release of platelets. However, it is not yet known if the translocation product represents an oncogene that triggers leukemogenesis, or if deregulation of normal MKL1 and/or Rbm15 are the cause of malignant transformation.

6.3 Involvement in progression of solid tumors and metastasis

The International Journal of Biochemistry & Cell Biology 42 (2010) 1911–1914

Contents lists available at ScienceDirect

The International Journal of Biochemistry & Cell Biology

journal homepage: www.elsevier.com/locate/biocel

Molecules in focus

Megakaryoblastic leukemia protein-1 (MKL1): Increasing evidence for an involvement in cancer progression and metastasis

Matthias A. Scharenberg, Ruth Chiquet-Ehrismann*, Maria B. Asparuhova

Friedrich Miescher Institute for Biomedical Research, Basel, Switzerland

ARTICLE INFO

Article history:
Received 5 August 2010
Received in revised form 23 August 2010
Accepted 24 August 2010
Available online 9 September 2010

Keywords:
Megakaryoblastic leukemia-1
Myocardin-related transcription factors
Cancer
Metastasis
Actin

ABSTRACT

Megakaryoblastic leukemia protein-1 (MKL1), also termed MAL, MRTF-A, and BSAC, belongs to the MRTF family of transcription factors that share evolutionary conserved domains required for actin-binding, homo- and heterodimerization, high-order chromatin organization and transcriptional activation. MKL1 regulates many processes, including muscle cell differentiation, cardiovascular development, remodeling of neuronal networks in the developing and adult brain, megakaryocytic differentiation and migration, modulation of cellular motile functions and epithelial–mesenchymal transition. Moreover, deregulation by genetic alterations and/or altered expression of MKL1 can contribute to a number of pathological processes such as coronary artery disease, sarcopenia, acute megakaryoblastic leukemia, and cancer. In this article, we review the structure, regulation and biological functions of MKL1. In addition, we discuss recent evidence that strongly suggests a dual role for MKL1 in oncogenic mechanisms, as a tumor-promoting or tumor-suppressing molecule. Future studies will be necessary to evaluate the potential clinical implications of MKL1 expression and activation in cancer.

1. Introduction

Gene expression is fine-tuned and tightly regulated through complex transcriptional signaling networks involving interactions of transcription factors and cofactors. Megakaryoblastic leukemia 1 (MKL1) is a member of the myocardin-related transcription factor (MRTF) family and functions as a co-activator for serum response factor (SRF), which regulates essential biological processes ranging from gastrulation and development to cell survival and apoptosis.

MKL1, also termed MAL (megakaryocytic acute leukemia), BSAC (basic, SAP and coiled-coil), and MRTF-A (myocardin-related transcription factor-A), was originally identified as a chromosome 22 encoded fusion partner of the t(1;22)(p13;q13) translocation causing acute megakaryoblastic leukemia (AMKL) in infants and children (Ma et al., 2001; Mercher et al., 2001). As a result of the translocation, the MKL1 gene is fused to the RNA-binding motif protein 15 (RBM15), also known as OTT gene, on chromosome 1 (Ma et al., 2001; Mercher et al., 2001). This fusion gene encodes the deregulated protein RBM15–MKL1 (OTT–MAL; Descot et al., 2008) with potential oncogenic properties (Mercher et al., 2009). MKL1 was also identified in a screen for genes that protect against tumor necrosis factor-induced cell death, and named BSAC (Sasazuki et al., 2002).

2. Structure

The human MKL1 gene encodes a 931-amino acid protein, which shares an overall homology of 35% with the other MRTF family members, and more than 60% homology in a series of conserved domains (Wang et al., 2002). The domain structures of MKL1 and RBM15–MKL1 proteins are represented in Fig. 1.

A strongly conserved region of the MRTF family members is the N-terminal homology domain. This region of ~120 amino acids contains two or three RPEL motifs depending on the isoform of the protein (Miralles et al., 2003). RPEL motifs are named after four of their conserved amino acids and are implicated in actin-association and Rho-dependent nuclear import of MKL1 (Miralles et al., 2003; Vartiainen et al., 2007).

The basic region 1 is required for MKL1 binding to SRF (Cen et al., 2003). A second basic region is located between RPEL motifs 2 and 3. Both basic regions are implicated in nuclear localization of MKL1 (Miralles et al., 2003). One of the notable features of the MRTF family members is the SAP domain, which is a conserved 35-amino acid motif composed of two amphipathic α-helices. SAP domains are known to regulate nuclear organization, chromosomal dynamics, and apoptosis (Aravind and Koonin, 2000). They are found in a variety of nuclear proteins including SAF-A/B, Acinus, and PIAS (Aravind

* Corresponding author at: Friedrich Miescher Institute for Biomedical Research, Novartis Research Foundation, Maulbeerstrasse 66, CH-4058 Basel, Switzerland. Tel.: +41 61 697 2494; fax: +41 61 697 3976.
E-mail addresses: matthias.scharenberg@fmi.ch (M.A. Scharenberg), chiquet@fmi.ch (R. Chiquet-Ehrismann), maria.asparuhova@fmi.ch (M.B. Asparuhova).

1357-2725/$ – see front matter © 2010 Elsevier Ltd. All rights reserved.
doi:10.1016/j.biocel.2010.08.014

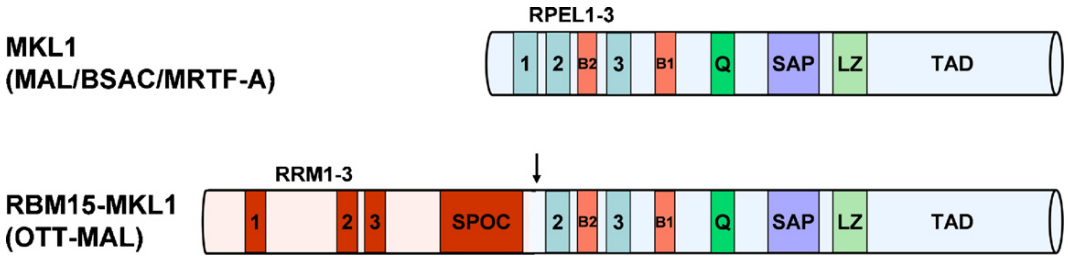

Fig. 1. Structure of MKL1 (MAL/BSAC/MRTF-A) and RBM15–MKL1 (OTT–MAL) proteins. Functional domains discussed in the text are shown. The RBM15–MKL1 contains almost the entire RBM15 (OTT) and MKL1 protein sequences, the fusion point is shown by an arrow. Abbreviations are: RPEL1–3, actin-binding motifs with Arg-Pro-X-X-X-Glu-Leu core consensus; B1 and B2, basic domains; Q, glutamine-rich domain; SAP, homology domain found in SAF-A/B, acinus, PIAS; LZ, leucine-zipper-like domain; TAD, transactivation domain; RRM, RNA recognition motif; SPOC, Spen paralogue and orthologue C-terminal domain.

and Koonin, 2000). However, deletion of the SAP domain of MKL1 had no effect on MKL1's transcriptional activity and MKL1–SRF complex formation (Cen et al., 2003; Miralles et al., 2003). A highly conserved coiled-coil leucine-zipper-like domain mediates homo- or heterodimerization among myocardin family members. Deletion of this domain had a modest effect on MKL1 activation of SRF-reporter genes (Cen et al., 2003). Finally, the transcriptional activity of MRTFs is mediated by powerful transcription-activation domains at the C-terminus of the proteins that share only low-level sequence identity between the three family members (Wang et al., 2002).

3. Expression, activation and turnover

MKL1 is expressed in nearly all adult tissues, with the strongest expression reported in heart, liver, lung, kidney, skeletal muscle, spleen, and brain (Wang et al., 2002).

The subcellular localization and transcriptional activity of MKL1 are directly regulated through its interaction with monomeric actin by means of the amino-terminal RPEL motifs (reviewed in Posern and Treisman, 2006). This regulatory mechanism involves the Rho-GTPase signaling (e.g. via RhoA, Rac1 or Cdc42) adjusting actin dynamics by integrating extracellular stimuli. In unstimulated fibroblasts, MKL1 is predominantly localized in the cytoplasm in association with G-actin. Upon RhoA activation, F-actin formation is increased and G-actin pools are depleted in both the cytoplasm and nucleus. This releases cytoplasmic MKL1 from G-actin, allowing nuclear import of MKL1 and subsequent activation of SRF-dependent transcription (Miralles et al., 2003). Interestingly, MKL1 also binds to G-actin in the nucleus, which plays an important role in modulating MKL1 functions (Vartiainen et al., 2007). Nuclear G-actin has been demonstrated to facilitate nuclear export of MKL1 and to prevent MKL1 from activating SRF target genes. Thus, cellular G-actin regulates MKL1 at three levels: nuclear import, nuclear export and nuclear activation/inactivation of MKL1-dependent transcription (Vartiainen et al., 2007).

This regulatory mechanism is likely to be triggered by every stimulus that can activate the RhoA-actin signaling pathway, including externally applied mechanical stress. We, as well as others, have observed translocation of MKL1 from the cytoplasm to the nucleus when mechanical strain was applied *in vitro* on mouse fibroblasts (Maier et al., 2008), rat cardiac fibroblasts (Zhao et al., 2007), primary smooth muscle cells or *in vivo*, in mechanically overloaded rat bladders (Hanna et al., 2009).

Other members of the small GTPase family, Rac1 and Cdc42 were also shown to regulate MKL1 nuclear localization and thus, smooth muscle actin promoter activity upon contact-dependent induction of epithelial–mesenchymal transition (EMT) (Busche et al., 2008).

In addition to Rho-GTPase signaling, MAPK pathways have been reported to regulate MKL1 activity. Activation of Erk1/2 promotes nuclear export of MKL1, thus negatively influencing the MKL1–SRF-dependent transcription (Muehlich et al., 2008). Furthermore, transcription factors other than SRF were shown to bind and regulate the activity of MKL1 for specific functions. For example, MKL1 was implicated in TGFβ-induced EMT via an interaction with Smad3 transcription factor. The MKL1–Smad3 complexes drive the expression of the human slug gene thereby prompting dissociation of cell–cell contacts (Morita et al., 2007).

MKL1 also forms complexes with Smad1/4 to activate transcription from the Id3-gene promoter, thus inhibiting myogenic differentiation (Iwasaki et al., 2008). Moreover, it has been shown that the forkhead transcription factor FOXO1 with a crucial role for myoblast fusion can also bind MKL1, thus preventing the association of the MKL1–Smad complex with the Id3 promoter (Iwasaki et al., 2008). Recently, a novel factor termed SCAI (suppressor of cancer cell invasion) has been identified as an MKL1-interacting protein (Brandt et al., 2009). SCAI inhibits the MKL1/SRF transcriptional complex, causing reduced expression of β1-integrins. The differential regulation of the MKL1-activity results in specific biological functions discussed in the next paragraph.

4. Biological function

Table 1 provides a summary of the known biological processes with the involvement of MKL1. Despite the diversity of functions in which MKL1 takes part, the majority of MKL1 knockout mice are viable and fertile (Li et al., 2006; Sun et al., 2006), possibly due to a functional redundancy between MKL1 and the other MRTF family members. However, 35% of the MKL1−/− embryos die from heart failure (Sun et al., 2006). Furthermore, females lacking MKL1 are unable to feed their pups owing to a defect in mammary gland myoepithelial cell differentiation (Li et al., 2006; Sun et al., 2006). In addition, knockout of MKL1 in mice leads to reduced platelet counts in peripheral blood, and reduced ploidy in bone marrow megakaryocytes, suggesting a role for MKL1 in megakaryocyte differentiation and maturation (Cheng et al., 2009). The phenotype of MKL1-deficient mice shows similarity to that of AMKL pathology associated with the chromosomal translocation t(1;22), in which the MKL1 and RBM15 genes are fused. It is not clear whether the leukemogenesis of this translocation results from reduced expression and altered specificity of RBM15 and/or MKL1, or whether the fusion protein possesses oncogenic properties. Recent studies have demonstrated that RBM15–MKL1 fusion protein is functionally deregulated and aberrantly activates SRF (Cen et al., 2003; Descot et al., 2008) as well as Notch-signaling (Mercher et al., 2009) shown to cause abnormal fetal megakaryopoiesis in the latter case.

In addition to the involvement in AMKL, MKL1 has been implicated in tumor cell invasion and metastasis (Medjkane et al., 2009). Downregulation of MKL1 by RNA interference decreased tumor cell motility in tumor xenografts of human breast carcinoma and mouse melanoma cells in mice, while cell proliferation was unaffected. In addition, MKL1-depleted breast tumor cells showed a

Table 1
Summary of MKL1 biological functions and known MKL1-dependent targets.

Development and tissue homeostasis	MKL1-dependent targets
Muscle cell differentiation	[1–3]SM22α, [1,2]SM α-actin, [2]SM MHC, [1]cardiac α-actin, [4]skeletal α-actin, [4]skeletal α-MHC, [5]miR-486 (inhibiting PTEN and Foxo1a expression)
Mammary gland myoepithelial cell differentiation	[6,7]SM α-actin, [6,7]MHC, [6,7]calponin 1, [6,7]Tpm2
Megakaryoblastic differentiation and migration	[8]GATA1, [8]GATA2, [8]GP5, [9]MYL9, [9]MMP9
Cardiovascular development[10] and adaptation to stress/myocardial infarction	[11]BNP, [11]SM α-actin, [11]skeletal α-actin, [11]SM22α, [12]Col1a1, [12]Col1a2, [12]Col3a1, [12]elastin, [1,12]ANF
Remodeling of neuronal networks in developing and adult brain[a]	[13]Gelsolin, [13]Pctaire1/Cdk16, [14]SM α-actin, [14]Slug/Snai2 (learning associated activation), [14]Tpm3
Modulation of actin dynamics and cellular motile functions	[15]SRF, [15,16]vinculin, [15]Jun-B, [15–17]Tpm1, [16]Tpm2, [16]zyxin, [16]caldesmon, [17]CTGF, [17]MYL9, [17]MYH9, [17,18]CCN1/CYR61, and others (reviewed in 19)
Cancer progression and metastasis	**MKL1-dependent targets**
Induction of epithelial–mesenchymal transition (EMT)	[20]Slug/Snai2, [20]Snail/Snai1, [20]Twist, [20–23]SM α-actin
Pathogenesis of acute megakaryoblastic leukemia (AMKL)[b]	[24]RBPJ-dependent genes (Notch signalling), [1,25]SRF-dependent genes (e.g. c-fos and egr-1)
Promotion of tumor cell invasion and metastasis	[17]MYL9, [17]MYH9, [26]β1-integrin, [27]ERα-dependent genes
Antiproliferative effects and tumor suppression	[28]mig6/errfi-1, [29]Eplin-α, [30]tropomyosin, [30]caldesmon

Publication details only provided for reports that are not listed under References. (1) Cen et al. (2003); (2) Du et al. J Biol Chem 2004;279:17578–86; (3) Wang et al. (2002); (4) Selvaraj and Prywes. J Biol Chem 2003;278:41977–87; (5) Small et al. Proc Natl Acad Sci U S A 2010;107:4218–23; (6) Sun et al. (2006); (7) Li et al. (2006); (8) Cheng et al. (2009); (9) Gilles et al. Blood 2009;114:4221–32; (10) Parmacek. Circ Res 2007;100:633–44; (11) Kuwahara et al. Mol Cell Biol 2010:00154–10; (12) Small et al. Circ Res 2010;107:294–304; (13) Mokalled et al. Development 2010;137:2365–74; (14) O'Sullivan et al. Cereb Cortex 2010;20:1915–25; (15) Selvaraj and Prywes. BMC Mol Biol 2004;5:13; (16) Morita et al. Exp Cell Res 2007;313:3432–45; (17) Medjkane et al. (2009); (18) Hanna et al. (2009); (19) Olson and Nordheim. Nat Rev Mol Cell Biol 2010;11:353–65; (20) Morita et al. (2007); (21) Fan et al. Mol Biol Cell 2007;18:1083–97; (22) Busche et al. (2008); (23) Sebe et al. Nephron Exp Nephrol 2010;114:e117–25; (24) Mercher et al. (2009); (25) Descot et al. (2008); (26) Brandt et al. (2009); (27) Huet et al. (2009); (28) Descot et al. (2009); (29) Leitner et al. (2010); and (30) Yoshio et al. (2010).

[a] Genes targeted by MKL1 and/or MKL2.

[b] Genes targeted by the fusion protein RBM15–MKL1/OTT–MAL rather than MKL1 alone, are listed.

reduced capability to form lung metastases following intravenous injection into the mouse tail vein. Moreover, expression of an MKL1-constitutive active protein potentiated lung colonization by otherwise poorly metastatic cells. Thus, at least in certain cell contexts, enhanced MKL1 activity can promote tumor cell metastasis.

Consistent with these observations, SCAI, a binding partner and inhibitor of MKL1 that is downregulated in various tumors has been identified (Brandt et al., 2009). The study suggests that MKL1–SRF signaling can upregulate β1-integrin expression, thus promoting tumor cell invasiveness, whereas SCAI significantly antagonizes this process. Furthermore, activation of the Rho-MKL1 signaling pathway resulted in reduced transactivation efficiency of estrogen receptor-α, diminishing its protective function in tumor progression and invasiveness (Huet et al., 2009) again supporting a protumorigenic role for MKL.

Interestingly, while downregulation of MKL1 does not affect proliferation (Medjkane et al., 2009), MKL1 overexpression elicits a strong antiproliferative effect in various fibroblast and epithelial cell lines (Descot et al., 2009). Several putative antiproliferative MKL1-target genes have been identified, including mig6/errfi-1, a negative regulator of the EGFR–MAPK pathway. Epithelial protein Lost in Neoplasm α (Eplin-α), a tumor suppressor gene, the expression of which inversely correlates with carcinoma aggressiveness, has been recently described as a direct target of the MKL1–SRF pathway (Leitner et al., 2010). Furthermore, Yoshio et al. (2010) have reported that expression of an MKL1-constitutive active form in oncogenic ras or src transformed rat intestinal epithelial cells, when injected into the spleen of nude mice, significantly suppressed tumor formation and reduced liver metastases. The enforced activation of MKL1 rescued the reduced tropomyosin and caldesmon expression levels in the transformed cells, thereby activating the tumor-suppressive properties of tropomyosin and reducing the caldesmon-dependent invadopodia formation (Yoshio et al., 2010). Moreover, the levels of expression and/or activation of MKL1 seem to determine the expression of specific sets of target genes, through which MKL1 exerts various and often opposing biological effects as a tumor-promoting or tumor-suppressing molecule depending on the cellular context.

Evidence supporting the above notion exists also for pathologies different than cancer. Decreased MKL1 expression levels were observed in the skeletal muscle of aged mice, which was proposed to induce sarcopenia (Sakuma et al., 2007). In addition, an MKL1 promoter single nucleotide polymorphism causing high MKL1 expression levels was associated with the progression of atherosclerosis and the susceptibility to coronary artery disease (Hinohara et al., 2009). Apparently, both up- and downregulation of MKL1 can play a role in the pathogenesis of diseases.

Collectively, the data reviewed here show that MKL1 may exert different biological functions depending on the cell type, tissue environment, and signaling pathways in which it is involved.

5. Possible medical applications

First steps in the development of novel pharmacological tools targeting transcriptional responses of MKL1 signaling in cancer were made with the recent development of compounds that selectively target the Rho/MKL1 signaling and inhibit the invasion of prostate cancer cells in a Matrigel model of metastasis (Evelyn et al., 2007). Given the incontestable involvement of MKL1 in tumorigenesis and the effects it exerts on tumor cell invasion and metastasis, it will be important to assess how MKL1 is integrated within the major signaling pathways that communicate extracellular signals and mechanical cues to the transcriptional machinery to alter the motility of cancer cells. Recognition of the differential regulation and function of MKL1 in tumors will ultimately provide a better understanding of the signaling pathways that can be therapeutically modulated.

References

Aravind L, Koonin EV. SAP—a putative DNA-binding motif involved in chromosomal organization. Trends Biochem Sci 2000;25:112–4.

Brandt DT, Baarlink C, Kitzing TM, Kremmer E, Ivaska J, Nollau P, et al. SCAI acts as a suppressor of cancer cell invasion through the transcriptional control of beta1-integrin. Nat Cell Biol 2009;11:557–68.

Busche S, Descot A, Julien S, Genth H, Posern G. Epithelial cell–cell contacts regulate SRF-mediated transcription via Rac–actin–MAL signalling. J Cell Sci 2008;121:1025–35.

Cen B, Selvaraj A, Burgess RC, Hitzler JK, Ma Z, Morris SW, et al. Megakaryoblastic Leukemia 1, a potent transcriptional coactivator for serum response factor (SRF), is required for serum induction of SRF target genes. Mol Cell Biol 2003;23:6597–608.

Cheng Ec, Luo Q, Bruscia EM, Renda MJ, Troy JA, Massaro SA, et al. Role for MKL1 in megakaryocytic maturation. Blood 2009;113:2826–34.

Descot A, Hoffmann R, Shaposhnikov D, Reschke M, Ullrich A, Posern G. Negative regulation of the EGFR–MAPK cascade by actin-MAL-mediated Mig6/Errfi-1 induction. Mol Cell 2009;35:291–304.

Descot A, Rex-Haffner M, Courtois G, Bluteau D, Menssen A, Mercher T, et al. OTT–MAL is a deregulated activator of serum response factor-dependent gene expression. Mol Cell Biol 2008;28:6171–81.

Evelyn CR, Wade SM, Wang Q, Wu M, Iñiguez-Lluhí JA, Merajver SD, et al. CCG-1423: A small-molecule inhibitor of RhoA transcriptional signaling. Mol Cancer Ther 2007;6:2249–60.

Hanna M, Liu H, Amir J, Sun Y, Morris SW, Siddiqui MAQ, et al. Mechanical regulation of the proangiogenic factor CCN1/CYR61 gene requires the combined activities of the myocardin-related transcription factor (MRTF)-A and CREB binding protein (CBP) histone acetyl transferase. J Biol Chem 2009;284:23125–36.

Hinohara K, Nakajima T, Yasunami M, Houda S, Sasaoka T, Yamamoto K, et al. Megakaryoblastic leukemia factor-1 gene in the susceptibility to coronary artery disease. Hum Genet 2009;126:539–47.

Huet G, Merot Y, Percevault F, Tiffoche C, Arnal JF, Boujrad N, et al. Repression of the estrogen receptor-+c transcriptional activity by the Rho/megakaryoblastic leukemia 1 signaling pathway. J Biol Chem 2009;284:33729–39.

Iwasaki K, Hayashi K, Fujioka T, Sobue K. Rho/Rho-associated kinase signal regulates myogenic differentiation via myocardin-related transcription factor-A/Smad-dependent transcription of the Id3 gene. J Biol Chem 2008;283:21230–41.

Leitner L, Shaposhnikov D, Descot A, Hoffmann R, Posern G. Epithelial protein lost in neoplasm alpha (Eplin-alpha) is transcriptionally regulated by G-actin and MAL/MRTF coactivators. Mol Cancer 2010;9:60.

Li S, Chang S, Qi X, Richardson JA, Olson EN. Requirement of a myocardin-related transcription factor for development of mammary myoepithelial cells. Mol Cell Biol 2006;26:5797–808.

Ma Z, Morris SW, Valentine V, Li M, Herbrick JA, Cui X, et al. Fusion of two novel genes RBM15 and MKL1, in the t(1;22)(p13;q13) of acute megakaryoblastic leukemia. Nat Genet 2001;28:220–1.

Maier S, Lutz R, Gelman L, Sarasa-Renedo A, Schenk S, Grashoff C, et al. Tenascin-C induction by cyclic strain requires integrin-linked kinase. Biochim Biophys Acta 2008;1783:1150–62.

Medjkane S, Perez-Sanchez C, Gaggioli C, Sahai E, Treisman R. Myocardin-related transcription factors and SRF are required for cytoskeletal dynamics and experimental metastasis. Nat Cell Biol 2009;11:257–68.

Mercher T, Coniat MB-L, Monni R, Mauchauffe M, Khac FN, Gressin L, et al. Involvement of a human gene related to the Drosophila spen gene in the recurrent t(1;22) translocation of acute megakaryocytic leukemia. Proc Natl Acad Sci U S A 2001;98:5776–9.

Mercher T, Raffel GD, Moore SA, Cornejo MG, Baudry-Bluteau D, Cagnard N, et al. The OTT–MAL fusion oncogene activates RBPJ-mediated transcription and induces acute megakaryoblastic leukemia in a knockin mouse model. J Clin Invest 2009;119:852–64.

Miralles F, Posern G, Zaromytidou AI, Treisman R. Actin dynamics control SRF activity by regulation of its coactivator MAL. Cell 2003;113:329–42.

Morita T, Mayanagi T, Sobue K. Dual roles of myocardin-related transcription factors in epithelial mesenchymal transition via slug induction and actin remodeling. J Cell Biol 2007;179:1027–42.

Muehlich S, Wang R, Lee SM, Lewis TC, Dai C, Prywes R. Serum-induced phosphorylation of the serum response factor coactivator MKL1 by the extracellular signal-regulated kinase 1/2 pathway inhibits its nuclear localization. Mol Cell Biol 2008;28:6302–13.

Posern G, Treisman R. Actin' together: serum response factor, its cofactors and the link to signal transduction. Trends Cell Biol 2006;16:588–96.

Sakuma K, Akiho M, Nakashima H, Akima H, Yasuhara M. Age-related reductions in expression of serum response factor and myocardin-related transcription factor A in mouse skeletal muscles. Biochim Biophys Acta (BBA) – Mol Basis Dis 2007;1782:453–61.

Sasazuki T, Sawada T, Sakon S, Kitamura T, Kishi T, Okazaki T, et al. Identification of a novel transcriptional activator, BSAC, by a functional cloning to inhibit tumor necrosis factor-induced cell death. J Biol Chem 2002;277:28853–60.

Sun Y, Boyd K, Xu W, Ma J, Jackson CW, Fu A, et al. Acute myeloid leukemia-associated Mkl1 (Mrtf-a) is a key regulator of mammary gland function. Mol Cell Biol 2006;26:5809–26.

Vartiainen MK, Guettler S, Larijani B, Treisman R. Nuclear actin regulates dynamic subcellular localization and activity of the SRF cofactor MAL. Science 2007;316:1749–52.

Wang DZ, Li S, Hockemeyer D, Sutherland L, Wang Z, Schratt G, et al. Potentiation of serum response factor activity by a family of myocardin-related transcription factors. Proc Natl Acad Sci U S A 2002;99:14855–60.

Yoshio T, Morita T, Tsujii M, Hayashi N, Sobue K. MRTF-A/B suppress the oncogenic properties of v-ras- and v-src-mediated transformants. Carcinogenesis 2010;31:1185–93.

Zhao XH, Laschinger C, Arora P, Szaszi K, Kapus A, McCulloch CA. Force activates smooth muscle alpha-actin promoter activity through the Rho signaling pathway. J Cell Sci 2007;120:1801–9.

6.4 Involvement in myofibroblast/cancer-associated fibroblast differentiation - a key player in tissue repair, fibrosis, and cancer

Over the past few years since the reports of the relatively mild embryonic phenotypes of MKL1$^{-/-}$ mice (Li et al., 2006; Sun et al., 2006b), important roles for MKL1 in postnatal physiological and pathological processes have been described. These were found in a variety of cell types, ranging from epithelial cells to smooth muscle cells. Strikingly, most of these processes involve MKL1 function as a crucial regulator of the smooth muscle cell (SMC)-specific gene expression program. Although MKL1 is not absolutely required for the differentiation of SMCs during embryonic development (see section 5), Du et al. (2004) showed that forced MKL1/SRF expression in undifferentiated SRF$^{-/-}$ embryonic stem cells and other non-SMCs induced the transcription of smooth muscle-specific genes. As discussed in section 4, myocardin is indispensible for SMC differentiation during embryogenesis, but is exclusively expressed in cardiac and smooth muscle cells and is not subjected to regulation by Rho and actin. Thus, a general function of MKL1 in postnatal processes involving the dynamic regulation of SMC-specific genes in various cell types seems plausible. As summarized in Figure 3, many reported functions of MKL1 in tissues other than brain and blood are connected to the differentiation into myofibroblast-like cells and to contractile protein expression.

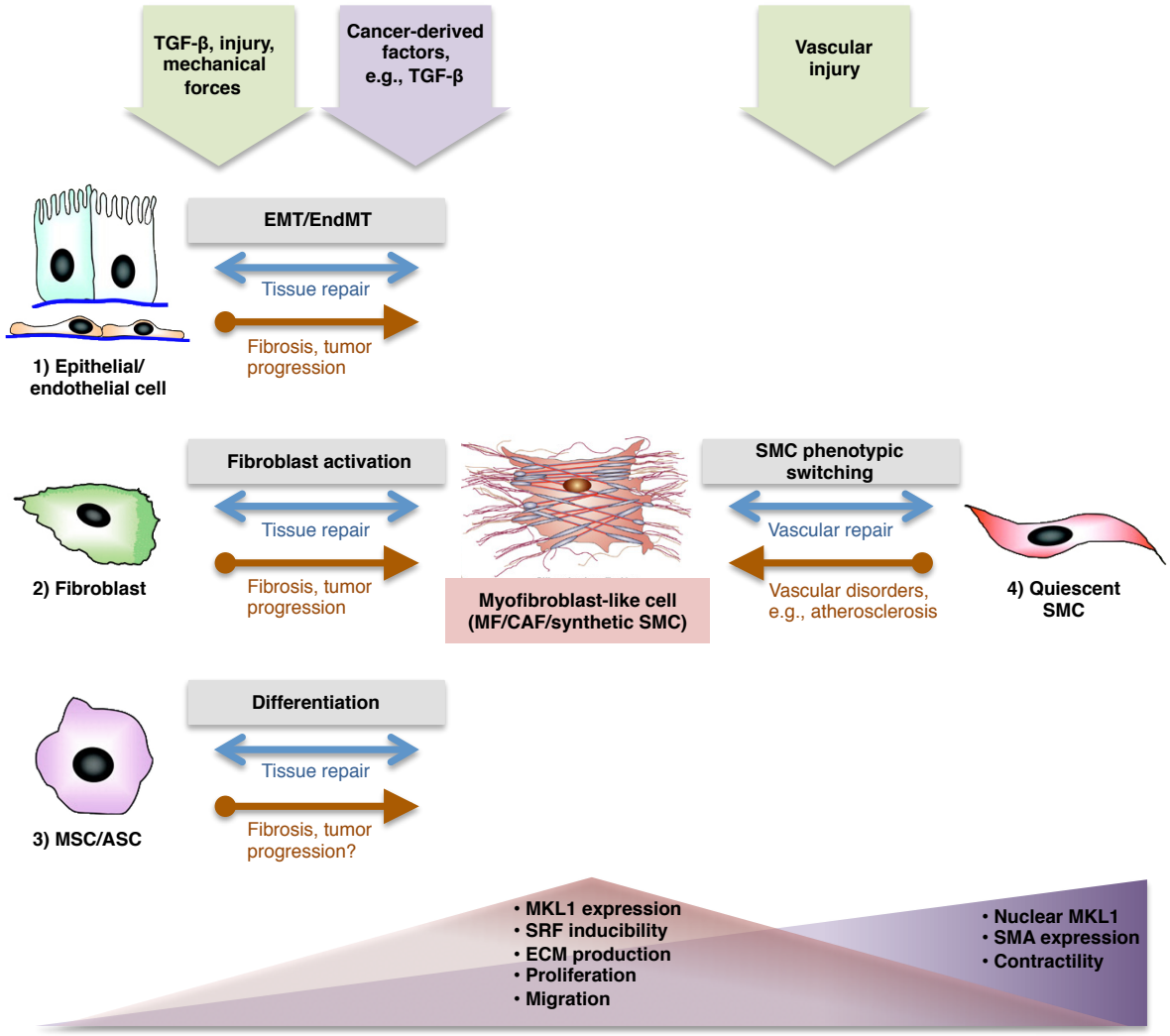

Figure 3: MKL1-dependent physiological and pathological processes related to the myofibroblast cell type.

Myofibroblast-like cells comprise myofibroblasts, cancer-associated (myo-)fibroblasts (CAFs), myoepithelial cells, and synthetic smooth muscle cells. All these cell types are contractile cells in-between a precursor cell and a smooth muscle cell, which resemble true myofibroblasts in many aspects. A double-headed arrow indicates the differentiation and the later resolution, either by dedifferentiation or apoptosis. The following publications reported a crucial role of MKL1-mediated gene expression during these dynamic transdifferentiation processes:

1) EMT/EMyT in renal fibrosis: Fan et al. (2007); Masszi et al. (2010); Morita et al. (2007); Charbonney et al. (2011); Elberg et al. (2008); EMT in lens epithelial cells: Gupta et al. (2013); EndMT: Mihira et al. (2012); Myoepithelial (MF-like) cell differentiation defect in MKL1$^{-/-}$ mice: Li et al. (2006); Sun et al. (2006b)

2) Cardiac fibrosis after myocardial infarction: Small et al. (2010); Cardiac hypertrophy, pressure or volume overload: Zhao et al. (2007); Pulmonary (lung) fibrosis: Huang et al. (2012);

Sandbo et al. (2011); Zhou et al. (2013); human MKL1 promoter SNP in coronary artery disease: Hinohara et al. (2009)

3) Tumor progression: Jeon et al. (2010); Siletz et al. (2013)

4) Vascular disorders, e.g., atherosclerosis, restenosis, and hypertension: Lagna et al. (2007); Minami et al. (2012)

ASC, adipose tissue-derived stromal cell; CAF, cancer-associated fibroblast; EMT/EndMT, epithelial/endothelial-to-mesenchymal transition; MF, myofibroblast; MSC, multipotent stromal cell; SMC, smooth muscle cell. Drawings of cell types were taken from Hinz et al. (2007); Tomasek et al. (2002).

Differentiation of a variety of cell types into myofibroblasts defines a major physiologic process that facilitates wound healing and tissue repair. Tissue damage leads to the loss of tensional homeostasis, the formation of a blood clot, and the release of soluble mediators. This drives the transformation of a variety of quiescent tissue-resident cells or invading circulating cells into a mesenchymal proliferative-migrative phenotype (termed proto-myofibroblast), involving the formation of smooth muscle α-actin (SMA)-negative stress fibers. Different cellular precursors have been described, including locally residing fibroblasts (Higashiyama et al., 2011), epithelial cells (EMT; reviewed in Kalluri and Weinberg, 2009; Masszi et al., 2010), endothelial cells (EndMT; Li and Jimenez, 2011; Potenta et al., 2008), pericytes (Rajkumar et al., 2005; Rajkumar et al., 2006), hepatic stellate cells (Desmoulière, 2007; Friedman, 2010), smooth muscle cells (Hao et al., 2006; reviewed in Owens et al., 2004), and multipotent stromal cells (MSCs) (Jahoda and Reynolds, 2001; van den Bogaerdt et al., 2009), as well as circulating bone marrow-derived MSCs (Direkze et al., 2004; Forbes et al., 2004) and fibrocytes (Abe et al., 2001; Yang et al., 2005). Proto-myofibroblasts are able to expand towards the wound and to differentiate into a contractile phenotype with characteristic SMA-positive stress fibers, then termed “myofibroblast” or “activated fibroblast”. The specialized cell type in-between a fibroblast and a smooth muscle cell mediates mechanical force generation and contraction of the wound (Desmoulière et al., 1993; Mayer and Leinwand, 1997). Furthermore, it produces large amounts of extracellular matrix proteins, such as type I collagen, fibronectin, tenascin-C, and matrix metalloproteinases (MMPs), contributing to the replacement of the granulation tissue and the scarring of the wound (reviewed in Sarrazy et al., 2011). Deregulation of this dynamic differentiation process inevitably

leads to pathological situations. Organ fibrosis and fibrotic scarring arise from excessive extracellular matrix deposition by persistent myofibroblasts. Fibrosis as part of chronic inflammation processes causes functional impairment of many organs, accounting for almost half of all natural deaths in the developed world.

Several studies showed an involvement of MKL1 in controlling myofibroblast differentiation and the fibrotic gene expression program (Figure 3). For instance, Small et al. (2010) compared the scar formation after experimentally induced myocardial infarction (MI) between wild-type mice and MKL1$^{-/-}$ mice. The authors found clearly reduced scar formation after MI in mice lacking MKL1. MI results in the loss of cardiomyocytes and fibrotic scarring of the tissue, which prevents the repair and replacement of the vasculature. Cardiac fibroblasts that transform into myofibroblasts upon injury are thought to be the major effector cell type (reviewed in van den Borne et al., 2010). Accordingly, the post-MI tissue of MKL1$^{-/-}$ mice contained less SMA-positive myofibroblasts and fibrosis-promoting genes were decreased compared to wild-type mice. Huang et al. (2012) and Zhou et al. (2013) identified the Rho-actin-MKL1-SRF pathway as a crucial mechanoresponsive pathway in converting matrix stiffening into the fibrotic gene program that drives myofibroblast differentiation in lung fibrosis. Several publications from the Kapus lab (see Figure 3) have established MKL1 as a crucial mediator of TGF-β-induced EMT in fibrosis. The molecular details of this regulation will be discussed in Manuscript 1. Similarly, Mihira et al. (2012) showed a role of MKL1 in the process of TGF-β-induced EndMT, in which myofibroblasts arise from the transformation of endothelial cells. Notably, the impaired mammary myoepithelial differentiation phenotype of MKL1$^{-/-}$ mice, which was discussed in section 4.2, is also related to the myofibroblast differentiation process. Myoepithelial cells differ from myofibroblasts as they are positive for keratins and negative for the mesenchymal marker vimentin. They show typical epithelial cell features, such as cadherin-mediated junctions and the association with a basement membrane that separates the cells from the stroma. However, the hormone-induced differentiation process from multipotent cap cells to myoepithelial cells during puberty involves the formation of stress fibers and the expression of smooth muscle-specific genes, such as SMA. These cytoskeletal structures enable the cells to contract and trigger milk ejection from the adjacent milk-secreting cells. In this respect, the inducible physiologic differentiation into mammary

myoepithelial cells resembles the differentiation into myofibroblasts and is likely to be controlled by similar MKL1-mediated mechanisms.

As mentioned before, a myofibroblast-like cell can be characterized as a cell type whose differentiation state resides in-between a precursor cell and a smooth muscle cell (SMC). The expression of contractility-promoting proteins and especially SMA increases steadily throughout the entire differentiation process from the precursor cell to the myofibroblast to the SMC (see Figure 3). Since the Rho-actin-MKL1-SRF pathway in known to regulate SMA expression, it seems plausible that MKL1 activity correlates with the level of SMA expression. Indeed, in smooth muscle cells MKL1 was found to be constitutively nuclear, reflecting the constant expression of contractility-promoting proteins. In contrast, MKL1 localizes in the cytosol of most unstimulated precursor cells, such as fibroblasts (Miralles et al., 2003). Whereas the differentiation process involves a steady increase of contractile protein expression, some characteristics of myofibroblasts are highly different from the two fully differentiated endpoints of this process. Quiescent precursor cells, such as epithelial cells or fibroblasts, as well as quiescent smooth muscle cells do not, e.g., proliferate or migrate, but serve other functions. However, in the case of a tissue injury and the concomitant loss of tissue homeostasis, quiescent cells need to temporarily switch to a specialized cell type that shows high proliferation, migration, and ECM production, which is the myofibroblast. Importantly, myofibroblasts cannot only derive from precursor cells such as epithelial cells or multipotent stromal cells (MSCs) as described before, but they can also arise from the dedifferentiation of quiescent smooth muscle cells (point 4 in Figure 3). This phenotypic switching is known for vascular smooth muscles cells (VSMCs). Quiescent or contractile VSMCs are not terminally differentiated and are able to temporarily switch back to a myofibroblast-like phenotype upon vascular injury, then being termed synthetic or proliferative VSMCs (reviewed in Owens et al., 2004). In contrast to the differentiation into myofibroblasts that was discussed before, the dedifferentiation process from VSMCs requires the downregulation of MKL activity and expression of contractility-promoting proteins. In addition to MKL1, differentiated smooth muscle cells also express myocardin, whereas MKL2 is specifically expressed in neural crest-derived SMCs. Minami et al. (2012) found a myocardin-induced and miR-1-mediated repression of MKL1 activity in differentiated SMCs (Figure 4). Since myocardin is constitutively active, genes of the contractile

apparatus are constantly expressed at high levels in SMCs. However, upon vascular injury myocardin and miR-1 get downregulated, resulting in an upregulation of MKL1. This causes a drop in basal SRF activity and concomitant contractile protein expression, but SRF inducibility via Rho-actin-mediated activation of MKL1 increases.

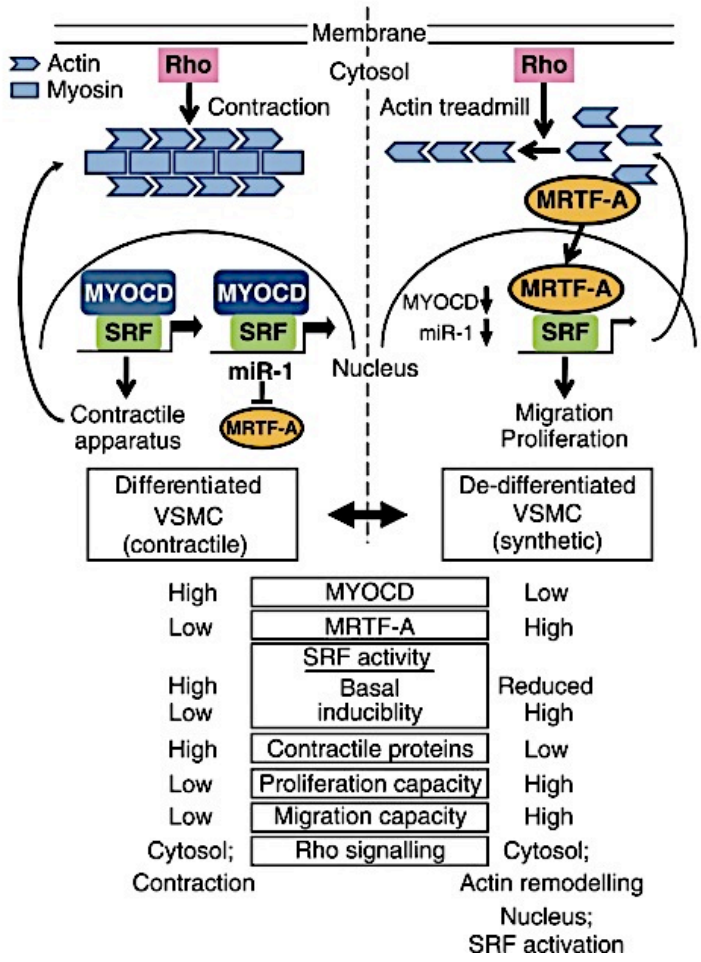

(From Minami et al., 2012)

Figure 4: Regulation of the phenotypic plasticity of vascular smooth muscle cells (VSMC) by MRTF family members.

Minami et al. (2012) proposed a model, according to which high levels of myocardin in differentiated VSMCs maintain high expression of contractile proteins and concomitant low expression of MKL1/MRTF-A via miR-1. Upon dedifferentiation into the synthetic phenotype, myocardin and miR-1 expression decrease and raise MKL1/MRTF-A transcription. Reduced contractility, a high inducibility of specific SRF transcription, as well as remodeling of the actin cytoskeleton enable the cell to migrate and produce ECM.

In addition, SRF coactivators from the TCF family seem to play an important role in the regulation of phenotypic SMC switching. A subset of proliferative genes that are expressed by the myofibroblast-like synthetic SMCs are controlled by members of this family. Forced expression of the ELK1 family member suppresses the transcription of SMC-specific contractile genes. The high phenotypic plasticity of VSMCs enables the closure of wounds in the vasculature, but it also predisposes these cells to contribute to vascular diseases, such as atherosclerosis, hypertension, or cancer, upon deregulation of the process.

Similarly to wounds, the "reactive stroma" of solid tumors can be considered as fibrotic tissue, and is stiffer than normal tissue. Cancer was therefore described as "a wound that does not heal" (Dvorak, 1986). In the tumor setting, myofibroblast-like cancer-associated fibroblasts (CAFs) accumulate in the tumor stroma and promote tumor progression (Barsky et al., 1984; Sugimoto et al., 2006). All myofibroblast precursor cells mentioned above for fibrotic processes similarly apply as putative sources for CAFs (Figure 5) (reviewed in Otranto et al., 2012). The process of type 3 epithelial-to-mesenchymal transition (EMT, reviewed in Kalluri and Weinberg (2009)) was shown to promote tumor invasiveness when transformed, neoplastic epithelial cells switch to a proliferative-migrative phenotype. These cells have the ability to spread, and eventually switch back to the epithelial phenotype to establish a secondary tumor (mesenchymal-to-epithelial transition, MET). However, EMT, in this case type 2 EMT, also serves as a source for myofibroblasts/CAFs that support cancer progression from the tumor microenvironment. Importantly, in contrast to CAFs that have differentiated from other precursor cell types, as e.g., from fibroblasts of the surrounding tumor stroma, these CAFs would have the altered genome of the transformed tumor cells. The exact contributions of the different precursor cell types to CAF-promoted tumor progression are not yet well understood. CAFs secrete pro-tumorigenic and pro-angiogenic factors, such as TGF-β, VEGF-A, or SDF-1/CXCL12, and some pro-inflammatory cytokines (De Wever et al., 2008). Additionally, they rebuild the ECM by secreting similar proteins as mentioned in the wound healing context, facilitating invasion (reviewed in Kalluri and Zeisberg, 2006). Thereby, CAFs importantly alter the physical properties of the tumor stroma. They cause tissue stiffening, leading to the differentiation of more CAFs. Tissue stiffness directly correlates with the risk of cancer, e.g., in breast tissues (Boyd et al.,

2007; Wolfe, 1976). In breast carcinomas, CAFs constitute about 80% of all stromal fibroblasts (Sappino et al., 1988). Notably, myofibroblast differentiation and fibrosis are common side effects of standard cancer treatments, including surgery, radio-, and chemotherapy (De Wever et al., 2008), which might in fact promote undesirable effects such as tumor recurrence and metastasis. It has become evident that interactions between cancer cells and stromal cells are an important factor driving tumor progression.

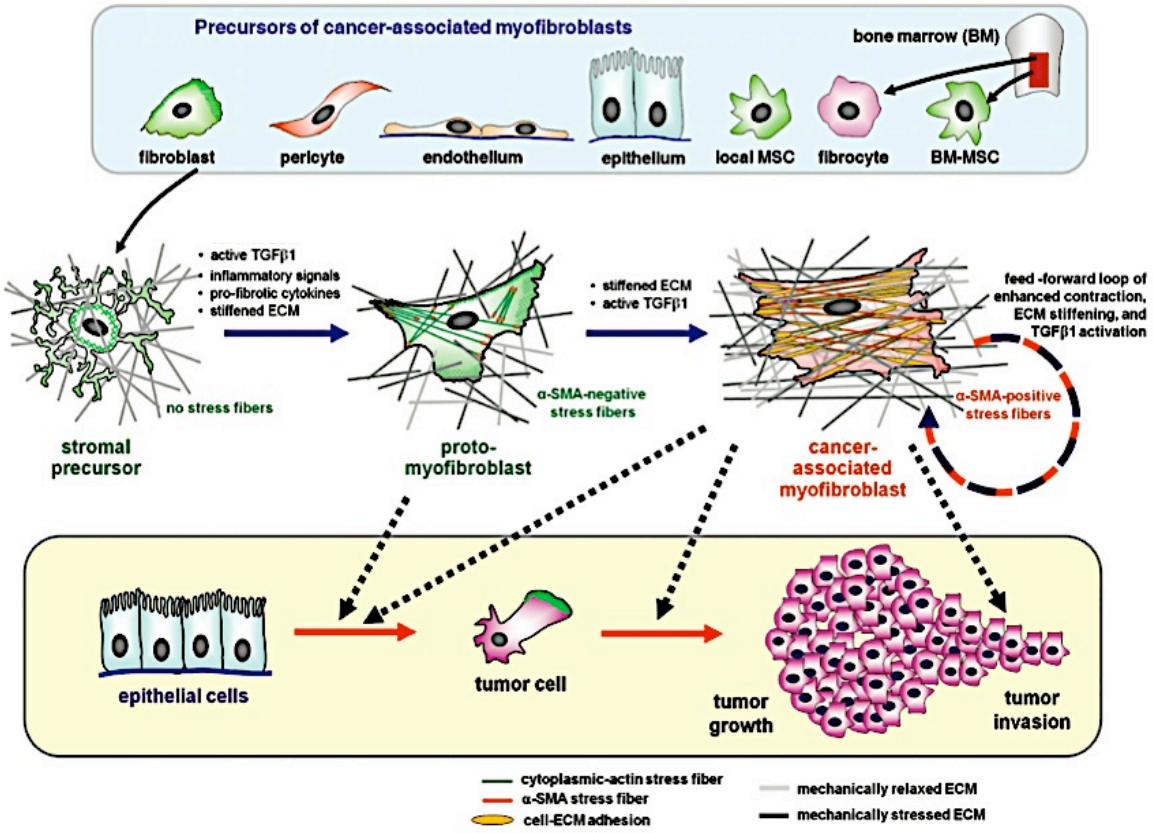

(Modified from Otranto et al., 2012)

Figure 5: Myofibroblast-like CAFs arise from different precursor cell types and promote tumor progression.

In the intact tissue, the extracellular matrix (ECM) maintains chemical and mechanical homeostasis and prevents quiescent cells from differentiating. When homeostasis is disturbed upon injury or by a nearby tumor, these cells get activated to proliferate, migrate, and secrete ECM. Autocrine TGF-β production and a stiffening ECM further promote the expression of contractile proteins, such as SMA, and the differentiation into CAFs. CAFs may support cancer cells at all stages of the tumorigenic process.

Siletz et al. (2013) identified SRF as a transcription factor whose activity was increased in both, a CAF cell line from human invasive ductal carcinoma and a normal mammary fibroblast (NMF) cell line that was induced to differentiate into CAFs by cancer cell-secreted factors, compared to non-induced NMF cells. Jeon et al. (2010) found an increase in MKL1 expression when they differentiated human adipose tissue-derived stem cells into SMA-positive CAFs by treating them with cancer cell-derived factors. siRNA-mediated depletion of MKL1 was sufficient to prevent SMA expression and full differentiation. To date, there have been only few publications implicating a function of the Rho-actin-MKL1-SRF pathway in the regulation of CAF differentiation (see Figure 3). However, since it is becoming increasingly clear that the Rho-actin-MKL1-SRF pathway is an important regulator of myofibroblast differentiation in the fibrosis context, it seems highly probable that similar mechanisms apply also in the tumor context.

The Rho-actin-MKL1 pathway emerges as a common pathway that controls myofibroblast/CAF differentiation in response to chemical or mechanical signals from the microenvironment, such as TGF-β or matrix stiffening, respectively. As such, this pathway is of central importance for physiologic tissue repair processes and modulating its activity is a novel option in Regenerative Medicine and Tissue Engineering. Moreover, targeting this pathway or its upstream effectors represents a promising strategy to interfere with the excessive and self-reinforcing myofibroblast/CAF differentiation that promotes fibrosis and cancer.

References

Abe, R., S. Donnelly, T. Peng, R. Bucala, and C. Metz. 2001. Peripheral blood fibrocytes: differentiation pathway and migration to wound sites. *Journal of immunology (Baltimore, Md. : 1950)*. 166:7556-7562.

Alberti, S., S. Krause, O. Kretz, U. Philippar, T. Lemberger, E. Casanova, F. Wiebel, H. Schwarz, M. Frotscher, G. Schütz, and A. Nordheim. 2005. Neuronal migration in the murine rostral migratory stream requires serum response factor. *Proceedings of the National Academy of Sciences of the United States of America*. 102:6148-6153.

Alberts, B., A. Johnson, J. Lewis, M. Raff, K. Roberts, and P. Walter. 2010. Molecular Biology of the Cell. New York: Garland Science; 2008. *Classic textbook now in its 5th Edition*.

Aravind, L., and E. Koonin. 2000. SAP - a putative DNA-binding motif involved in chromosomal organization. *Trends in Biochemical Sciences*. 25:112-114.

Arsenian, S., B. Weinhold, M. Oelgeschläger, U. Rüther, and A. Nordheim. 1998. Serum response factor is essential for mesoderm formation during mouse embryogenesis. *The EMBO Journal*. 17:6289-6299.

Asparuhova, M., J. Ferralli, M. Chiquet, and R. Chiquet-Ehrismann. 2011. The transcriptional regulator megakaryoblastic leukemia-1 mediates serum response factor-independent activation of tenascin-C transcription by mechanical stress. *FASEB journal : official publication of the Federation of American Societies for Experimental Biology*. 25:3477-3488.

Audet, M., and M. Bouvier. 2012. Restructuring G-protein- coupled receptor activation. *Cell*. 151:14-23.

Baarlink, C., H. Wang, and R. Grosse. 2013. Nuclear Actin Network Assembly by Formins Regulates the SRF Coactivator MAL. *Science (New York, N.Y.)*.

Barsky, S., W. Green, G. Grotendorst, and L. Liotta. 1984. Desmoplastic breast carcinoma as a source of human myofibroblasts. *The American Journal of Pathology*. 115:329-333.

Belaguli, N., J. Sepulveda, V. Nigam, F. Charron, M. Nemer, and R. Schwartz. 2000. Cardiac tissue enriched factors serum response factor and GATA-4 are mutual coregulators. *Molecular and Cellular Biology*. 20:7550-7558.

Boxer, L., R. Prywes, R. Roeder, and L. Kedes. 1989. The sarcomeric actin CArG-binding factor is indistinguishable from the c-fos serum response factor. *Molecular and Cellular Biology*. 9:515-522.

Boyd, N., H. Guo, L. Martin, L. Sun, J. Stone, E. Fishell, R. Jong, G. Hislop, A. Chiarelli, S. Minkin, and M. Yaffe. 2007. Mammographic density and the risk and detection of breast cancer. *The New England Journal of Medicine*. 356:227-236.

Brandt, D., C. Baarlink, T. Kitzing, E. Kremmer, J. Ivaska, P. Nollau, and R. Grosse. 2009. SCAI acts as a suppressor of cancer cell invasion through the transcriptional control of beta1-integrin. *Nature Cell Biology*. 11:557-568.

Bryant, D., and K. Mostov. 2008. From cells to organs: building polarized tissue. *Nature Reviews. Molecular Cell Biology*. 9:887-901.

Cen, B., A. Selvaraj, R. Burgess, J. Hitzler, Z. Ma, S. Morris, and R. Prywes. 2003. Megakaryoblastic leukemia 1, a potent transcriptional coactivator for serum response factor (SRF), is required for serum induction of SRF target genes. *Molecular and Cellular Biology*. 23:6597-6608.

Cen, B., A. Selvaraj, and R. Prywes. 2004. Myocardin/MKL family of SRF coactivators: key regulators of immediate early and muscle specific gene expression. *Journal of Cellular Biochemistry*. 93:74-82.

Charbonney, E., P. Speight, A. Masszi, H. Nakano, and A. Kapus. 2011. β-catenin and Smad3 regulate the activity and stability of myocardin-related transcription factor during epithelial-myofibroblast transition. *Molecular Biology of the Cell*. 22:4472-4485.

Chen, C., and R. Schwartz. 1996. Recruitment of the tinman homolog Nkx-2.5 by serum response factor activates cardiac alpha-actin gene transcription. *Molecular and Cellular Biology*. 16:6372-6384.

Cheng, E.-C., Q. Luo, E. Bruscia, M. Renda, J. Troy, S. Massaro, D. Tuck, V. Schulz, S. Mane, N. Berliner, Y. Sun, S. Morris, C. Qiu, and D. Krause. 2009. Role for MKL1 in megakaryocytic maturation. *Blood*. 113:2826-2834.

Chiquet, M., L. Gelman, R. Lutz, and S. Maier. 2009. From mechanotransduction to extracellular matrix gene expression in fibroblasts. *Biochimica et Biophysica Acta*. 1793:911-920.

Cook, D., and P. Genever. 2013. Regulation of mesenchymal stem cell differentiation. *Advances in Experimental Medicine and Biology*. 786:213-229.

Cordes, K., N. Sheehy, M. White, E. Berry, S. Morton, A. Muth, T.-H. Lee, J. Miano, K. Ivey, and D. Srivastava. 2009. miR-145 and miR-143 regulate smooth muscle cell fate and plasticity. *Nature*. 460:705-710.

Creemers, E., L. Sutherland, J. McAnally, J. Richardson, and E. Olson. 2006a. Myocardin is a direct transcriptional target of Mef2, Tead and Foxo proteins during cardiovascular development. *Development (Cambridge, England)*. 133:4245-4256.

Creemers, E., L. Sutherland, J. Oh, A. Barbosa, and E. Olson. 2006b. Coactivation of MEF2 by the SAP domain proteins myocardin and MASTR. *Molecular Cell*. 23:83-96.

De Wever, O., P. Demetter, M. Mareel, and M. Bracke. 2008. Stromal myofibroblasts are drivers of invasive cancer growth. *International journal of cancer. Journal international du cancer*. 123:2229-2238.

Descot, A., M. Rex-Haffner, G. Courtois, D. Bluteau, A. Menssen, T. Mercher, O. Bernard, R. Treisman, and G. Posern. 2008. OTT-MAL is a deregulated activator of serum response factor-dependent gene expression. *Molecular and Cellular Biology*. 28:6171-6181.

Desmoulière, A. 2007. Hepatic stellate cells: the only cells involved in liver fibrogenesis? A dogma challenged. *Gastroenterology*. 132:2059-2062.

Desmoulière, A., A. Geinoz, F. Gabbiani, and G. Gabbiani. 1993. Transforming growth factor-beta 1 induces alpha-smooth muscle actin expression in granulation tissue myofibroblasts and in quiescent and growing cultured fibroblasts. *The Journal of Cell Biology*. 122:103-111.

Direkze, N., K. Hodivala-Dilke, R. Jeffery, T. Hunt, R. Poulsom, D. Oukrif, M. Alison, and N. Wright. 2004. Bone marrow contribution to tumor-associated myofibroblasts and fibroblasts. *Cancer Research*. 64:8492-8495.

Du, K., M. Chen, J. Li, J. Lepore, P. Mericko, and M. Parmacek. 2004. Megakaryoblastic leukemia factor-1 transduces cytoskeletal signals and induces smooth muscle cell differentiation from undifferentiated embryonic stem cells. *The Journal of Biological Chemistry*. 279:17578-17586.

DuFort, C., M. Paszek, and V. Weaver. 2011. Balancing forces: architectural control of mechanotransduction. *Nature Reviews. Molecular Cell Biology*. 12:308-319.

Dupont, S., L. Morsut, M. Aragona, E. Enzo, S. Giulitti, M. Cordenonsi, F. Zanconato, J. Le Digabel, M. Forcato, S. Bicciato, N. Elvassore, and S. Piccolo. 2011. Role of YAP/TAZ in mechanotransduction. *Nature*. 474:179-183.

Dvorak, H. 1986. Tumors: wounds that do not heal. Similarities between tumor stroma generation and wound healing. *The New England Journal of Medicine*. 315:1650-1659.

Elberg, G., L. Chen, D. Elberg, M. Chan, C. Logan, and M. Turman. 2008. MKL1 mediates TGF-beta1-induced alpha-smooth muscle actin expression in human renal epithelial cells. *American Journal of Physiology. Renal Physiology*. 294:28.

Fan, L., A. Sebe, Z. Péterfi, A. Masszi, A. Thirone, O. Rotstein, H. Nakano, C. McCulloch, K. Szászi, I. Mucsi, and A. Kapus. 2007. Cell contact-dependent regulation of epithelial-myofibroblast transition via the rho-rho kinase-phospho-myosin pathway. *Molecular Biology of the Cell*. 18:1083-1097.

Forbes, S., F. Russo, V. Rey, P. Burra, M. Rugge, N. Wright, and M. Alison. 2004. A significant proportion of myofibroblasts are of bone marrow origin in human liver fibrosis. *Gastroenterology*. 126:955-963.

Friedman, S. 2010. Evolving challenges in hepatic fibrosis. *Nature Reviews. Gastroenterology and Hepatology*. 7:425-436.

Gilles, L., D. Bluteau, S. Boukour, Y. Chang, Y. Zhang, T. Robert, P. Dessen, N. Debili, O. Bernard, W. Vainchenker, and H. Raslova. 2009. MAL/SRF complex is involved in platelet formation and megakaryocyte migration by regulating MYL9 (MLC2) and MMP9. *Blood*. 114:4221-4232.

Guettler, S., M. Vartiainen, F. Miralles, B. Larijani, and R. Treisman. 2008. RPEL motifs link the serum response factor cofactor MAL but not myocardin to Rho signaling via actin binding. *Molecular and Cellular Biology*. 28:732-742.

Gupta, M., A. Korol, and J. West-Mays. 2013. Nuclear translocation of myocardin-related transcription factor-A during transforming growth factor beta-induced epithelial to mesenchymal transition of lens epithelial cells. *Molecular Vision*. 19:1017-1028.

Hao, H., G. Gabbiani, E. Camenzind, M. Bacchetta, R. Virmani, and M.-L. Bochaton-Piallat. 2006. Phenotypic modulation of intima and media smooth muscle cells in fatal cases of coronary artery lesion. *Arteriosclerosis, Thrombosis, and Vascular Biology*. 26:326-332.

Higashiyama, R., S. Nakao, Y. Shibusawa, O. Ishikawa, T. Moro, K. Mikami, H. Fukumitsu, Y. Ueda, K. Minakawa, Y. Tabata, G. Bou-Gharios, and Y. Inagaki. 2011. Differential contribution of dermal resident and bone marrow-derived cells to collagen production during wound healing and fibrogenesis in mice. *The Journal of Investigative Dermatology*. 131:529-536.

Hinohara, K., T. Nakajima, M. Yasunami, S. Houda, T. Sasaoka, K. Yamamoto, B.-S. Lee, H. Shibata, Y. Tanaka-Takahashi, M. Takahashi, T. Arimura, A. Sato, T. Naruse, J. Ban, H. Inoko, Y. Yamada, M. Sawabe, J.-E. Park, T. Izumi, and A. Kimura. 2009. Megakaryoblastic leukemia factor-1 gene in the susceptibility to coronary artery disease. *Human Genetics*. 126:539-547.

Hinz, B., S. Phan, V. Thannickal, A. Galli, M.-L. Bochaton-Piallat, and G. Gabbiani. 2007. The myofibroblast: one function, multiple origins. *The American Journal of Pathology*. 170:1807-1816.

Hinz, B., S. Phan, V. Thannickal, M. Prunotto, A. Desmoulière, J. Varga, O. De Wever, M. Mareel, and G. Gabbiani. 2012. Recent developments in myofibroblast biology: paradigms for connective tissue remodeling. *The American Journal of Pathology*. 180:1340-1355.

Hirano, H., and Y. Matsuura. 2011. Sensing actin dynamics: structural basis for G-actin-sensitive nuclear import of MAL. *Biochemical and Biophysical Research Communications*. 414:373-378.

Huang, X., N. Yang, V. Fiore, T. Barker, Y. Sun, S. Morris, Q. Ding, V. Thannickal, and Y. Zhou. 2012. Matrix stiffness-induced myofibroblast differentiation is mediated by intrinsic mechanotransduction. *American Journal of Respiratory Cell and Molecular Biology*. 47:340-348.

Hynes, R. 2009. The extracellular matrix: not just pretty fibrils. *Science (New York, N.Y.)*. 326:1216-1219.

Jahoda, C., and A. Reynolds. 2001. Hair follicle dermal sheath cells: unsung participants in wound healing. *Lancet*. 358:1445-1448.

Jeon, E., S. Heo, I. Lee, Y. Choi, J. Park, K. Choi, D.Y. Park, D. Suh, M. Yoon, and J. Kim. 2010. Ovarian cancer-derived lysophosphatidic acid stimulates secretion of VEGF and stromal cell-derived factor-1 alpha from human mesenchymal stem cells. *Experimental and Molecular Medicine*. 42:280-293.

Jones, D., and A. Wagers. 2008. No place like home: anatomy and function of the stem cell niche. *Nature Reviews. Molecular Cell Biology*. 9:11-21.

Juliano, R. 2009. SCAI blocks MAL-evolent effects on cancer cell invasion. *Nature Cell Biology*. 11:540-542.

Kalluri, R., and R.A. Weinberg. 2009. The basics of epithelial-mesenchymal transition. *The Journal of Clinical Investigation*. 119:1420-1428.

Kalluri, R., and M. Zeisberg. 2006. Fibroblasts in cancer. *Nature Reviews. Cancer*. 6:392-401.

Kumar, A., S. Lnu, R. Malya, D. Barron, J. Moore, D. Corry, and A. Boriek. 2003. Mechanical stretch activates nuclear factor-kappaB, activator protein-1, and mitogen-activated protein kinases in lung parenchyma: implications in asthma. *FASEB journal : official publication of the Federation of American Societies for Experimental Biology*. 17:1800-1811.

Lagna, G., M. Ku, P. Nguyen, N. Neuman, B. Davis, and A. Hata. 2007. Control of phenotypic plasticity of smooth muscle cells by bone morphogenetic protein signaling through the myocardin-related transcription factors. *The Journal of Biological Chemistry*. 282:37244-37255.

Lemmon, M., and J. Schlessinger. 2010. Cell signaling by receptor tyrosine kinases. *Cell*. 141:1117-1134.

Li, J., X. Zhu, M. Chen, L. Cheng, D. Zhou, M. Lu, K. Du, J. Epstein, and M. Parmacek. 2005. Myocardin-related transcription factor B is required in cardiac neural crest for smooth muscle differentiation and cardiovascular development. *Proceedings of the National Academy of Sciences of the United States of America*. 102:8916-8921.

Li, S., S. Chang, X. Qi, J. Richardson, and E. Olson. 2006. Requirement of a myocardin-related transcription factor for development of mammary myoepithelial cells. *Molecular and Cellular Biology*. 26:5797-5808.

Li, S., D.-Z. Wang, Z. Wang, J. Richardson, and E. Olson. 2003. The serum response factor coactivator myocardin is required for vascular smooth muscle development. *Proceedings of the National Academy of Sciences of the United States of America*. 100:9366-9370.

Li, Z., and S. Jimenez. 2011. Protein kinase Cδ and c-Abl kinase are required for transforming growth factor β induction of endothelial-mesenchymal transition in vitro. *Arthritis and Rheumatism*. 63:2473-2483.

Liu, N., S. Bezprozvannaya, A. Williams, X. Qi, J. Richardson, R. Bassel-Duby, and E. Olson. 2008. microRNA-133a regulates cardiomyocyte proliferation and suppresses smooth muscle gene expression in the heart. *Genes and Development*. 22:3242-3254.

Lu, P., K. Takai, V. Weaver, and Z. Werb. 2011. Extracellular matrix degradation and remodeling in development and disease. *Cold Spring Harbor Perspectives in Biology*. 3.

Ma, Z., S. Morris, V. Valentine, M. Li, J. Herbrick, X. Cui, D. Bouman, Y. Li, P. Mehta, D. Nizetic, Y. Kaneko, G. Chan, L. Chan, J. Squire, S. Scherer, and J. Hitzler. 2001. Fusion of two novel genes, RBM15 and MKL1, in the t(1;22)(p13;q13) of acute megakaryoblastic leukemia. *Nature Genetics*. 28:220-221.

Maier, S., R. Lutz, L. Gelman, A. Sarasa-Renedo, S. Schenk, C. Grashoff, and M. Chiquet. 2008. Tenascin-C induction by cyclic strain requires integrin-linked kinase. *Biochimica et Biophysica Acta*. 1783:1150-1162.

Masszi, A., P. Speight, E. Charbonney, M. Lodyga, H. Nakano, K. Szászi, and A. Kapus. 2010. Fate-determining mechanisms in epithelial-myofibroblast transition: major inhibitory role for Smad3. *The Journal of Cell Biology*. 188:383-399.

Mayer, D., and L. Leinwand. 1997. Sarcomeric gene expression and contractility in myofibroblasts. *The Journal of Cell Biology*. 139:1477-1484.

Mercher, T., M. Coniat, R. Monni, M. Mauchauffe, F. Nguyen Khac, L. Gressin, F. Mugneret, T. Leblanc, N. Dastugue, R. Berger, and O. Bernard. 2001. Involvement of a human gene related to the Drosophila spen gene in the recurrent t(1;22) translocation of acute megakaryocytic leukemia. *Proceedings of the National Academy of Sciences of the United States of America*. 98:5776-5779.

Miano, J., X. Long, and K. Fujiwara. 2007. Serum response factor: master regulator of the actin cytoskeleton and contractile apparatus. *American Journal of Physiology. Cell Physiology*. 292:81.

Miano, J., N. Ramanan, M. Georger, K. de Mesy Bentley, R. Emerson, R. Balza, Q. Xiao, H. Weiler, D. Ginty, and R. Misra. 2004. Restricted inactivation of serum response factor to the cardiovascular system. *Proceedings of the National Academy of Sciences of the United States of America*. 101:17132-17137.

Mihira, H., H. Suzuki, Y. Akatsu, Y. Yoshimatsu, T. Igarashi, K. Miyazono, and T. Watabe. 2012. TGF-β-induced mesenchymal transition of MS-1 endothelial cells requires Smad-dependent cooperative activation of Rho signals and MRTF-A. *Journal of Biochemistry*. 151:145-156.

Minami, T., K. Kuwahara, Y. Nakagawa, M. Takaoka, H. Kinoshita, K. Nakao, Y. Kuwabara, Y. Yamada, C. Yamada, J. Shibata, S. Usami, S. Yasuno, T. Nishikimi, K. Ueshima, M. Sata, H. Nakano, T. Seno, Y. Kawahito, K. Sobue, A. Kimura, R. Nagai, and K. Nakao. 2012. Reciprocal expression of MRTF-A and myocardin is crucial for pathological vascular remodelling in mice. *The EMBO Journal*. 31:4428-4440.

Miralles, F., G. Posern, A.-I. Zaromytidou, and R. Treisman. 2003. Actin dynamics control SRF activity by regulation of its coactivator MAL. *Cell*. 113:329-342.

Morita, T., T. Mayanagi, and K. Sobue. 2007. Dual roles of myocardin-related transcription factors in epithelial mesenchymal transition via slug induction and actin remodeling. *The Journal of Cell Biology*. 179:1027-1042.

Mouilleron, S., C. Langer, S. Guettler, N. McDonald, and R. Treisman. 2011. Structure of a pentavalent G-actin*MRTF-A complex reveals how G-actin controls nucleocytoplasmic shuttling of a transcriptional coactivator. *Science Signaling*. 4.

Muehlich, S., R. Wang, S.-M. Lee, T. Lewis, C. Dai, and R. Prywes. 2008. Serum-induced phosphorylation of the serum response factor coactivator MKL1 by the extracellular signal-regulated kinase 1/2 pathway inhibits its nuclear localization. *Molecular and Cellular Biology*. 28:6302-6313.

Niu, Z., W. Yu, S. Zhang, M. Barron, N. Belaguli, M. Schneider, M. Parmacek, A. Nordheim, and R. Schwartz. 2005. Conditional mutagenesis of the murine serum response factor gene blocks cardiogenesis and the transcription of downstream gene targets. *The Journal of Biological Chemistry*. 280:32531-32538.

Nombela-Arrieta, C., J. Ritz, and L. Silberstein. 2011. The elusive nature and function of mesenchymal stem cells. *Nature Reviews. Molecular Cell Biology*. 12:126-131.

Norman, C., M. Runswick, R. Pollock, and R. Treisman. 1988. Isolation and properties of cDNA clones encoding SRF, a transcription factor that binds to the c-fos serum response element. *Cell*. 55:989-1003.

Oh, J., J. Richardson, and E. Olson. 2005. Requirement of myocardin-related transcription factor-B for remodeling of branchial arch arteries and smooth muscle

differentiation. *Proceedings of the National Academy of Sciences of the United States of America*. 102:15122-15127.

Olson, E., and A. Nordheim. 2010. Linking actin dynamics and gene transcription to drive cellular motile functions. *Nature Reviews. Molecular Cell Biology*. 11:353-365.

Otranto, M., V. Sarrazy, F. Bonté, B. Hinz, G. Gabbiani, and A. Desmoulière. 2012. The role of the myofibroblast in tumor stroma remodeling. *Cell adhesion & migration*. 6:203-219.

Owens, G., M. Kumar, and B. Wamhoff. 2004. Molecular regulation of vascular smooth muscle cell differentiation in development and disease. *Physiological Reviews*. 84:767-801.

Parlakian, A., D. Tuil, G. Hamard, G. Tavernier, D. Hentzen, J.-P. Concordet, D. Paulin, Z. Li, and D. Daegelen. 2004. Targeted inactivation of serum response factor in the developing heart results in myocardial defects and embryonic lethality. *Molecular and Cellular Biology*. 24:5281-5289.

Parmacek, M. 2007. Myocardin-related transcription factors: critical coactivators regulating cardiovascular development and adaptation. *Circulation Research*. 100:633-644.

Pawłowski, R., E. Rajakylä, M. Vartiainen, and R. Treisman. 2010. An actin-regulated importin α/β-dependent extended bipartite NLS directs nuclear import of MRTF-A. *The EMBO Journal*. 29:3448-3458.

Philippar, U., G. Schratt, C. Dieterich, J. Müller, P. Galgóczy, F. Engel, M. Keating, F. Gertler, R. Schüle, M. Vingron, and A. Nordheim. 2004. The SRF target gene Fhl2 antagonizes RhoA/MAL-dependent activation of SRF. *Molecular Cell*. 16:867-880.

Pipes, G., E. Creemers, and E. Olson. 2006. The myocardin family of transcriptional coactivators: versatile regulators of cell growth, migration, and myogenesis. *Genes and Development*. 20:1545-1556.

Posern, G., and R. Treisman. 2006. Actin' together: serum response factor, its cofactors and the link to signal transduction. *Trends in Cell Biology*. 16:588-596.

Potenta, S., E. Zeisberg, and R. Kalluri. 2008. The role of endothelial-to-mesenchymal transition in cancer progression. *British Journal of Cancer*. 99:1375-1379.

Rajkumar, V., K. Howell, K. Csiszar, C. Denton, C. Black, and D. Abraham. 2005. Shared expression of phenotypic markers in systemic sclerosis indicates a convergence of pericytes and fibroblasts to a myofibroblast lineage in fibrosis. *Arthritis Research and Therapy*. 7:23.

Rajkumar, V., X. Shiwen, M. Bostrom, P. Leoni, J. Muddle, M. Ivarsson, B. Gerdin, C. Denton, G. Bou-Gharios, C. Black, and D. Abraham. 2006. Platelet-derived growth factor-beta receptor activation is essential for fibroblast and pericyte recruitment during cutaneous wound healing. *The American Journal of Pathology*. 169:2254-2265.

Ramanan, N., Y. Shen, S. Sarsfield, T. Lemberger, G. Schütz, D. Linden, and D. Ginty. 2005. SRF mediates activity-induced gene expression and synaptic plasticity but not neuronal viability. *Nature Neuroscience*. 8:759-767.

Sandbo, N., A. Lau, J. Kach, C. Ngam, D. Yau, and N. Dulin. 2011. Delayed stress fiber formation mediates pulmonary myofibroblast differentiation in response to TGF-β. *American Journal of Physiology. Lung Cellular and Molecular Physiology*. 301:66.

Sappino, A., O. Skalli, B. Jackson, W. Schürch, and G. Gabbiani. 1988. Smooth-muscle differentiation in stromal cells of malignant and non-malignant breast tissues. *International journal of cancer. Journal international du cancer*. 41:707-712.

Sarrazy, V., F. Billet, L. Micallef, B. Coulomb, and A. Desmoulière. 2011. Mechanisms of pathological scarring: role of myofibroblasts and current developments. *Wound repair and regeneration : official publication of the Wound Healing Society [and] the European Tissue Repair Society*. 19 Suppl 1:5.

Sasazuki, T., T. Sawada, S. Sakon, T. Kitamura, T. Kishi, T. Okazaki, M. Katano, M. Tanaka, M. Watanabe, H. Yagita, K. Okumura, and H. Nakano. 2002. Identification of a novel transcriptional activator, BSAC, by a functional cloning to inhibit tumor necrosis factor-induced cell death. *The Journal of Biological Chemistry*. 277:28853-28860.

Schratt, G., U. Philippar, J. Berger, H. Schwarz, O. Heidenreich, and A. Nordheim. 2002. Serum response factor is crucial for actin cytoskeletal organization and focal adhesion assembly in embryonic stem cells. *The Journal of Cell Biology*. 156:737-750.

Schröter, H., P. Shaw, and A. Nordheim. 1987. Purification of intercalator-released p67, a polypeptide that interacts specifically with the c-fos serum response element. *Nucleic Acids Research*. 15:10145-10158.

Selvaraj, A., and R. Prywes. 2003. Megakaryoblastic leukemia-1/2, a transcriptional co-activator of serum response factor, is required for skeletal myogenic differentiation. *The Journal of Biological Chemistry*. 278:41977-41987.

Selvaraj, A., and R. Prywes. 2004. Expression profiling of serum inducible genes identifies a subset of SRF target genes that are MKL dependent. *BMC molecular biology*. 5:13.

Siletz, A., E. Kniazeva, J. Jeruss, and L. Shea. 2013. Transcription factor networks in invasion-promoting breast carcinoma-associated fibroblasts. *Cancer microenvironment : official journal of the International Cancer Microenvironment Society*. 6:91-107.

Small, E., J. Thatcher, L. Sutherland, H. Kinoshita, R. Gerard, J. Richardson, J. Dimaio, H. Sadek, K. Kuwahara, and E. Olson. 2010. Myocardin-related transcription factor-a controls myofibroblast activation and fibrosis in response to myocardial infarction. *Circulation Research*. 107:294-304.

Smith, E., A. Teixeira, R. Chen, L. Wang, Y. Gao, K. Hahn, and D. Krause. 2013. Induction of megakaryocyte differentiation drives nuclear accumulation and transcriptional function of MKL1 via actin polymerization and RhoA activation. *Blood*. 121:1094-1101.

Sugimoto, H., T. Mundel, M. Kieran, and R. Kalluri. 2006. Identification of fibroblast heterogeneity in the tumor microenvironment. *Cancer Biology and Therapy*. 5:1640-1646.

Sun, Q., G. Chen, J. Streb, X. Long, Y. Yang, C. Stoeckert, and J. Miano. 2006a. Defining the mammalian CArGome. *Genome Research*. 16:197-207.

Sun, Y., K. Boyd, W. Xu, J. Ma, C. Jackson, A. Fu, J. Shillingford, G. Robinson, L. Hennighausen, J. Hitzler, Z. Ma, and S. Morris. 2006b. Acute myeloid leukemia-associated Mkl1 (Mrtf-a) is a key regulator of mammary gland function. *Molecular and Cellular Biology*. 26:5809-5826.

Tomasek, J., G. Gabbiani, B. Hinz, C. Chaponnier, and R. Brown. 2002. Myofibroblasts and mechano-regulation of connective tissue remodelling. *Nature Reviews. Molecular Cell Biology*. 3:349-363.

Treisman, R. 1986. Identification of a protein-binding site that mediates transcriptional response of the c-fos gene to serum factors. *Cell*. 46:567-574.

Treisman, R. 1987. Identification and purification of a polypeptide that binds to the c-fos serum response element. *The EMBO Journal*. 6:2711-2717.

van den Bogaerdt, A., V. van der Veen, P. van Zuijlen, L. Reijnen, M. Verkerk, R. Bank, E. Middelkoop, and M. Ulrich. 2009. Collagen cross-linking by adipose-derived mesenchymal stromal cells and scar-derived mesenchymal cells: Are mesenchymal stromal cells involved in scar formation? *Wound repair and regeneration : official publication of the Wound Healing Society [and] the European Tissue Repair Society*. 17:548-558.

van den Borne, S., J. Diez, W. Blankesteijn, J. Verjans, L. Hofstra, and J. Narula. 2010. Myocardial remodeling after infarction: the role of myofibroblasts. *Nature Reviews. Cardiology*. 7:30-37.

Vartiainen, M., S. Guettler, B. Larijani, and R. Treisman. 2007. Nuclear actin regulates dynamic subcellular localization and activity of the SRF cofactor MAL. *Science (New York, N.Y.)*. 316:1749-1752.

Wang, D., P. Chang, Z. Wang, L. Sutherland, J. Richardson, E. Small, P. Krieg, and E. Olson. 2001. Activation of cardiac gene expression by myocardin, a transcriptional cofactor for serum response factor. *Cell*. 105:851-862.

Wang, D.-Z., S. Li, D. Hockemeyer, L. Sutherland, Z. Wang, G. Schratt, J. Richardson, A. Nordheim, and E. Olson. 2002. Potentiation of serum response factor activity by a family of myocardin-related transcription factors. *Proceedings of the National Academy of Sciences of the United States of America*. 99:14855-14860.

Wang, Z., D.-Z. Wang, D. Hockemeyer, J. McAnally, A. Nordheim, and E. Olson. 2004. Myocardin and ternary complex factors compete for SRF to control smooth muscle gene expression. *Nature*. 428:185-189.

Weinhold, B., G. Schratt, S. Arsenian, J. Berger, K. Kamino, H. Schwarz, U. Rüther, and A. Nordheim. 2000. Srf(-/-) ES cells display non-cell-autonomous impairment in mesodermal differentiation. *The EMBO Journal*. 19:5835-5844.

Wolfe, J. 1976. Risk for breast cancer development determined by mammographic parenchymal pattern. *Cancer*. 37:2486-2492.

Yang, L., P. Scott, C. Dodd, A. Medina, H. Jiao, H. Shankowsky, A. Ghahary, and E. Tredget. 2005. Identification of fibrocytes in postburn hypertrophic scar. *Wound repair and regeneration : official publication of the Wound Healing Society [and] the European Tissue Repair Society*. 13:398-404.

Zaromytidou, A.-I., F. Miralles, and R. Treisman. 2006. MAL and ternary complex factor use different mechanisms to contact a common surface on the serum response factor DNA-binding domain. *Molecular and Cellular Biology*. 26:4134-4148.

Zhang, S., E. Garcia-Gras, D. Wycuff, S. Marriot, N. Kadeer, W. Yu, E. Olson, D. Garry, M. Parmacek, and R. Schwartz. 2005. Identification of direct serum-response factor gene targets during Me2SO-induced P19 cardiac cell differentiation. *The Journal of Biological Chemistry*. 280:19115-19126.

Zhao, X.-H., C. Laschinger, P. Arora, K. Szászi, A. Kapus, and C. McCulloch. 2007. Force activates smooth muscle alpha-actin promoter activity through the Rho signaling pathway. *Journal of Cell Science*. 120:1801-1809.

Zhao, Y., E. Samal, and D. Srivastava. 2005. Serum response factor regulates a muscle-specific microRNA that targets Hand2 during cardiogenesis. *Nature*. 436:214-220.

Zhou, Y., X. Huang, L. Hecker, D. Kurundkar, A. Kurundkar, H. Liu, T.-H. Jin, L. Desai, K. Bernard, and V. Thannickal. 2013. Inhibition of mechanosensitive signaling in

myofibroblasts ameliorates experimental pulmonary fibrosis. *The Journal of Clinical Investigation*. 123:1096-1108.

Zolotukhin, A., H. Uranishi, S. Lindtner, J. Bear, G. Pavlakis, and B. Felber. 2009. Nuclear export factor RBM15 facilitates the access of DBP5 to mRNA. *Nucleic Acids Research*. 37:7151-7162.

Results

Manuscript I

TGF-β-induced differentiation into myofibroblasts involves specific regulation of two MKL1 isoforms.

Results

Manuscript I

TGF-β-induced differentiation into myofibroblasts involves specific regulation of two MKL1 isoforms.

Matthias A. Scharenberg[1,2], Benjamin E. Pippenger[3], Ragna Sack[1], Dominik Zingg[1], Susanne Schenk[4], Jacqueline Ferralli[1], Ivan Martin[2], Ruth Chiquet-Ehrismann[1,2,*]

[1] Friedrich Miescher Institute for Biomedical Research, Department of Mechanisms of Cancer, Maulbeerstrasse 66, CH-4058, Basel, Switzerland

[2] University of Basel, Faculty of Sciences, CH-4056, Basel, Switzerland

[3] University Hospital Basel, Departments of Surgery and Biomedicine, Hebelstrasse 20, CH-4031, Basel, Switzerland

[4] Pharmazentrum Basel, Division of Pharmaceutical Technology, Klingelbergstrasse 50, CH-4056 Basel, Switzerland

* Corresponding author:
Friedrich Miescher Institute for Biomedical Research, Maulbeerstrasse 66, CH-4058 Basel, Switzerland; e-mail: ruth.chiquet@fmi.ch
telephone: +41 (0)61 697 24 94; fax: +41 (0)61 697 39 76

Abstract

Cellular transformation into myofibroblasts is a central physiological process enabling tissue repair. Its deregulation promotes fibrosis and carcinogenesis. TGF-β is the main inducer of the contractile gene program that drives myofibroblast/cancer-associated fibroblast differentiation from various precursor cell types. Crucial regulators of this transcriptional program are SRF and its cofactor MKL1/MRTF-A. However, the exact mechanism of the crosstalk between TGF-β signaling and MKL1 remains unclear. Here, we report the discovery of a novel MKL1 variant/isoform, MKL1_S, being transcribed from an alternative promoter and uncover a novel translation start of the published human isoform, MKL1_L. Using a human adipose-derived mesenchymal stem cell differentiation model, we show that TGF-β specifically up-regulates MKL1_S during the initial phase of myofibroblast/CAF differentiation. We identified a functional N-terminal motif in MKL1_S that allows specific induction of a group of genes including ECM modifiers MMP-16 and SPOCK3/testican-3. We propose that TGF-β-mediated induction of MKL1_S initiates progression to later stages of differentiation towards a stationary myofibroblast.

Abbreviations

9aa	TAD 9-amino acid transactivation domain
CAF	cancer-associated (myo-)fibroblast
hASC	adipose tissue-derived mesenchymal stem cell
LPA	lysophosphatidic acid
MKL1	megakaryoblastic leukemia 1
MMP	matrix metalloproteinase
pPCR	quantitative RT-PCR
SMA	smooth muscle α-actin
SPC	sphingosylphosphorylcholine
SRF	serum response factor
SVF	stromal vascular fraction

Introduction

Differentiation of a variety of cell types into myofibroblasts defines a major physiological process that facilitates wound healing and tissue repair. Tissue damage leads to the formation of a blood clot and the release of soluble mediators. This drives the transformation of diverse quiescent tissue-resident cells or invading circulating cells into a mesenchymal proliferative-migratory phenotype (termed proto-myofibroblast) involving the formation of smooth muscle α-actin (SMA)-negative stress fibers. Different cellular precursors have been described, including locally residing fibroblasts (Ross et al., 1970), epithelial cells (Iwano et al., 2002), endothelial cells (Frid et al., 2002), pericytes (Rajkumar et al., 2005), hepatic stellate cells (Gressner and Weiskirchen, 2006), smooth muscle cells (Hao et al., 2006), and mesenchymal stem/multipotent stromal cells (MSCs) (van den Bogaerdt et al., 2009), as well as circulating bone marrow-derived MSCs (Forbes et al., 2004) and fibrocytes (Abe et al., 2001). Proto-myofibroblasts are able to expand towards the wound and differentiate into a contractile phenotype with characteristic SMA-positive stress fibers, then known as a "myofibroblast" or "activated fibroblast". This specialized cell type that shares characteristics with a fibroblast and a smooth muscle cell mediates mechanical force generation and contraction of the wound (Desmoulière et al., 1993; Mayer and Leinwand, 1997). Furthermore, it produces large amounts of extracellular matrix (ECM) proteins, such as type I collagen, fibronectin, tenascin-C, and matrix metalloproteinases (MMPs), contributing to the replacement of the granulation tissue and the scarring of the wound (Sarrazy et al., 2011). Deregulation of this dynamic differentiation process inevitably leads to pathological situations. Organ fibrosis and fibrotic scarring arise from excessive extracellular matrix deposition by persistent myofibroblasts, which can occur after tissue damage, but also in the context of chronic inflammation and ageing. It causes functional impairment of many organs and therefore constitutes a major health problem.

Similarly to wounds, the "reactive stroma" of solid tumors can be considered as fibrotic tissue, and is stiffer than normal tissue. Cancer was therefore described as "a wound that does not heal" (Dvorak, 1986). In the tumor setting, cancer-associated (myo-)fibroblasts (CAFs) accumulate in the tumor stroma and promote tumor progression (Barsky et al., 1984; Sugimoto et al., 2006). All myofibroblast precursor cell types mentioned above

similarly apply as putative sources for CAFs (Otranto et al., 2012). In both tissue repair and tumorigenesis, TGF-β represents the prototypic inducer of myofibroblast/CAF differentiation from all precursor cell types. Therefore, interfering with TGF-β signaling currently poses one of the main therapeutic approaches for fibrosis and cancer (Hinz et al., 2012). TGF-β can be mechanically released from the ECM, as in the case of myofibroblast-mediated stiffening of the stroma (Wipff et al., 2007), and is secreted by platelets, immune cells, and tumor cells (Jotzu et al., 2011). The Rho-actin-MKL1-SRF and Smad signaling pathways were identified as major drivers to elicit the contractile gene expression program. Key regulators of these pathways are the transcription factors megakaryoblastic leukemia 1 (MKL1)/myocardin-related transcription factor-A (MRTF-A) and Smad3, respectively (Charbonney et al., 2011; Crider et al., 2011; Small, 2012). Rho-dependent association of serum response factor (SRF) with members of the MRTF family has recently been described as a mechano- and growth factor-sensitive pathway that regulates expression of many cytoskeletal, ECM, and contractile proteins (Wang et al., 2001; Wang et al., 2002). Its activity is directly dependent on the polymerization status of the actin cytoskeleton. In quiescent cells, binding to G-actin renders MKL1 inactive, keeping it mainly in the cytosol. Rearrangement of the actin cytoskeleton in response to stimulation from the extracellular environment depletes G-actin and liberates MKL1, which can accumulate in the nucleus to activate SRF transcription (Miralles et al., 2003).

Here we characterized human MKL1 in different cell types and tissues and discovered that two human MKL1 mRNAs are transcribed from alternative promoters. This results in two isoforms that differ in their N-terminal domains as well as in their functions. We identified the specific induction of a group of genes, including the ECM regulators MMP-16 and SPOCK3/testican-3, by the shorter MKL1_S isoform. Furthermore, using a human adipose tissue-derived stem cell (hASC)-based myofibroblast/CAF differentiation model, we found the MKL1_S isoform to be strongly up-regulated during the initial phase of TGF-β-induced differentiation, suggesting a specific function of its target genes in subsequent steps of differentiation.

Materials and methods

MKL1 plasmid constructs and expression of recombinant MKL1 variants

The published human MKL1 cDNA (NM_020831) was amplified from total RNA from fetal human brain (ams Biotechnology) and cloned into the pcDNA3.1 expression vector (Life Technologies). This sequence comprising the full 5'UTR region ends at the published stop codon at nucleotide position 3388 of NM_020831 and was termed 5'UTR-full length MKL1_L. From this, ΔN-MKL1 was designed starting with the published ATG translation initiation codon at position 593 of NM_020831. For MKL1_S, the 5'UTR sequence was amplified by 5'RACE experiments on total RNA from fetal (male, 24 weeks of age) and adult (male, 24 years of age) human brain (ams Biotechnology) using the 5'/3' RACE kit, 2nd generation (Roche) according to the manufacturer's instructions. Reverse MKL1-specific primers SP1, SP2, SP3 were designed to anneal to the published human MKL1 mRNA downstream of the published ATG translation start (see Supplemental Table S1). Nucleotide sequencing of the purified amplification products was performed after cloning the fragments into the pBluescript II KS vector (Agilent Technologies) and transformation into competent XL-10 Gold bacteria. The MKL1_S 5'UTR (see Supplemental Fig. 1S) was appended in front of the ΔN-full length MKL1 construct using an overlapping PCR strategy (construct 5'UTR-full length MKL1_S). All ΔC constructs finish after the N-terminal half of the published human MKL1 sequence at nucleotide position 1984 of NM_020831. For MKL1_L_S fusion, the corresponding 5'UTR sequence of MKL1_L (containing the suggested translation start at GTG/Val-100) was engineered in front of the MKL1_S isoform-coding sequence starting with the first in-frame ATG. In the MKL1_S 9aa_L and the MKL1_L 9aa_S constructs the predicted 9aa TAD in MKL1_S (MAVQSVLQL) was exchanged with the corresponding sequence of MKL1_L (SERKNVLQL) or vice versa. For MKL1_S 9aa mut, the predicted 9aa TAD was mutated to KRGHSVLQL, a sequence that does not meet several of the criteria for 9aa TADs (Piskacek et al., 2007). Site-directed mutagenesis was performed as described in (Zheng et al., 2004). For the expression of recombinant MKL1 variants, HEK293 cells (EcR293 variant, Life Technologies/Invitrogen) were cultured at 37 °C and 6 % CO_2 in Dulbecco's Modified Eagle Medium (D-MEM; Seromed) containing 10 % fetal calf serum (FCS; Life Technologies/Gibco). Cells were transfected using jetPEI™ (Polyplus-transfection SA). To generate HEK293 cells stably

overexpressing MKL1 variants, cells were selected with 800 µg/ml G-418 (Roche) and pooled clones were cultured with 200 µg/ml G-418.

Antibodies and immunoblotting

Monoclonal antibodies against a) human MKL1 total (recognizing both MKL1_L and MKL1_S), and b) human MKL1_S were generated as described previously (Maier et al., 2008). For the former, referred to as "anti-MKL1 total mAb", three Balb-c mice were immunized with a 6x His-tagged 19.5 kDa peptide comprising the amino acids 215-395 of human MKL1 (NP_065882.1, NM_020831.3) expressed in E. coli and purified by using ProBond nickel-chelating resin beads (Life Technologies/Invitrogen). For the latter, referred to as "anti-MKL1_S mAb", two Wistar rats were immunized with a peptide comprising the 15 amino acids that are unique for human MKL1_S (MTLLEPEMLMMAVQS) and a single C-terminal cysteine residue for conjugation to a carrier molecule. The peptide was synthesized by EnoGene Biotech Co., Ltd. Monoclonal antibodies were purified from cell culture supernatants of positive hybridoma clones via ProteinG-Sepharose 4 Fast Flow (GE Healthcare) following the manufacturer's instructions. Polyclonal antibodies against human MKL1 total ("anti-MKL1 total pAb") were generated at Harlan Laboratories Ltd. Here, two New Zealand White rabbits were immunized with the same peptide as for the "anti-MKL1 total mAb". Anti-β-tubulin was from Sigma Aldrich. For immunoblotting whole cell extracts or purified protein solutions in Laemmli buffer/100 mM dithiothreitol (DTT) were separated on NuPAGE 4-12 % Bis-Tris gels (Life Technologies/Invitrogen) and transferred to a BioTrace PVDF membrane (PALL LifeSciences). After blocking with 50 % Odyssey Blocking Buffer (LI-COR Biosciences) in PBS/0.1 % Tween, primary antibodies were applied overnight at 4 °C. Secondary antibodies were applied for 1.5 h at room temperature (RT). Goat AlexaFluor 680 secondary antibodies against mouse or rat (Molecular Probes/Life Technologies) and donkey anti-rabbit IRDye 800 (Rockland) were used for visualization with the Odyssey Imaging System (LI-COR Biosciences).

Affinity purification of MKL1 and Mass Spectrometry

Purified mAb were coupled to $CNBr^-$-activated Sepharose beads 4B (GE Healthcare) according to the manufacturer's instructions and the beads were poured into a

purification column. The column was washed with 3 cycles of elution buffer (0.2 M Glycine-HCl, pH3) and loading buffer (TST buffer = 50 mM Tris, pH7.6; 150 mM NaCl; 0.05 % Tween20). Whole cell extracts were prepared in lysis buffer (50 mM Hepes, pH 7.5; 140 mM NaCl; 1 % Triton X-100; Roche Complete Inhibitor Cocktail) and an equal volume of loading buffer was added before running the extract over the column overnight at 4°C. After washing, retained proteins were eluted in elution buffer and neutralized. Protein-containing fractions were pooled, trichloro acetic acid-precipitated, and resuspended in Laemmli buffer/100 mM DTT. Cysteine residues were alkylated with 200 mM iodoacetamide before separating the proteins via SDS-PAGE. Protein bands were excised, washed with 25 mM NH4HCO3 and twice with 25 mM NH4HCO3/acetonitrile (1:1) for 30 min each at RT, and then digested with 100 ng endoproteinase AspN (Roche) overnight at 37 °C. Peptides were analyzed by liquid chromatography-mass spectrometry (LTQ Orbitrap Velos, Thermo Fisher Scientific).

Cell cultures and qPCR analysis

RCH-ACV Leukemia cells and Epithelial Bladder 5637 cells were obtained from the German Collection of Microorganisms and Cell Cultures. HeLa Cells were obtained from the European Cell Collection Porton Down UK. U343MG, U373, T98G, and LN319 cells were kindly provided by Dr. Brian Hemmings (Friedrich Miescher Institute, Basel, Switzerland). These cell lines were maintained at 37 °C and 6 % CO_2 in D-MEM containing 10 % FCS. Primary lung fibroblasts and airway smooth muscle cells were established from non-diseased peripheral lung tissue samples obtained from patients undergoing lung resection following approval by the ethics committee (kindly provided by Katrin E. Hostettler-Haack, Clinic of Respiratory Medicine, University Hospital Basel, Switzerland). Primary cells were grown in RPMI 1640 medium (Cambrex Bio Science) supplemented with 10% FCS and 1% MEM-vitamins (Cambrex Bio Science). Total RNA from cultured cells was extracted using the RNeasy and QiaShredder kits (Qiagen). 2 µg of total RNA each was transcribed into cDNA using the High Capacity cDNA ReverseTranscription kit (Life Technologies/Applied Biosystems) with random primers. Relative quantification (ΔΔCt method) or Relative Standard Curve quantification was performed using the SYBR qPCR Supermix W/ROX from Invitrogen/Life Technologies and human GAPDH as internal reference gene. Exon-

spanning primers were designed for each MKL1 isoform and for MKL1 total (see Supplemental Table S1 for primer sequences). Experiments were performed on the StepOnePlus™ Real-Time PCR system (Life Technologies/Applied Biosystems).

Human adipose tissue-derived stem cell (hASC) isolation

Adipose tissue in the form of liposuction was obtained from a healthy donor following informed consent and according to a protocol approved by the local ethical committee (EKBB, Ref. 78/07). The donor was male and younger than 20 years of age. Liposuction samples were digested with 0.075 % collagenase type II (355 U/mg, Worthington) for 60–90 min at 37 °C. After centrifugation at 190 g for 10 min, the lipid-rich layer was discarded and the cellular pellet was washed once with phosphate buffered saline (PBS, Life Technologies/Gibco). Red blood cells were lysed by incubation in ammonium chloride solution following the manufacturer's protocol (Stemcell Technologies). The resulting SVF cells were then resuspended in α-MEM (Life Technologies/Gibco) containing 10 % FCS, 1 mM sodium pyruvate, 10 mM HEPES buffer, 100 U/mL penicillin, 100 µg/mL streptomycin, and 0.29 mg/mL l-glutamate (complete medium, CM) (all from Life Technologies/Gibco). For monolayer expansion, 3.5 x 10^3 cells/cm^2 were seeded onto tissue culture plates, cultured in CM supplemented with 5 ng/mL FGF-2 (R&D Systems), and serially replated when reaching subconfluence. The expanded adipose-derived cells are referred to as hASCs. To verify the presence of a mesenchymal population within the expanded hASCs, cells were detached and phenotypically analyzed for cell surface markers using flow cytofluorometric analysis. Cells were incubated for 30 min with antibodies against the mesenchymal markers CD105 (FITC-conjugated, Serotec), CD90 (FITC-conjugated, BD Bioscience) and CD73 (APC-conjugated, BD Bioscience) and against the endothelial markers CD45, CD31 and CD34 (FITC-, PE- and APC-conjugated, respectively) (all from BD Bioscience). Cells were washed, resuspended in PBS and analyzed by using a FACSCalibur flow cytometer (BD Bioscience). Positive expression was defined as the level of fluorescence greater than 99 % of corresponding control.

hASC differentiation

hASCs between passage numbers 1 and 3 were plated in 6-well culture dishes at a density of 3.5 x 10^3 cells/cm^2, starved the next day for 20 h in serum-free α-MEM, and cultured in serum-free α-MEM substituted with 2 ng/ml human TGF-β1 (R&D Systems), 2 µM sphingosylphosphorylcholine (SPC), or 5 µM Oleoyl-α-lysophosphatidic acid (LPA) (both Sigma-Aldrich) for 24 or 96 h. For differentiation into chondrocytes, hASCs were plated at a density of 1.5 x 10^4 cells/cm^2, starved for 20 h, and cultured in chondrogenic medium (D-MEM supplemented with ITS^{+1} (Sigma-Aldrich), 0.1 mM ascorbic acid 2-phosphate, 1.25 mg/mL human serum albumin, 1x 10^{-7} M dexamethasone, and 10 ng/mL TGF-β1) for 24 or 96 h. For mechanically induced hASC differentiation, hASCs were seeded at a density of 3.5 x 10^3 cells/cm^2 on flexible silicone membranes coated with fibronectin (BioFlex® 6-well culture plates; Flexcell International) as described previously (Chiquet et al., 2004; Maier et al., 2008). Cells were starved for 20 h in serum-free α-MEM before applying 5 % equibiaxial cyclic strain at 1 Hz for 24 h, using a computer-controlled vacuum system (Flexcell FX-4000; Flexcell International). Transcript levels were measured either directly (24 h timepoint), or after 72 h with serum-free α-MEM (96 h timepoint).

Immunofluorescence staining and nuclear translocation assays

HEK293 cells overexpressing MKL1 variants were grown on poly-L-lysine-precoated 4-compartment plastic tissue culture dishes (Greiner Bio-One) and, after starvation in serum-free D-MEM for 20 h, stimulated with 2 µM Cytochalasin D (Calbiochem), 50 µM LPA (Sigma-Aldrich), or 15 % FCS. Cells were then fixed with 4 % paraformaldehyde for 20 min. After permeabilization with 0.1 % Triton X-100 for 5 min, anti-MKL1 total mAb was added for 1.5 h at RT. After washing, goat anti-mouse AlexaFluor 568 (Invitrogen/Life Technologies) was applied for 1.5 h at RT to visualize the MKL1 staining. Coverslips were mounted using ProLong Gold Antifade reagent (Life Technologies/Invitrogen). Fluorescent images were taken with a Zeiss Axioskop linked to a Hamamatsu ORCA-ER camera and controlled by the Zeiss AxioVision software (version 4.7). Adjustments of brightness and contrast were made with Adobe Photoshop (CS4). Overexpressing cells were classified according to their predominant MKL1 localization into “nuclear”, “pancellular”, or “cytosolic”.

Promoter-reporter assays

The pSRE-SEAP vector containing three tandem copies of the CArG box sequence fused to the thymidine kinase (TK) promoter was purchased from Clontech. HEK293 cells grown in 6-well plates were co-transfected with 1 µg of this reporter construct, 1 µg of an MKL1 construct in the pcDNA3.1 vector, and 0.02 µg of the Ready-To-Glow secreted luciferase reporter (Clontech) for normalizing on transfection efficiencies. After transfection, cells were cultured in 0.3 % FCS/D-MEM for 24 h. SEAP activity (using the chemiluminescent SEAP Reporter Gene Assay, Roche) and secreted luciferase activity in the culture medium were determined according to the manufacturers' instructions. Luminescent intensities were measured with the Luminometer Mithras LB940 (Berthold Technologies).

DNA microarray analysis

HEK293 cells constitutively expressing: Condition 1) the empty pcDNA3.1 vector, Condition 2) the 5'UTR-full-length MKL_L construct, or Condition 3) the 5'UTR-full-length MKL_S construct were grown in triplicates until they reached 70 % confluence. Cells were starved for 16 h in D-MEM/0.3 % FCS and treated with 50 µM LPA for 4 h. Total RNA was extracted using the RNeasy and QiaShredder kits (Qiagen). RNA was converted into labeled sense-strand cDNA with the Ambion WT expression kit (Life Technologies) and hybridized to Affymetrix Human Gene 1.0 arrays (Affymetrix) with a hybridization time of 16 h. Raw data were normalized using rma as implemented in the Biodonductor 2.15 package *affy*. Differentially expressed genes with a minimum average expression value of 4.0 ($\log_2$) were identified using the empirical Bayes method (*F* test) implemented in the *limma* package from Bioconductor. Contrasts were calculated for Condition 2) vs. Condition 1), Condition 3) vs. Condition 1), and Condition 3) vs. Condition 2) with a non-adjusted *P*-value threshold of 0.001 (with Benjamini-Hochberg false discovery correction) and a minimum absolute linear fold change difference of 1.5.

Statistical analysis

Data are represented as stated in the Figure legends. t-tests were used for comparing 2 groups and 1-way ANOVA (Holm-Sidak method) when comparing several groups.

Statistical analysis was performed using SigmaPlot for Windows Version 12.0. Stars indicate statistical significance with * P <0.05. ** P <0.01; *** P <0.001; n. s., not significant.

Results

Translation of the published human MKL1 mRNA starts at an upstream GTG start.

Common protein databases at the time of submission of this article listed human MKL1 (Q969V6; NP_065882.1; CAG30408.1) as a 931-amino acid protein with translation starting at the first ATG start codon. This protein would contain only two actin-binding RPEL motifs, despite a third highly conserved RPEL motif being encoded within the 5' untranslated region (5'UTR; Fig. 1A). Therefore, Miralles and colleagues (Miralles et al., 2003) suggested for an orthologous mouse MKL1 transcript that translation starts at CTG/Leu-92 or shortly upstream of it, embedding the RPEL1 motif within the coding sequence (Fig. 1A). Since then, publications were either based on this CTG/Leu-92 or the published ATG/Met translation start to study the function of human MKL1. To identify the actual translation start of the human protein, we expressed a human cDNA construct comprising the full 5'UTR and the sequence coding for the N-terminal half of the published MKL1 protein (5'UTR-ΔC) in HEK293 cells and compared its size to the corresponding construct starting at the published ATG (ATG-ΔC). As suspected, only a minor product was found to co-migrate with ATG-ΔC and the main translation product migrated less, indicating an upstream translation start (Fig. 1B). To identify its exact position, we purified MKL1 that was translated in HEK293 cells from a 5'UTR-full length MKL1 construct by antibody affinity chromatography. Using endoproteinase AspN cleavage and detection of peptides by LC-MS, we achieved a full coverage of the in-frame translated 5'UTR of MKL1. The most N-terminal sequence that we identified is preceded by a putative GTG start codon, which would normally code for a valine at position -100 of the published ATG/Met start (Fig. 1A). Since cleavage of the initiating amino acid is a common mechanism, this GTG was considered as the candidate start codon. By aligning the human 5'UTR nucleotide sequence to that from other species, this GTG codon depicts the most upstream putative start codon that is conserved in mouse and Xenopus MKL1 (Fig. 1C).

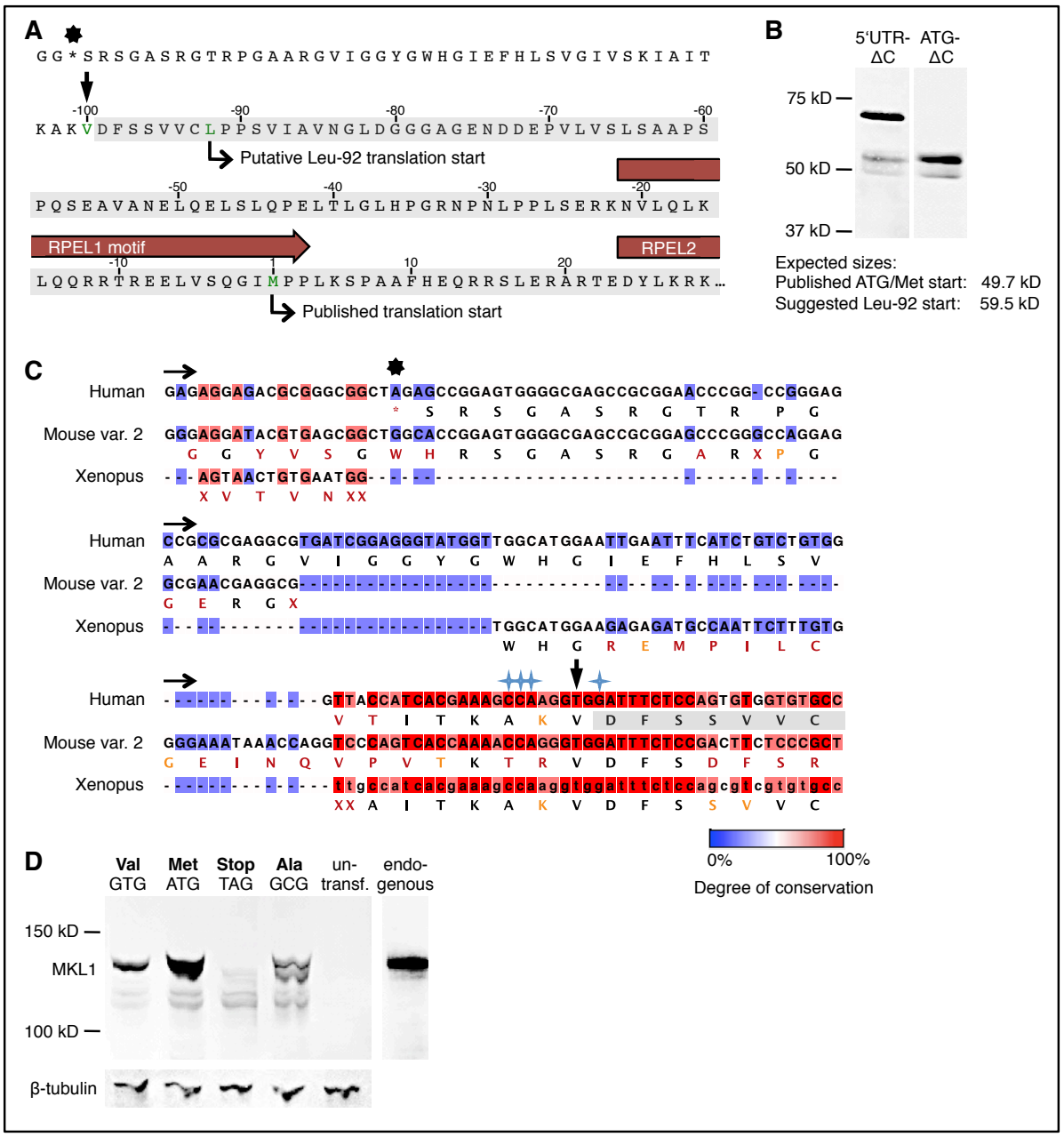

Figure 1. Identification of an unusual translation start of the published human MKL1.

A) Human 5'UTR-full length MKL1 was overexpressed in HEK293 cells, the translated MKL1 was affinity purified, and the major product AspN digested. Peptides were identified by LC-MS using the in-frame translated MKL1 5'UTR sequence as reference. Highlighted in gray: Peptide coverage. Black star: In-frame stop codon. Green letters: Suggested ATG, CTG or GTG translation initiation codons (coding for M, L, and V, respectively). Vertical arrow: Putative GTG/Val-100 start. **B)** ATG-ΔC and 5'UTR-ΔC constructs were overexpressed in HEK293 cells and MKL1 was detected by immunoblotting with anti-MKL1 total mAb. Expected sizes were calculated from the putative amino acid sequences. **C)** Alignment of the human MKL1 5'UTR region with those of mouse (variant 2) and Xenopus. Horizontal arrows: 5' to 3' direction. Black 8-point star: In-frame stop codon. Vertical arrow: Suggested GTG/Val-100 start. Blue 4-point star: Nucleotides

complying with the Kozak consensus sequence. **D)** Point mutations targeting the suggested GTG/Val-100 start codon were introduced into the construct from B), the resulting constructs were transiently overexpressed in HEK293 cells, and MKL1 was detected by immunoblotting with anti-MKL1 total mAb. Endogenous human MKL1 had been purified from untransfected (untransf.) HEK293 cells as in B).

In addition, with a G in position +4 and a purine base at -3 this nucleotide is flanked by a strong Kozak consensus sequence (Kozak, 1989), the major requirement for a GTG to serve as an unusual start codon. To experimentally test the function of this GTG as the translation start, we introduced the following mutations into the 5'UTR-full length MKL1 construct (Fig. 1D). Introduction of the more potent ATG start codon into this context increased translation efficiency, and the resulting product migrated at the same position as from the GTG construct and the endogenous protein. Replacing the GTG start codon with GCG (Ala) greatly diminished translation and resulted in two different translation products, proving the importance of the GTG/Val-100 codon as the translation initiation codon of human MKL1. Finally, introduction of a stop codon abolished translation most efficiently, excluding the existence of further downstream translation starts. The eight additional amino acids that are included with the GTG/Val-100 translation start, but not present with the CTG/Leu-92 start are predicted to form two out of four β-strands within the N-terminal 36-amino acid stretch (Supplemental Fig. S1).

Human cells express a second, shorter MKL1 isoform (MKL1_S).

To investigate endogenous MKL1 transcripts in human tissues we performed 5'RACE on total RNA from fetal and adult brain extracts, amplifying the region upstream of the published ATG start codon (Fig. 2A). Interestingly, we detected two major products of different sizes. Nucleotide sequencing revealed the expression of a second human transcript (for sequence see Supplemental Fig. S2), which is homologous in sequence to the mouse MKL1 variant 1 (NM_153049.2). An alignment with the human genome depicts that in this variant a single alternative exon is found between previously known exons 3 and 4, which represents an alternative 5' end of the MKL1 gene and thus implies the existence of an alternative promoter for this transcript (Fig. 2B). The novel exon

contains an in-frame ATG start codon. Thus, translation of this transcript is expected to yield a second MKL1 isoform that we termed MKL1_S (S for short), since it is shorter than the MKL1_L (L for long) isoform derived from the GTG/Leu-100 start of the published mRNA. MKL1_S carries a stretch of only 15 variant-specific amino acids at its N-terminus, whereas MKL1_L has a long tail of 80 variant-specific amino acids. Both isoforms are otherwise identical and both of them harbor all three RPEL repeats. To investigate whether the two MKL1 isoforms are indeed expressed in human cells on protein level, we generated two monoclonal antibodies, one detecting a region of human MKL1 that is shared by both isoforms (detecting "MKL1 total") and one that is specifically recognizing the N-terminus of the novel MKL1_S. Affinity purification from whole cell extracts of U343MG glioblastoma cells using the antibody against MKL1 total was used to enrich the endogenous MKL1 proteins. As shown in Figure 2C, two distinct MKL1 isoforms could be detected which corresponded in size with the overexpressed proteins translated from 5'UTR-full length constructs of the two MKL1 transcripts. Using the MKL1_S-specific antibody we confirmed that the observed lower band indeed constituted the novel isoform MKL1_S (Fig. 2C).

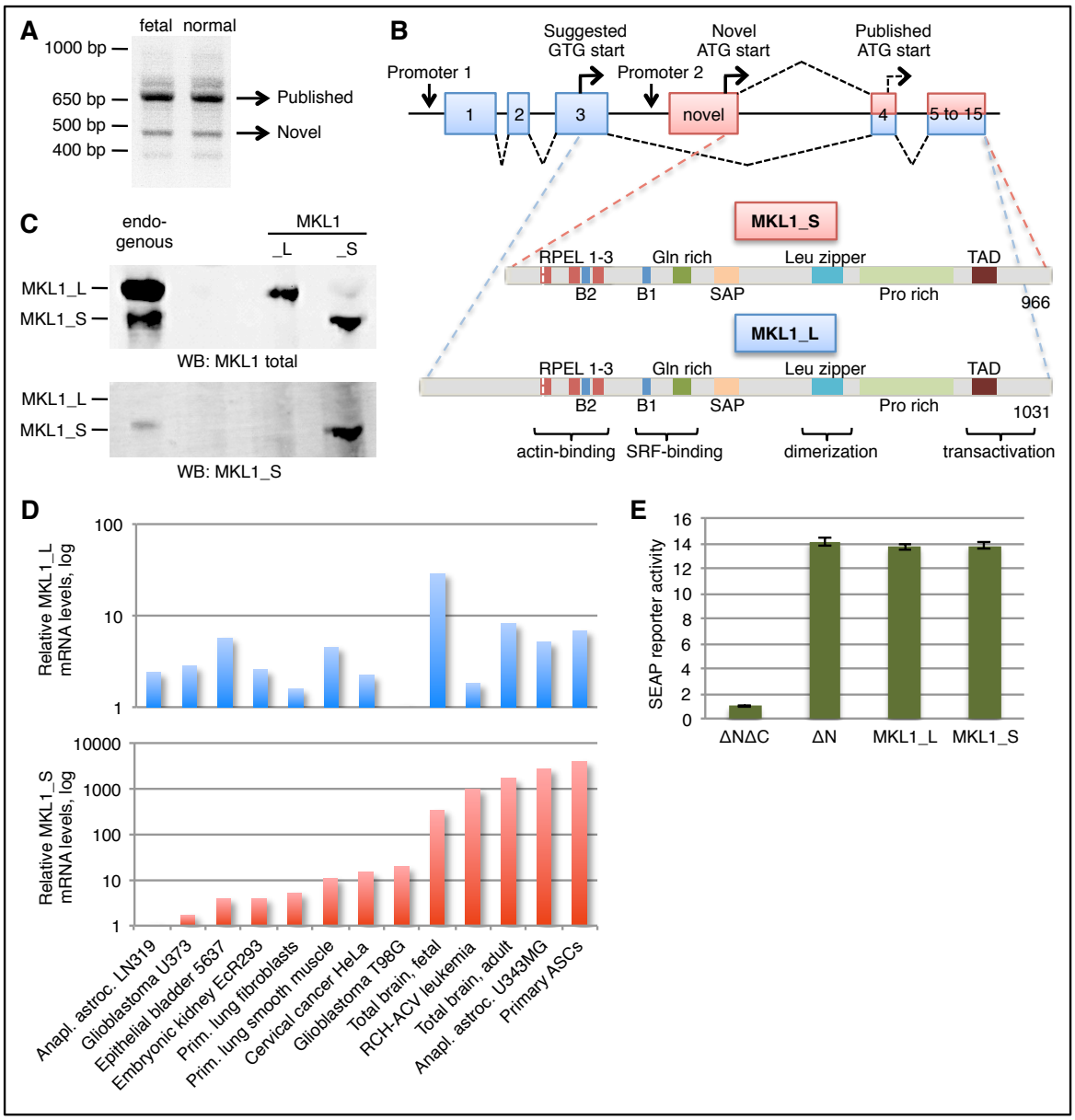

Figure 2. Identification of a second human MKL1 isoform.

A) 5'RACE on total RNA from human brain extracts. The MKL1 5'UTR region was amplified using a reverse primer located 3' of the published ATG/Met start codon and the main products were sequenced. **B)** Alignment of the two MKL1 transcripts with the human genome. An alternative exon with an upstream ATG/Met start codon results in the translation of the shorter MKL1_S isoform. Translation starting at the suggested GTG/Val-100 codon of the published transcript results in the longer MKL1_L isoform. Downstream of the white dashed line the two isoforms are identical. B = basic motif; TAD = transactivation domain. **C)** Western Blot detection of both human isoforms on the protein level. Detection on the same membrane was achieved by 2-channel detection of two antibodies with the LI-COR Odyssey system. Left: Endogenous MKL1 was affinity purified from U343MG glioblastoma cell extract with the anti-MKL1 total mAb. Right: Cell extracts from HEK293 cells stably overexpressing either MKL1_L or MKL1_S. **D)** Total

RNAs from human cell lines and tissues were subjected to quantitative RT-PCR analysis with primers specific for each MKL1 isoform. Isoform levels relative to GAPDH were calculated by using the relative standard curve method. Averages of triplicate measurements from single batches of RNA are shown (n = 1). Attention should be paid to the logarithmic scale for MKL1_S. Anapl. astroc. = anaplastic astrocytoma; prim. = primary. **E)** SEAP (SEcreted Alkaline Phosphatase) promoter-reporter assay. HEK293 cells were transiently co-transfected with an MKL1 construct and a 3x CArG box SEAP reporter construct. 18 h after LPA stimulation the amount of secreted alkaline phosphatase was determined. Constructs: ΔNΔC = published ATG/Met start (ΔN) with the C-terminal half of MKL1 missing (ΔC); ΔN = published ATG/Met start full length MKL1; MKL1_L = 5'UTR-full length MKL1_L; MKL1_S = 5'UTR-full length MKL1_S. Data are represented as mean +/- sd of 4 independent experiments (n = 4).

No protein band of the size of the published ATG/Met start protein (smaller than MKL1_S) was detected, implicating that MKL1_L and MKL1_S identified in our experiments are the main isoforms expressed in human cells. To assess the expression patterns of both isoforms in different human cells and tissues, we performed quantitative RT-PCR (qPCR) analysis with primers specific for each isoform (Fig. 2D). Estimated from the Ct values, MKL1_L was the major isoform in most of the cell types and tissues analyzed. MKL1_L expression levels were comparable in all samples, whereas MKL1_S levels varied greatly. In the majority of samples MKL1_S was expressed at very low level, within a relative range of 1- to 20-fold above the lowest expressing cell line. However, a group of cell lines and tissues, including fetal and adult brain, expressed MKL1_S at much higher levels. For this group, the relative difference in expression of MKL1_S spanned 2 to 3 orders of magnitude compared to the lowest expressing cell line. Primary ASCs showed the highest expression of MKL1_S, which was approximately 4x 10^3-fold higher than that of the anaplastic astrocytoma cell line LN319. Notably, the purification of the endogenous protein isoforms from U343MG cells in Figure 2C illustrates that even in cells that belong to the group with high relative MKL1_S expression (Fig. 2D), protein levels were lower than those of MKL1_L.

MKL1_L and MKL1_S show similar SRF-dependent transcriptional activities, Rho-responsiveness and nuclear translocation.

To assess whether the different N-termini of the two MKL1 isoforms result in differential transcriptional activities, Rho-responsiveness or nuclear translocation, we investigated the transactivation of SRF and the kinetics of MKL1 isoform nuclear accumulation after stimulation of the Rho-actin-MKL1 pathway. Promoter-reporter assays after co-transfection of different MKL1 constructs with a 3x CArG box promoter construct are shown in Figure 2E. We did not observe any difference in activation of the SRF reporter construct by MKL1 constructs harboring the different translation starts of MKL1. However, the ability to induce SRF activity was strongly impaired in a C-terminally truncated construct lacking the transactivation domain.

MKL1 staining in HEK293 cells that overexpressed either of the two isoforms revealed comparable nuclear accumulation kinetics for MKL1_L and MKL1_S after stimulation with FCS, LPA, and cytochalasin D (Fig. 3). With FCS and LPA, two classical activators of the Rho-actin-MKL1 pathway, nuclear accumulation of each MKL1 isoform was visible already after 5 min of treatment (Fig. 3A and 3B). In case of FCS treatment, about 80% of all cells showed nuclear accumulation of each isoform and the peak was reached already after 5 min. With LPA we observed a more pronounced nuclear accumulation for MKL1_S than for MKL1_L, which increased within 60 min to about 75 % for MKL1_S and 60 % for MKL1_L. However, this difference was not statistically significant. To assess possible differences in nuclear import or export rates between the two isoforms, we treated the cells with the actin polymerization inhibitor cytochalasin D. This drug binds to G-actin and thereby liberates MKL1 from actin inhibition. Independent of the MKL1 isoform, 100 % of cells showed nuclear MKL1 localization already after 5 – 60 min of cytochalasin D treatment (Fig. 3C). We therefore conclude that despite the small differences after LPA stimulation, MKL1_L and MKL1_S exhibit similar SRF-dependent transcriptional activities, Rho-responsiveness and nuclear import and export efficiencies.

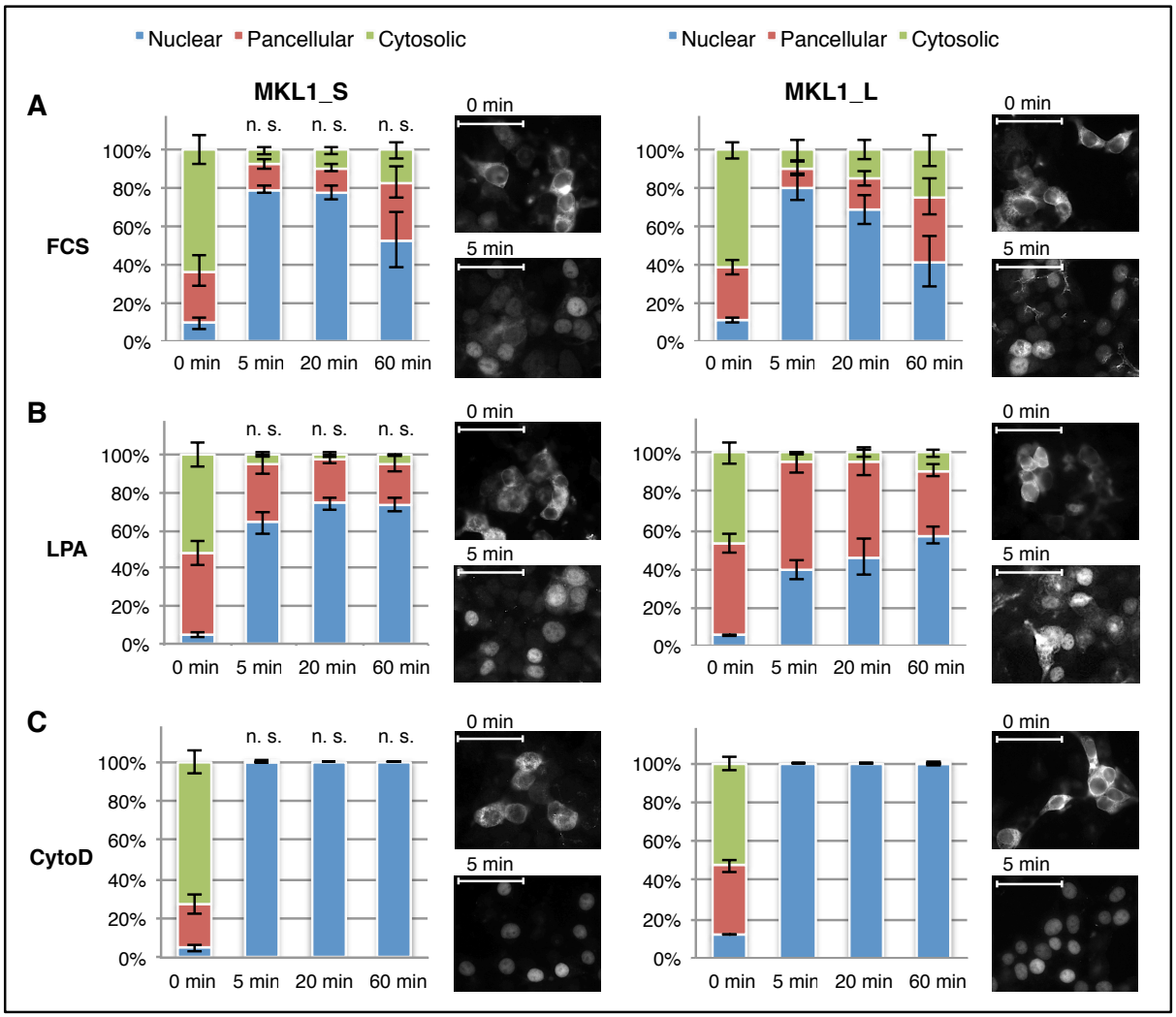

Figure 3. MKL1_S and MKL1_L show similar nuclear translocation properties.

HEK293 cells stably overexpressing 5'UTR-full length MKL1_S or MKL1_L constructs were starved and treated with **A)** 15% FCS, **B)** 50 µM LPA, or **C)** 2 µM Cytochalasin D (CytoD) for 0 - 60 min. Cells were then stained with the anti-MKL1 total mAb and fluorescent images were taken. Overexpressing cells were classified according to their predominant subcellular localization of MKL1 into "nuclear", "pancellular", or "cytosolic". At least 30 cells were counted in each of three independent experiments for each treatment at each time point. The percentage of cells in each category was calculated for each experiment and then averaged. Data are represented as mean +/- SEM of 3 independent experiments (n = 3). n. s. = not significant in comparison to MKL1_L under the same conditions in an unpaired t-test. Scale bars are 50 µm in length.

The initial phase of TGF-β1-induced myofibroblastic differentiation involves specific up-regulation of MKL1_S expression.

MKL1 is known to act as a crucial regulator of the contractile gene transcription program of myofibroblast-like cells. Since we have found that hASCs express two different MKL1 isoforms, we aimed to understand the isoform-specific regulation of MKL1 during this process. Therefore, we isolated the stromal vascular fraction (SVF) of cells from patient adipose tissue, which was confirmed to contain a large proportion of MSCs expressing the mesenchymal markers CD73, CD90, and CD105 (Fig. 4A). Adherent cells were expanded to obtain a population of primary hASCs. Treatment of these cells with serum-free medium containing 2 ng/ml TGF-β1 for 96 h clearly induced their differentiation, as documented by their change in morphology compared to cells incubated with the control medium (Fig. 4B). We analyzed the transcript levels of various myofibroblast/CAF markers and the MKL1 isoforms 24 h and 96 h after the start of the TGF-β1-induced differentiation. Expression of the contractility-promoting genes calponin-1/*CNN1*, SM22α/*TAGLN*, and SMA/*ACTA2*, the prototypic marker of the myofibroblast/CAF cell type, increased significantly compared to the mock-treated cells. The transcript level of the secreted marker tenascin-C/*TNC* also increased within 96 h of treatment, confirming the differentiation of the hASCs into myofibroblasts/CAFs (Fig. 4C). As reported by others (Mihira et al., 2012; Minami et al., 2012; Sandbo et al., 2011), we also observed an increase in total MKL1 levels compared to control cells (Fig. 4D).

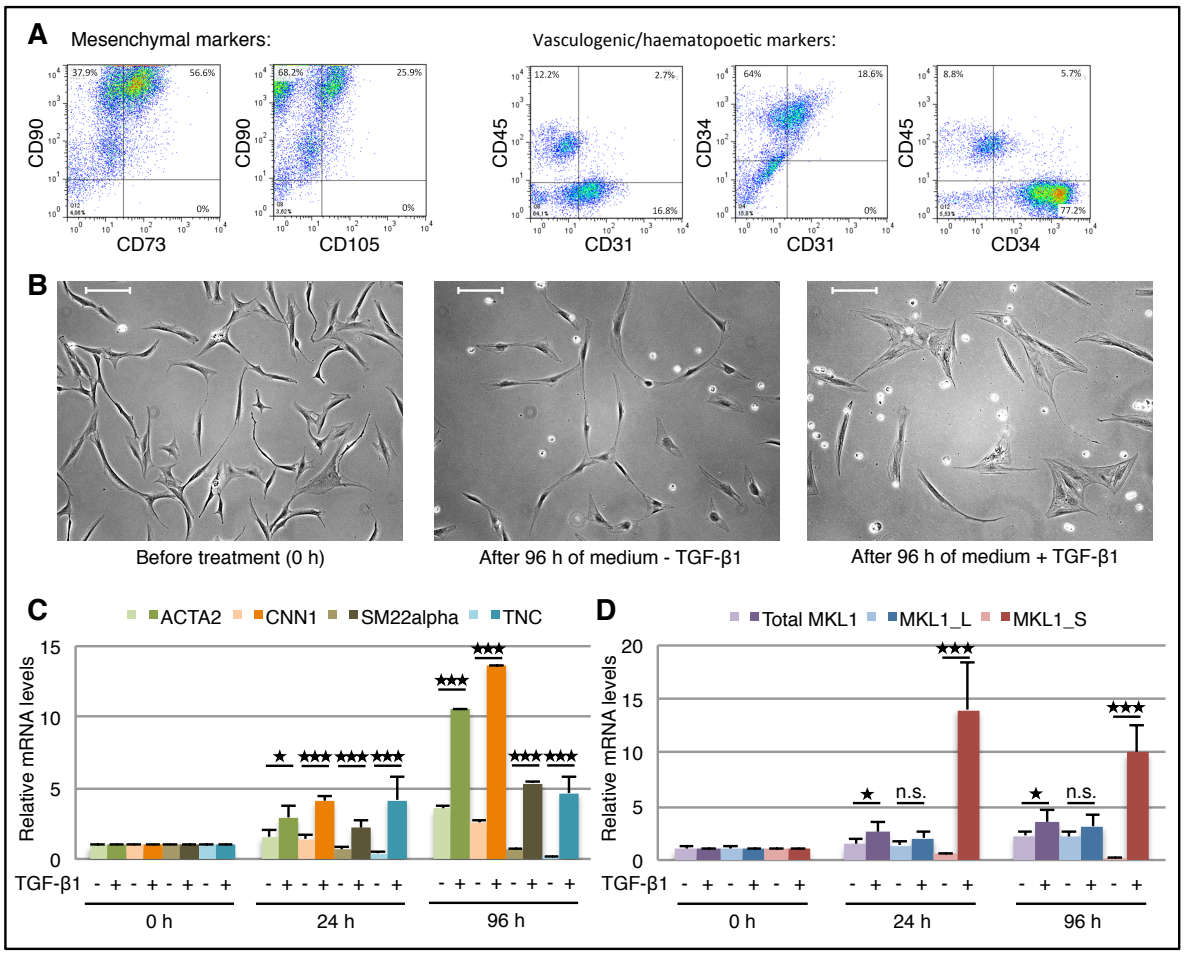

Figure 4. Specific up-regulation of MKL1_S during the initial phase of TGF-β-induced myofibroblast/CAF differentiation.

A) Cytofluorimetric profile of the SVF from which the adherent cells generated the hASC population that was used for differentiation experiments. **B)** Phase contrast pictures of TGF-β1-induced differentiation of hASCs. Cells were starved and kept in serum-free medium with or without 2 ng/ml TGF-β1 for 96 h. Scale bars are 200 µm in length. **C)** qPCR analysis of myofibroblast/CAF marker levels relative to GAPDH during the initial phase of TGF-β1-induced myofibroblast/CAF differentiation. **D)** qPCR analysis of MKL1 isoform levels relative to GAPDH during the initial phase of TGF-β1-induced myofibroblastic differentiation. Data in C) and D) are represented as mean +/- sd of 4 independent experiments (n = 4). Statistical significance was determined using an unpaired t-test, with * $P < 0.05$, *** $P < 0.001$, and n. s. = not significant.

However, the use of isoform-specific primers revealed that expression of the major human isoform MKL1_L did not change significantly in response to TGF-β1, whereas expression of the novel isoform MKL1_S was induced more than 10-fold within 24 h of differentiation and remained high after 96 h (Fig. 4D). The small effect of this strong

MKL1_S induction on total MKL1 levels can be explained by the fact that MKL1_S basal levels were clearly lower than MKL1_L basal levels in the undifferentiated hASCs (estimated from the Ct values). Our data suggest that the known increase of MKL1 expression during TGF-β-induced myofibroblast/CAF differentiation is mainly driven by a strong induction of MKL1_S transcript levels. Thus, TGF-β1 seems to be a potent isoform-specific inducer of MKL1_S, and TGF-β1-induced differentiation of hASCs into myofibroblasts/CAFs involves a strong up-regulation of the MKL1_S mRNA level during the initial 24 h of differentiation.

MKL1_S up-regulation is specific for TGF-β1-induced differentiation.

To assess whether MKL1_S up-regulation constitutes a general mechanism during hASC differentiation, we used other media to differentiate hASCs/MSCs into different cell types. With chondrogenic medium containing TGF-β1 at a concentration of 10 ng/ml, we obtained a comparably strong up-regulation of MKL1_S after 24 h and 96 h as with TGF-β1 alone (Fig. 5A). LPA was reported to induce expression of total MKL1 in hASCs (Jeon et al., 2010; Jeon et al., 2008a), but in our experiments using 5 µM LPA we did neither observe an up-regulation of total MKL1 transcript levels compared to control cells, nor of one of the MKL1 isoforms alone (Fig. 5B). Likewise, the stimulation of hASCs to differentiate towards a smooth muscle phenotype using 2 µM SPC (Jeon et al., 2008b), or 5 % uniaxial cyclic strain (Kurpinski et al., 2009) did not result in obvious changes of the transcript levels of total MKL1 or one of the MKL1 isoforms (Fig. 5C, 5D). Therefore, the observed strong and isoform-specific induction of MKL1_S expression within the initial phase of hASC differentiation seems to be a mechanism that is specifically triggered by TGF-β1.

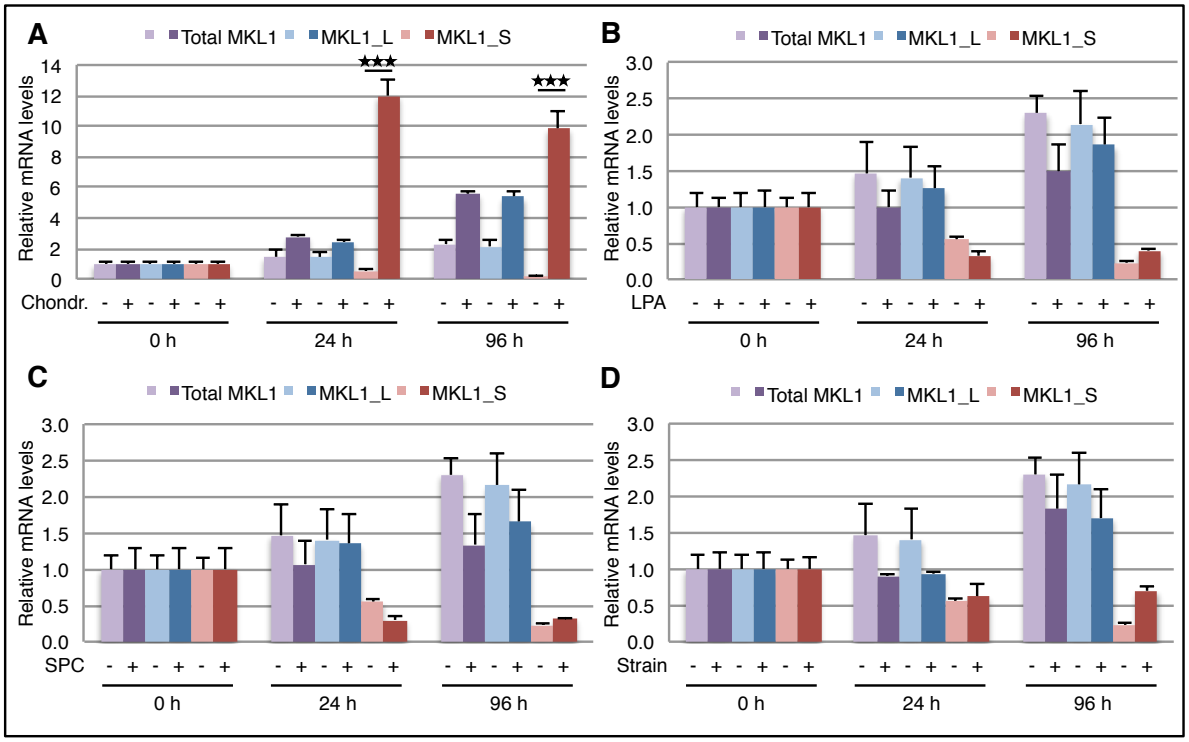

Figure 5. TGF-β1 is required to specifically up-regulate MKL1_S during hASC differentiation. qPCR analysis of MKL1 isoform levels during the initial phase of hASC differentiation induced by **A)** chondrogenic medium (= chondr.) containing 10 ng/ml TGF-β1, **B)** 5 µM LPA, **C)** 2 µM SPC, and **D)** 5 % uniaxial cyclic strain at 1 Hz for the initial 24 hours. Levels are relative to GAPDH. Data are represented as mean +/- sd of 4 independent experiments (n = 4). Statistical significance was determined using an unpaired t-test, with *** $P < 0.001$.

MKL1_S activates a group of genes in an isoform-specific manner.

According to published work (Morita et al., 2007; Sandbo et al., 2011), TGF-β promotes the translocation of MKL1 to the nucleus only after 24-48 h, meaning in a strongly delayed fashion compared to the direct stimulation of Rho-actin-MKL1 signaling. However, we observed a strong induction of MKL1_S transcription by TGF-β within the first 24 h of myofibroblast/CAF differentiation. Thus, TGF-β treatment seems to induce MKL1_S in a rapid and direct fashion, before it indirectly activates the Rho-actin-MKL1 signaling pathway. Therefore, we addressed a potential specific role of MKL1_S for the later phase of myofibroblast/CAF differentiation by identifying MKL1_S-specific target genes. Due to inefficient transient transfection of primary hASCs and the impossibility to select stable overexpression/knockdown clones from primary cells without the loss of

their multipotent properties, we used a cell line that reacts to MKL1 transfection with the induction of the myofibroblast marker *ACTA2* (SMA) for these exeriments. We tested the easily transfectable HEK293 cells to reveal the transcriptional activities of the two MKL1 isoforms. We imitated the TGF-β-induced increase of the MKL1_S/_L ratio during the initial phase of myofibroblast/CAF differentiation by stable overexpression of MKL1_S in the background of the endogenously low MKL1_S/_L ratio of HEK293 cells (see Fig. 2D). As a direct stimulation of the Rho-actin-MKL1 pathway we treated the cells with LPA and assessed MKL1_S-dependent gene regulation by gene expression profiling. The majority of genes that were significantly up- or down-regulated in the MKL1_S-overexpressing cells were comparably regulated by overexpression of MKL1_L. This group of common target genes contained *ACTA2* (SMA) and other genes that have been described before as direct targets of MKL1 or SRF (Table 1, Table S1). The observation that both MKL1 isoforms seem to similarly induce SRF-dependent transcription is in agreement with the results from promoter-reporter assays shown before (Fig. 2E).

In addition, the gene expression analysis revealed a group of genes that were differentially affected by the MKL1 isoform overexpression (Table 1; Table S1). Within this group, most transcripts showed higher expression with MKL1_S than with MKL1_L overexpression. Some of these transcripts were more strongly inhibited by MKL1_L than by MKL1_S when compared to the empty vector control, which might point towards an increased inhibitory function of MKL1_L. Importantly, although MKL1_S was clearly less overexpressed than MKL_L compared to endogenous MKL1 levels in the empty vector control, several genes were significantly more strongly induced by MKL1_S. On the contrary, only a single gene of the top 10 differentially regulated genes was specifically up-regulated with the MKL1_L isoform. This argues for a specific effect of the 15-amino acid N-terminal stretch of MKL1_S on transcription.

Table 1. MKL1_S and MKL1_L overexpression induce a common and an MKL1_S-specific transcriptional activity.

Gene name	Description	MKL_S vs. empty vector [a]	MKL_L vs. empty vector [a]	MKL_S vs. MKL_L [a]
Genes similarly regulated by the two isoforms:				
POM121 L1P	POM121 membrane glycoprotein-like 1 pseudogene	+3.89 (2.6E-04)	+5.83 (4.2E-05)	**< 1.50**
NAP1L3	nucleosome assembly protein 1-like 3	+.2.78 (2.4E-06)	+1.86 (1.0E-04)	**< 1.50**
ACTA2	actin, alpha 2, smooth muscle	+2.02 (3.0E-05)	+1.86 (7.2E-05)	**< 1.50**
ESRRG	estrogen-related receptor gamma	+1.93 (4.5E-08)	+1.71 (2.2E-07)	**< 1.50**
MDGA2	MAM domain containing GPI anchor 2	+1.83 (1.8E-05)	+2.43 (9.4E-07)	**< 1.50**
DACH2	dachshund homolog 2 (*Drosophila*)	+1.82 (1.5E-05)	+1.61 (8.0E-05)	**< 1.50**
SLC8A1	solute carrier family 8 (sodium/ calcium exchanger), member 1	+1.67 (1.7E-05)	+2.18 (6.6E-07)	**< 1.50**
PDGFD	platelet derived growth factor D	+1.61 (8.3E-06)	+1.50 (2.6E-05)	**< 1.50**
ESRP1	epithelial splicing regulatory protein 1	-4.20 (2.3E-08)	-2.88 (2.6E-07)	**< 1.50**
IFI16	interferon, gamma-inducible protein 16	-2.96 (2.3E-07)	-3.35 (9.8E-08)	**< 1.50**
MEOX2	mesenchyme homeobox 2	-2.62 (2.1E-06)	-3.15 (5.5E-07)	**< 1.50**
PION	pigeon homolog (*Drosophila*)	-2.48 (4.3E-05)	-2.47 (4.4E-05)	**< 1.50**
LGALS8	lectin, galactoside-binding, soluble, 8	-2.22 (1.1E-04)	-2.43 (5.3E-05)	**< 1.50**
Genes differentially regulated by the two isoforms:				
MMP16	matrix metallopeptidase 16 (membrane-inserted)	+5.86 (1.4E-07)	+2.30 (4.5E-05)	**+2.54** (2.0E-05)
SPOCK3	sparc/osteonectin, cwcv and kazal-like domains proteoglycan (testican) 3	+5.04 (8.5E-09)	+2.31 (1.6E-06)	**+2.18** (2.7E-06)
OSTN	Osteocrin (musclin)	+2.23 (3.5E-05)	< 1.20	**+1.92** (1.6E-04)
ODZ1	odz, odd Oz/ten-m homolog 1 *(Drosoph.)*	-1.85 (2.6E-05)	-3.55 (1.0E-07)	**+1.91** (1.8E-05)
NRG3	neuregulin 3	< 1.20	-1.71 (1.5E-05)	**+1.70** (1.5E-05)
AMBN	ameloblastin (enamel matrix protein)	+5.14 (2.0E-07)	+3.09 (3.7E-06)	**+1.67** (1.0E-03)
ADAM21	ADAM metallopeptidase domain 21	+1.38 (3.7E-06)	-1.36 (8.4E-04)	**+1.65** (3.0E-05)
MAP7D2	MAP7 domain containing 2	-1.77 (3.8E-06)	-2.77 (4.1E-08)	**+1.56** (2.5E-05)
CNTN4	contactin 4	< 1.20	-1.72 (1.3E-06)	**+1.54** (8.3E-06)
FABP6	fatty acid binding protein 6	< 1.20	+2.00 (7.7E-07)	**-1.78** (3.0E-06)

[a] Averaged fold-regulations of genes are given with *P*-values in parentheses.
Genes that were specifically induced by MKL1_S are highlighted in gray.

Interestingly, several genes that code for extracellular proteins such as proteases (e.g., MMP-16), MMP regulators (e.g., SPOCK3/testican-3), or ECM components (e.g., osteocrin/musclin) were specifically upregulated by MKL_S. MMP-16 showed the strongest MKL1_S-specific up-regulation. To test whether this transcriptional regulation also occurs during hASC differention, we analyzed MMP-16 transcript levels during differentiation induced by TGF-β, LPA, SPC, or cyclic strain. MMP-16 levels were elevated after 96 h of TGF-β-induced myofibroblast/CAF differentiation, but down-regulated compared to the medium control with all other stimuli (Fig. 6). This may reflect the effect of the TGF-β-mediated induction of MKL1_S transcript levels in myofibroblast/CAF differentiation, which could control MMP-16 expression in a delayed fashion.

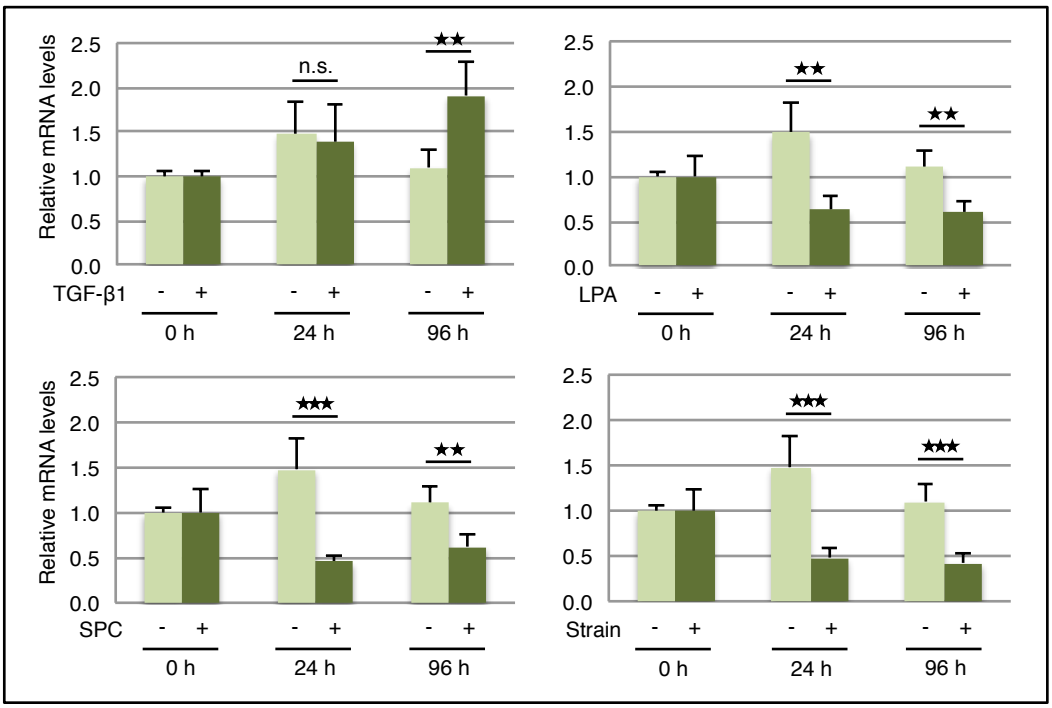

Figure 6. SRF activation by MKL1 isoforms and MMP-16 up-regulation during myofibroblast/CAF differentiation.

qPCR analysis of the MKL1_S target gene MMP-16 during the initial phase of hASC differentiation induced by 2 ng/ml TGF-β, 5 µM LPA, 2 µM SPC, or 5 % uniaxial cyclic strain at 1 Hz for the initial 24 h. Levels are relative to GAPDH. Data are represented as mean +/- sd of 4 independent experiments (n = 4). Statistical significance was determined using an unpaired t-test, with * $P < 0.05$, ** $P < 0.01$, *** $P < 0.001$, and n. s. = not significant.

MKL1_S specific transcriptional activity requires a novel N-terminal domain.

The observations of a strong and partly specific transcriptional activity of MKL1_S and an increased suppressive effect of MKL1_L led us to consider that their unique N-termini were responsible for these differential activities. Bioinformatical analyses of the N-terminal sequences, predicted a 9-amino acid transactivation domain (9aa TAD) within the specific 15 N-terminal amino acids (MAVQSVLQL) of MKL1_S. 9aa TADs have been described as the smallest known denominator in the transactivation domains of a variety of transcription factors, ranging from yeast to mammals (Martin, 2009; Piskacek et al., 2007). Due to the fact that the border between the isoform-specific parts and the shared sequence lies within this motif, the corresponding sequence in MKL1_L (SERKNVLQL) does not fulfill the criteria for such a domain (Fig. 7A). Furthermore, secondary structure predictions (by CLC Main Workbench version 6.7) predicted a more extended α-helix upstream of the RPEL1 motif in MKL1_S than in MKL1_L (Fig. 7A). In addition to the predicted N-terminal 9aa TAD in MKL1_S, the algorithm detected another 9aa TAD in the C-terminal region that is common to both isoforms (DDLFDILIQ). This C-terminal region harbors the only MKL1 transactivation domain described so far.

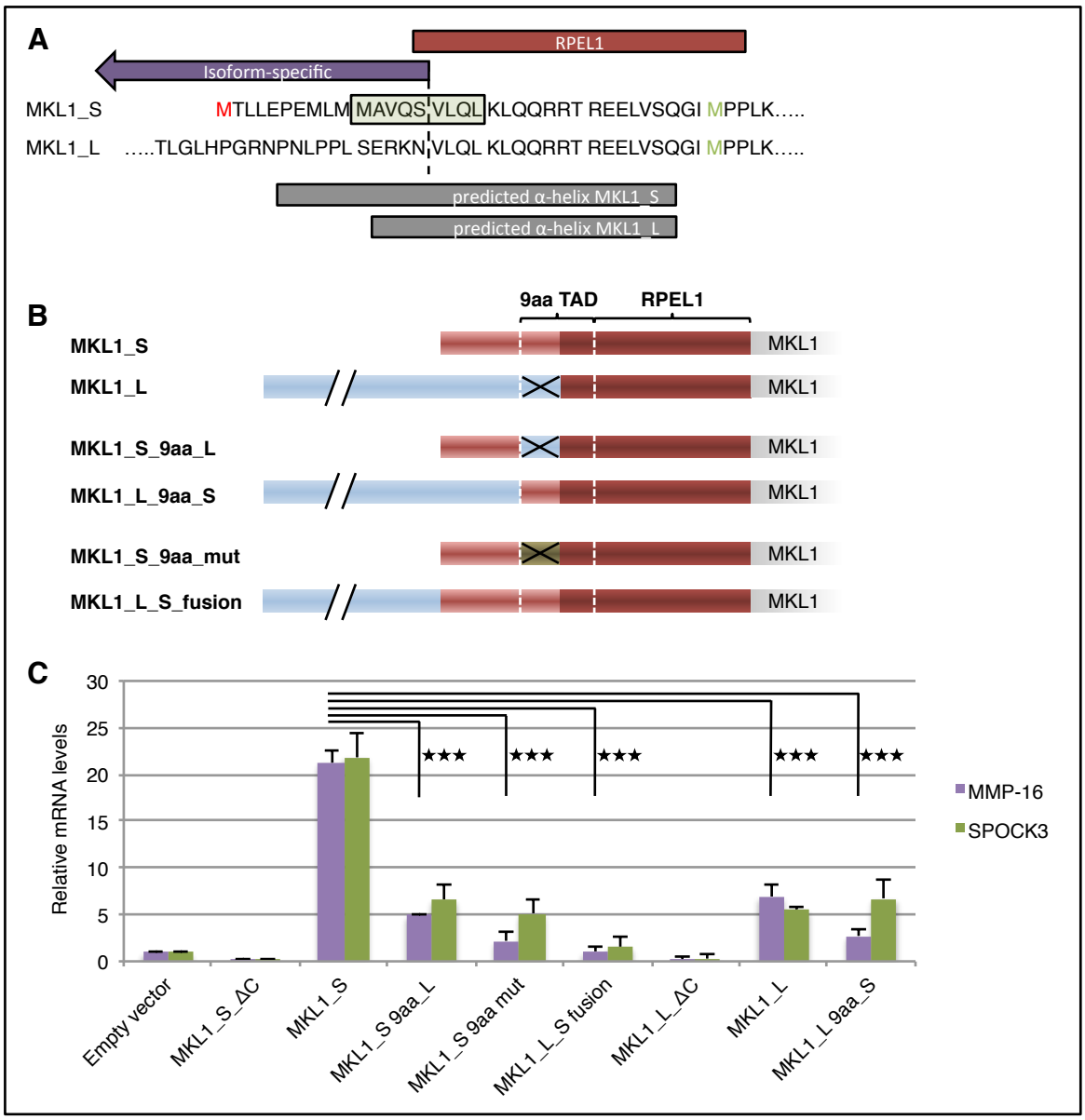

Figure 7. Identification of a functional domain in MKL1_S that allows specific transcriptional activity.

A) Alignment of MKL1 isoform N-terminal amino acid sequences. Green box: Predicted 9aa TAD in MKL1_S. Green letter: Published ATG/Met start of MKL1_L. Red letter: ATG/Met start of MKL1_S. **B)** Constructs were generated in which the 5 specific amino acids of the predicted 9aa TAD in MKL1_S were mutated, exchanged with the corresponding amino acids in MKL1_L, or vice versa. The MKL1_L_S fusion construct contains the full length MKL1_S coding sequence preceded by the MKL1_L-specific N-terminal tail. A cross indicates a sequence that does not fulfill the 9aa TAD criteria. **C)** qPCR analysis of MKL1_S-specific target genes. Constructs depicted in B) were stably overexpressed in HEK293 cells. Before RNA extraction, cells were starved and MKL1 activity stimulated with LPA. MKL1_L and MKL1_S: 5'UTR-full length constructs. ΔC constructs: MKL1 missing its C-terminal half. Data are represented as mean +/- sd

of 2 independent experiments each with 2 independently created overexpressing cell lines. Statistical significance is given for MMP-16 levels with *** $P < 0.001$ in 1-way ANOVA (Holm-Sidak method).

To test the hypothesis that the newly identified N-terminal motif in MKL1_S contributes to its specific transcriptional activity, we transfected HEK293 cells with different constructs containing altered or exchanged N-terminal motifs (Fig. 7B, for expression of the translated proteins see Supplemental Fig. S3). After stimulation of the Rho-actin-MKL pathway by LPA treatment, we isolated RNA and analyzed the expression levels of the two MKL1_S-specific targets MMP-16 and SPOCK3. Constructs missing the C-terminal half of MKL1, regardless of which N-terminal isoform sequence was used (MKL1_L_ΔC or MKL1_S_ΔC), did not support an increased MMP-16 or SPOCK3 expression compared to empty vector transfected control cells (Fig. 7C). Thus, the activation of MKL1_S-specific target genes requires the C-terminal half of MKL1, including the C-terminal transactivation domain. Similarly to what we observed before in the gene expression profiling, overexpression of MKL1_S triggered MMP-16 and SPOCK3 transcription 3 to 4-fold more efficiently than did overexpression of MKL1_L. However, when we mutated the predicted 9aa TAD in MKL1_S into a sequence that did not meet several of the criteria for 9aa TADs (KRGHSVLQL, MKL1_S 9aa mut), MMP-16 and SPOCK3 expression dropped to roughly the level in MKL1_L-overexpressing cells. Moreover, when we exchanged this motif with the corresponding sequence of MKL1_L (MKL1_S 9aa_L), we observed the same drop of activity, suggesting that the identified motif in MKL1_S indeed confers higher activity towards certain target genes. However, we did not observe any enhancement of MKL1_L-mediated gene expression of MMP-16 and SPOCK3 when we replaced its corresponding sequence with the functional domain of MKL1_S (MKL1_L 9aa_S) in the context of its long N-terminal tail. Furthermore, expression of a fusion construct between both isoforms (MKL1_L_S fusion), in which we fused the long N-terminal tail of MKL1_L to the N-terminus of MKL1_S, resulted in similarly low expression of MMP-16 and SPOCK3. In summary these results argue for a functional activating motif in MKL1_S when present in its natural context, as well as for a dominant inhibitory function of the MKL1_L-specific tail.

Discussion

Over the past years, the Rho-actin-MKL1-SRF pathway has been implicated in several physiological and pathological processes based on the reversible differentiation of different precursor cell types into myofibroblasts/CAFs (Small, 2012). Within this pathway, MKL1 activity has emerged as the crucial relay between the status of the actin cytoskeleton and the transcription of a substantial part of SRF target genes (Selvaraj and Prywes, 2004; Wang et al., 2002). Here, we analyzed the exact molecular structure of the human MKL1 protein, its gene architecture, and its regulation during myofibroblast/CAF differentiation. Before this study, human MKL1 was either assumed to start at the first in-frame ATG/Met start codon (Wang et al., 2002) resulting in a protein missing the first conserved RPEL1 motif, or at an unusual CTG/Leu-92 start codon (Miralles et al., 2003). In our experiments we found no evidence of either of these two translation starts. Instead, we provide experimental evidence for translation starting at the upstream unusual GTG/Val-100 codon. Thus, the published MKL1 transcript translates into a protein (MKL1_L) that is 100 amino acids longer than originally thought, and contains three actin-binding RPEL motifs. Compared to the suggested upstream CTG/Leu-92 codon this novel translation start includes eight more amino acids in the protein, which are predicted to form two short β-strands within a 4-β-strand motif at the MKL1_L N-terminus. Identification of this putative N-terminal domain points out the importance of using the GTG/Val-100 start that we describe here when studying MKL1_L structure and function.

Moreover, we show for the first time that a second human MKL1 transcript variant arises from the utilization of an alternative promoter and is translated into the shorter MKL1_S. This isoform also contains 3 RPEL motifs, but a much shorter N-terminal domain than MKL1_L. In opposition to the MKL1_L transcript, which showed ubiquitous and robust expression, we observed highly variable expression of the novel transcript, pointing towards more tissue-specific functions. Most studies published so far exclusively addressed total MKL1 levels by utilizing antibodies, PCR primers, or RNAi targeting the common part of the two MKL1 isoforms. Most studies based on overexpression of MKL1 constructs used either mouse MKL1_S, which was considered the major MKL1 protein in this species (Sasazuki et al., 2002; Wang et al., 2002), or engineered MKL1_L variants, with translation starts other than the GTG/Val-100 start.

Therefore, some of the earlier findings on MKL1 function will have to be reevaluated with regard to the specific contributions of the two isoforms. Indeed, we found differential effects on gene expression by the two isoforms. In addition to a common transcriptional activity of MKL1_S and MKL1_L that comprised, e.g., the regulation of SMA, the prototypic marker of the myofibroblast/CAF cell type, we identified a specific transcriptional activity of MKL1_S. We provide evidence that this activity is dependent on the initial 5 amino acids of a predicted 9aa TAD in the unique N-terminal stretch of MKL1_S. Appending the long N-terminal tail of MKL1_L to MKL1_S erased the MKL1_S-specific induction of its target genes MMP-16 and SPOCK3. Thus, the presence of this large extension might interfere with the binding of an unknown factor to the predicted 9aa TAD. For instance, this motif was suggested to interact with general transcriptional coactivators, such as the transcription initiation factor TFIID subunit 9 (TAF9) (Martin, 2009; Piskacek et al., 2007). Our experiments suggest a dual mode by which MKL1_L is disabled to induce certain MKL1_S target genes: (1) it is lacking the potential 9aa TAD, and (2) the presence of its long N-terminal tail has an inhibitory function.

In our study we used primary hASCs as a differentiation model to study the two human MKL1 isoforms. In contrast to bone marrow, adipose tissue constitutes an easily accessible source for large numbers of patient-derived MSCs, which have an enormous potential for future applications in tissue regeneration (Zuk, 2010). Importantly, hASCs were shown to differentiate into CAFs under the influence of tumor-secreted factors such as TGF-β, and to promote the *in vitro* invasiveness of breast cancer cells (Jeon et al., 2010; Jotzu et al., 2011). We found that MKL1_S, but not MKL1_L was strongly upregulated in primary hASCs within 24 h of TGF-β-induced myofibroblast/CAF differentiation. Current models suggest a complex interplay between the Smad3 and the Rho-actin-MKL1 signaling pathways during myofibroblast/CAF differentiation (Charbonney et al., 2011; Masszi et al., 2010; Small, 2012). TGF-β is a known direct inducer of Smad signaling. Several studies also showed that TGF-β up-regulates total MKL1 expression and triggers the nuclear accumulation of MKL1, but not MKL2, in different precursor cells (Gupta et al., 2013; Mihira et al., 2012; Minami et al., 2012; Morita et al., 2007; Sandbo et al., 2011). However, MKL1 only translocates after 24-48 h of TGF-β stimulation, meaning in a strongly delayed fashion compared to direct stimulation of the Rho-actin-MKL1 pathway. To explain the delayed activation, several

models have been suggested that divide TGF-β-induced myofibroblast/CAF differentiation into different phases. Masszi and colleagues (Masszi et al., 2010) suggested that the direct induction of Smad signaling by TGF-β defines an early "Smad-promoted" phase of the myofibroblast differentiation process, in which Smad3 competes with SRF for binding to MKL1 and thus inhibits progression to the later stage (cf. Fig. 8). Sandbo et al. (2011) proposed that TGF-β/Smad signaling induces the transcription of yet unknown factors that indirectly activate the Rho-actin-MKL1 pathway, thus initiating the later phase of differentiation with a delay. We propose in our model (Fig. 8) to term this phase, which includes the expression of SMA and other contractility-promoting proteins, "Rho-actin-MKL1-promoted" phase. Such a mechanism is supported by studies from Fan et al. (2007) and Masszi et al. (2004) who found that for myofibroblastic differentiation of kidney tubular cells an epithelial cell injury is required as a 2nd hit, which directly activates the Rho-actin-MKL1 pathway.

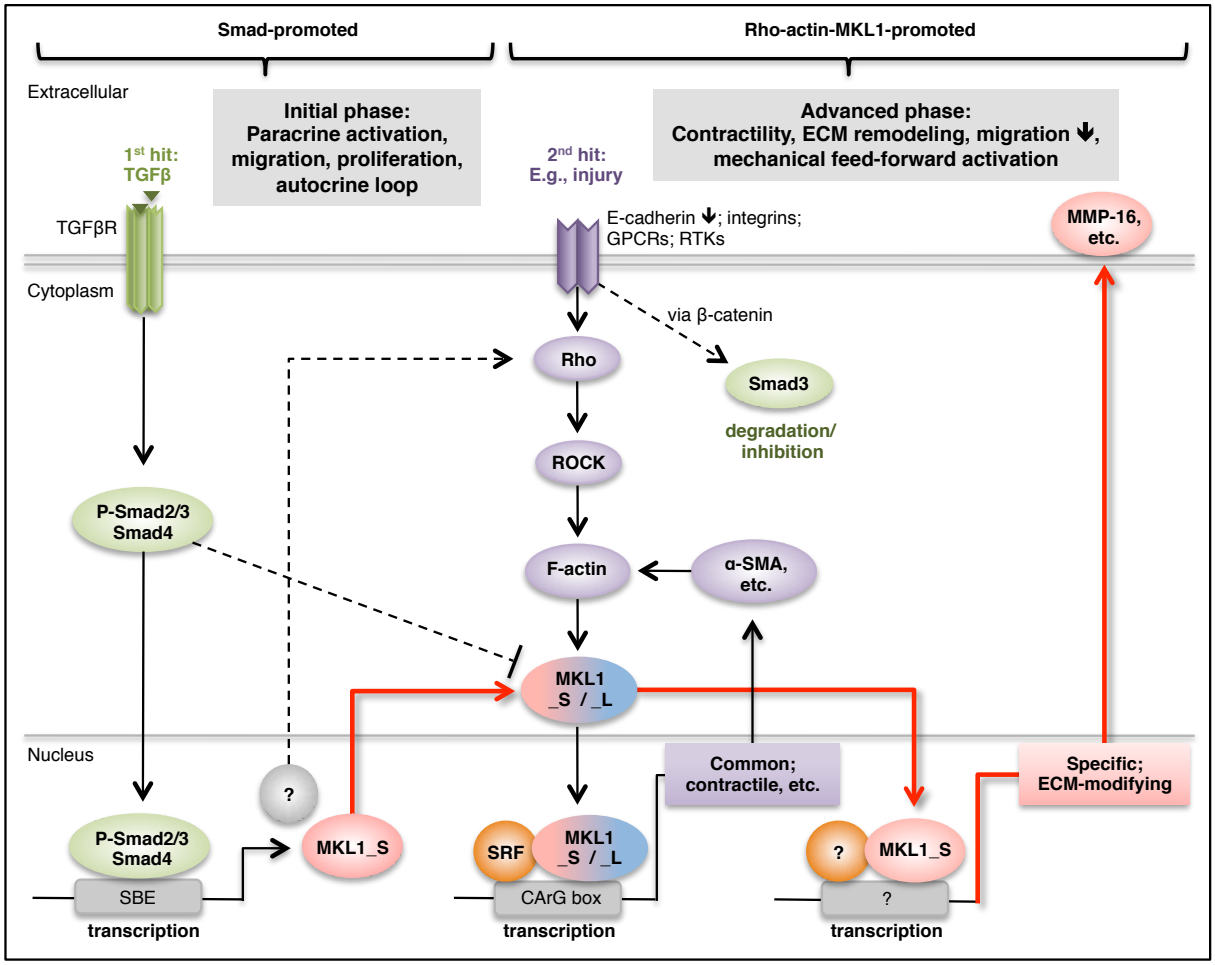

Figure 8. Model for TGF-β-induced myofibroblast/CAF differentiation involving MKL1 isoform-specific activities.

Based on published models that seek to explain the delayed activation of the Rho-actin-MKL1 pathway by TGF-β during myofibroblast/CAF differentiation (Masszi et al., 2010; Sandbo et al., 2011), we propose that MKL1_S is one of the factors whose expression is directly induced by Smad signaling during the initial phase of differentiation. Direct activation of the Rho-actin-MKL1 pathway by a second hit and/or the indirect activation via Smad signaling and MKL1_S induction are then likely to have two consequences. Firstly, the SRF-mediated expression of contractility-promoting smooth muscle-specific genes such as SMA, which is induced by either MKL1 isoform. Secondly, the expression of genes coding for ECM(-modifying) proteins, which is regulated specifically by MKL1_S. We hypothesize that MKL1_S-specific transcription contributes to the progression to the advanced phase of myofibroblast/CAF differentiation involving ECM modifications and the down-regulation of migration.

Our data suggest that one of the factors that is rapidly transcribed by Smad signaling during the initial Smad-promoted phase is the MKL1_S isoform (Fig. 8). As a result, the generally low MKL1_S/MKL1_L ratio is raised significantly. Our gene expression analyses suggest that this results in MKL1_S-specific transcription of genes coding for extracellular proteins, including ECM proteins, proteases, and MMP regulators. In addition to SRF-dependent expression of contractility-promoting proteins, which seemed to be similarly induced by both MKL1 isoforms, the MKL1_S-specific gene regulation is likely to contribute to myofibroblast/CAF-mediated modification of the ECM. The protein products of *MMP-16* and *SPOCK3*, the genes with the strongest MKL1_S-specific up-regulation, are both known to regulate MMP-2 activity (Nakada et al., 2001). The pro-migratory gene *MMP-2* was found to be down-regulated by TGF-β in the later phase of fibroblast transformation into myofibroblasts (Howard et al., 2012). Furthermore, MMP-2 is known to cleave latent TGF-β during the activation process of TGF-β from the ECM (Yu and Stamenkovic, 2000). Thus, MKL1_S might control the activation of MMP-2 and in this way influence the motility of myofibroblasts/CAFs, or their feed-forward activation via mechanical release of latent TGF-β from the ECM and its subsequent activation by MMP-2.

The myofibroblast effector cell type has emerged as the major target for anti-fibrotic therapies (Hinz et al., 2012). Remarkably, inhibition of the mechanosensitive Rho-actin-MKL1 pathway, e.g., by genetic ablation of *MKL1*, was recently found to induce apoptosis in myofibroblasts and to inhibit experimental lung fibrosis (Zhou et al., 2013). Because of its specific and strong up-regulation, the MKL1_S isoform has the potential to become a valuable biomarker for the TGF-β-induced differentiation into myofibroblasts/CAFs. Here, we reported the successful production of an antibody that specifically recognizes this isoform. Our findings also indicate that modulating MKL1 isoform-specific activities might become an important strategy in Regenerative Medicine, e.g., for the engineering of myofibroblast- or smooth muscle-like cells from hASCs. Furthermore, MKL1_S may become a novel target for the pharmacological intervention with persistent myofibroblast activation during fibrosis and cancer.

Acknowledgements

We thank the Functional Genomics Facility of the Friedrich Miescher Institute and Tim Roloff for their help with the transcript profiling and Matthias Chiquet and Richard P. Tucker for critical reading of the manuscript. This work was supported by grants 31003A_120235 and 31003A_135584 from the Swiss National Science Foundation.

Conflicts of interest

The authors declare to have no conflict of interest.

References

Abe, R., S. Donnelly, T. Peng, R. Bucala, and C. Metz. 2001. Peripheral blood fibrocytes: differentiation pathway and migration to wound sites. *Journal of immunology (Baltimore, Md. : 1950)*. 166:7556-7562.

Barsky, S., W. Green, G. Grotendorst, and L. Liotta. 1984. Desmoplastic breast carcinoma as a source of human myofibroblasts. *The American Journal of Pathology*. 115:329-333.

Charbonney, E., P. Speight, A. Masszi, H. Nakano, and A. Kapus. 2011. β-catenin and Smad3 regulate the activity and stability of myocardin-related transcription factor during epithelial-myofibroblast transition. *Molecular Biology of the Cell*. 22:4472-4485.

Chiquet, M., A. Sarasa-Renedo, and V. Tunç-Civelek. 2004. Induction of tenascin-C by cyclic tensile strain versus growth factors: distinct contributions by Rho/ROCK and MAPK signaling pathways. *Biochimica et Biophysica Acta*. 1693:193-204.

Crider, B., G. Risinger, C. Haaksma, E. Howard, and J. Tomasek. 2011. Myocardin-related transcription factors A and B are key regulators of TGF-β1-induced fibroblast to myofibroblast differentiation. *The Journal of Investigative Dermatology*. 131:2378-2385.

Desmoulière, A., A. Geinoz, F. Gabbiani, and G. Gabbiani. 1993. Transforming growth factor-beta 1 induces alpha-smooth muscle actin expression in granulation tissue myofibroblasts and in quiescent and growing cultured fibroblasts. *The Journal of Cell Biology*. 122:103-111.

Dvorak, H. 1986. Tumors: wounds that do not heal. Similarities between tumor stroma generation and wound healing. *The New England Journal of Medicine*. 315:1650-1659.

Fan, L., A. Sebe, Z. Péterfi, A. Masszi, A. Thirone, O. Rotstein, H. Nakano, C. McCulloch, K. Szászi, I. Mucsi, and A. Kapus. 2007. Cell contact-dependent regulation of epithelial-myofibroblast transition via the rho-rho kinase-phospho-myosin pathway. *Molecular Biology of the Cell*. 18:1083-1097.

Forbes, S., F. Russo, V. Rey, P. Burra, M. Rugge, N. Wright, and M. Alison. 2004. A significant proportion of myofibroblasts are of bone marrow origin in human liver fibrosis. *Gastroenterology*. 126:955-963.

Frid, M., V. Kale, and K. Stenmark. 2002. Mature vascular endothelium can give rise to smooth muscle cells via endothelial-mesenchymal transdifferentiation: in vitro analysis. *Circulation Research*. 90:1189-1196.

Gressner, A., and R. Weiskirchen. 2006. Modern pathogenetic concepts of liver fibrosis suggest stellate cells and TGF-beta as major players and therapeutic targets. *Journal of Cellular and Molecular Medicine*. 10:76-99.

Gupta, M., A. Korol, and J. West-Mays. 2013. Nuclear translocation of myocardin-related transcription factor-A during transforming growth factor beta-induced epithelial to mesenchymal transition of lens epithelial cells. *Molecular Vision*. 19:1017-1028.

Hao, H., G. Gabbiani, E. Camenzind, M. Bacchetta, R. Virmani, and M.-L. Bochaton-Piallat. 2006. Phenotypic modulation of intima and media smooth muscle cells in fatal cases of coronary artery lesion. *Arteriosclerosis, Thrombosis, and Vascular Biology*. 26:326-332.

Hinz, B., S. Phan, V. Thannickal, M. Prunotto, A. Desmoulière, J. Varga, O. De Wever, M. Mareel, and G. Gabbiani. 2012. Recent developments in myofibroblast biology: paradigms for connective tissue remodeling. *The American Journal of Pathology*. 180:1340-1355.

Howard, E., B. Crider, D. Updike, E. Bullen, E. Parks, C. Haaksma, D. Sherry, and J. Tomasek. 2012. MMP-2 expression by fibroblasts is suppressed by the myofibroblast phenotype. *Experimental Cell Research*. 318:1542-1553.

Iwano, M., D. Plieth, T. Danoff, C. Xue, H. Okada, and E. Neilson. 2002. Evidence that fibroblasts derive from epithelium during tissue fibrosis. *The Journal of Clinical Investigation*. 110:341-350.

Jeon, E., S. Heo, I. Lee, Y. Choi, J. Park, K. Choi, D.Y. Park, D. Suh, M. Yoon, and J. Kim. 2010. Ovarian cancer-derived lysophosphatidic acid stimulates secretion of VEGF and stromal cell-derived factor-1 alpha from human mesenchymal stem cells. *Experimental and Molecular Medicine*. 42:280-293.

Jeon, E., H. Moon, M. Lee, H. Song, Y. Kim, M. Cho, D.-S. Suh, M.-S. Yoon, C. Chang, J. Jung, and J. Kim. 2008a. Cancer-derived lysophosphatidic acid stimulates differentiation of human mesenchymal stem cells to myofibroblast-like cells. *Stem cells (Dayton, Ohio)*. 26:789-797.

Jeon, E., W. Park, M. Lee, Y. Kim, J. Han, and J. Kim. 2008b. A Rho kinase/myocardin-related transcription factor-A-dependent mechanism underlies the sphingosylphosphorylcholine-induced differentiation of mesenchymal stem cells into contractile smooth muscle cells. *Circulation Research*. 103:635-642.

Jotzu, C., E. Alt, G. Welte, J. Li, B. Hennessy, E. Devarajan, S. Krishnappa, S. Pinilla, L. Droll, and Y.-H. Song. 2011. Adipose tissue derived stem cells differentiate into carcinoma-associated fibroblast-like cells under the influence of tumor derived factors. *Cellular oncology (Dordrecht)*. 34:55-67.

Kozak, M. 1989. Context effects and inefficient initiation at non-AUG codons in eucaryotic cell-free translation systems. *Molecular and Cellular Biology*. 9:5073-5080.

Kurpinski, K., J. Chu, D. Wang, and S. Li. 2009. Proteomic Profiling of Mesenchymal Stem Cell Responses to Mechanical Strain and TGF-beta1. *Cellular and molecular bioengineering*. 2:606-614.

Maier, S., R. Lutz, L. Gelman, A. Sarasa-Renedo, S. Schenk, C. Grashoff, and M. Chiquet. 2008. Tenascin-C induction by cyclic strain requires integrin-linked kinase. *Biochimica et Biophysica Acta*. 1783:1150-1162.

Martin, P. 2009. Common Transactivation Motif 9aaTAD recruits multiple general co-activators TAF9, MED15, CBP and p300. *Nature Precedings*.

Masszi, A., P. Speight, E. Charbonney, M. Lodyga, H. Nakano, K. Szászi, and A. Kapus. 2010. Fate-determining mechanisms in epithelial-myofibroblast transition: major inhibitory role for Smad3. *The Journal of Cell Biology*. 188:383-399.

Mayer, D., and L. Leinwand. 1997. Sarcomeric gene expression and contractility in myofibroblasts. *The Journal of Cell Biology*. 139:1477-1484.

Mihira, H., H. Suzuki, Y. Akatsu, Y. Yoshimatsu, T. Igarashi, K. Miyazono, and T. Watabe. 2012. TGF-β-induced mesenchymal transition of MS-1 endothelial cells requires Smad-dependent cooperative activation of Rho signals and MRTF-A. *Journal of Biochemistry*. 151:145-156.

Minami, T., K. Kuwahara, Y. Nakagawa, M. Takaoka, H. Kinoshita, K. Nakao, Y. Kuwabara, Y. Yamada, C. Yamada, J. Shibata, S. Usami, S. Yasuno, T. Nishikimi, K. Ueshima, M. Sata, H. Nakano, T. Seno, Y. Kawahito, K. Sobue, A. Kimura, R. Nagai, and K. Nakao. 2012. Reciprocal expression of MRTF-A and myocardin is crucial for pathological vascular remodelling in mice. *The EMBO Journal*. 31:4428-4440.

Miralles, F., G. Posern, A.-I. Zaromytidou, and R. Treisman. 2003. Actin dynamics control SRF activity by regulation of its coactivator MAL. *Cell*. 113:329-342.

Morita, T., T. Mayanagi, and K. Sobue. 2007. Dual roles of myocardin-related transcription factors in epithelial mesenchymal transition via slug induction and actin remodeling. *The Journal of Cell Biology*. 179:1027-1042.

Nakada, M., A. Yamada, T. Takino, H. Miyamori, T. Takahashi, J. Yamashita, and H. Sato. 2001. Suppression of membrane-type 1 matrix metalloproteinase (MMP)-mediated MMP-2 activation and tumor invasion by testican 3 and its splicing variant gene product, N-Tes. *Cancer Research*. 61:8896-8902.

Otranto, M., V. Sarrazy, F. Bonté, B. Hinz, G. Gabbiani, and A. Desmoulière. 2012. The role of the myofibroblast in tumor stroma remodeling. *Cell adhesion & migration*. 6:203-219.

Piskacek, S., M. Gregor, M. Nemethova, M. Grabner, P. Kovarik, and M. Piskacek. 2007. Nine-amino-acid transactivation domain: establishment and prediction utilities. *Genomics*. 89:756-768.

Rajkumar, V., K. Howell, K. Csiszar, C. Denton, C. Black, and D. Abraham. 2005. Shared expression of phenotypic markers in systemic sclerosis indicates a convergence of pericytes and fibroblasts to a myofibroblast lineage in fibrosis. *Arthritis Research and Therapy*. 7:23.

Ross, R., N. Everett, and R. Tyler. 1970. Wound healing and collagen formation. VI. The origin of the wound fibroblast studied in parabiosis. *The Journal of Cell Biology*. 44:645-654.

Sandbo, N., A. Lau, J. Kach, C. Ngam, D. Yau, and N. Dulin. 2011. Delayed stress fiber formation mediates pulmonary myofibroblast differentiation in response to TGF-β. *American Journal of Physiology. Lung Cellular and Molecular Physiology*. 301:66.

Sarrazy, V., F. Billet, L. Micallef, B. Coulomb, and A. Desmoulière. 2011. Mechanisms of pathological scarring: role of myofibroblasts and current developments. *Wound repair and regeneration : official publication of the Wound Healing Society [and] the European Tissue Repair Society*. 19 Suppl 1:5.

Sasazuki, T., T. Sawada, S. Sakon, T. Kitamura, T. Kishi, T. Okazaki, M. Katano, M. Tanaka, M. Watanabe, H. Yagita, K. Okumura, and H. Nakano. 2002. Identification of a novel transcriptional activator, BSAC, by a functional cloning to inhibit tumor necrosis factor-induced cell death. *The Journal of Biological Chemistry*. 277:28853-28860.

Selvaraj, A., and R. Prywes. 2004. Expression profiling of serum inducible genes identifies a subset of SRF target genes that are MKL dependent. *BMC molecular biology*. 5:13.

Small, E. 2012. The actin-MRTF-SRF gene regulatory axis and myofibroblast differentiation. *Journal of Cardiovascular Translational Research*. 5:794-804.

Sugimoto, H., T. Mundel, M. Kieran, and R. Kalluri. 2006. Identification of fibroblast heterogeneity in the tumor microenvironment. *Cancer Biology and Therapy*. 5:1640-1646.

van den Bogaerdt, A., V. van der Veen, P. van Zuijlen, L. Reijnen, M. Verkerk, R. Bank, E. Middelkoop, and M. Ulrich. 2009. Collagen cross-linking by adipose-derived mesenchymal stromal cells and scar-derived mesenchymal cells: Are mesenchymal stromal cells involved in scar formation? *Wound repair and regeneration : official publication of the Wound Healing Society [and] the European Tissue Repair Society*. 17:548-558.

Wang, D., P. Chang, Z. Wang, L. Sutherland, J. Richardson, E. Small, P. Krieg, and E. Olson. 2001. Activation of cardiac gene expression by myocardin, a transcriptional cofactor for serum response factor. *Cell*. 105:851-862.

Wang, D.-Z., S. Li, D. Hockemeyer, L. Sutherland, Z. Wang, G. Schratt, J. Richardson, A. Nordheim, and E. Olson. 2002. Potentiation of serum response factor activity by a family of myocardin-related transcription factors. *Proceedings of the National Academy of Sciences of the United States of America*. 99:14855-14860.

Wipff, P.-J., D.B. Rifkin, J.-J. Meister, and B. Hinz. 2007. Myofibroblast contraction activates latent TGF-1 from the extracellular matrix. *Science Signaling*. 179:1311.

Yu, Q., and I. Stamenkovic. 2000. Cell surface-localized matrix metalloproteinase-9 proteolytically activates TGF-beta and promotes tumor invasion and angiogenesis. *Genes and Development*. 14:163-176.

Zheng, L., U. Baumann, and J.-L. Reymond. 2004. An efficient one-step site-directed and site-saturation mutagenesis protocol. *Nucleic Acids Research*. 32.

Zhou, Y., X. Huang, L. Hecker, D. Kurundkar, A. Kurundkar, H. Liu, T.-H. Jin, L. Desai, K. Bernard, and V. Thannickal. 2013. Inhibition of mechanosensitive signaling in myofibroblasts ameliorates experimental pulmonary fibrosis. *The Journal of Clinical Investigation*. 123:1096-1108.

Zuk, P. 2010. The adipose-derived stem cell: looking back and looking ahead. *Molecular Biology of the Cell*. 21:1783-1787.

Supplementary Material

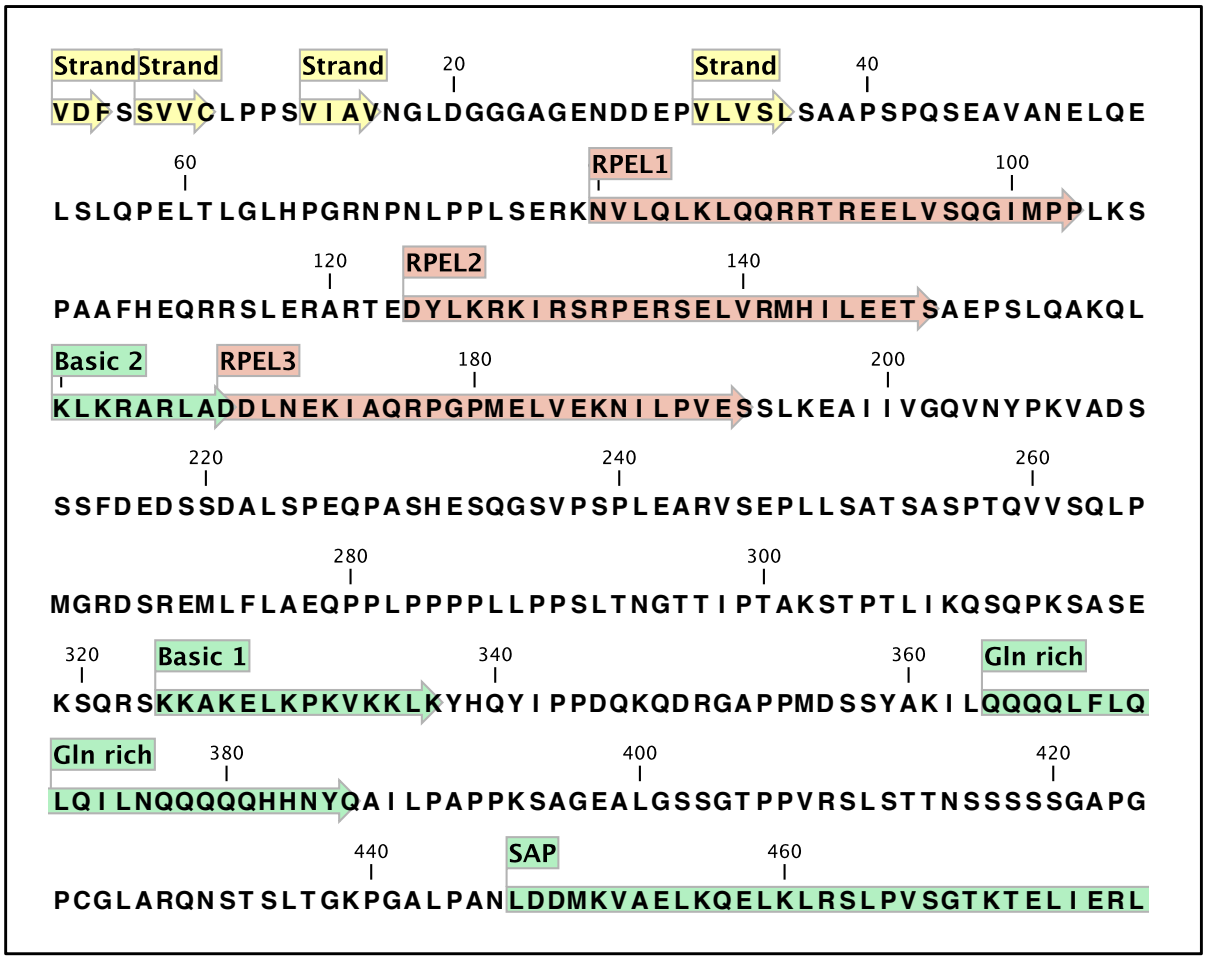

Figure S1: Predicted β-strand secondary structures in MKL1_L (GTG/Val start). Amino acids 1-8 would not be included with the suggested CTG/Leu-92 translation start (Miralles et al., 2003). Amino acids 1-100 would not be included with the published ATG/Met translation start. β-strand secondary structures were predicted with CLC Main Workbench version 6.7.

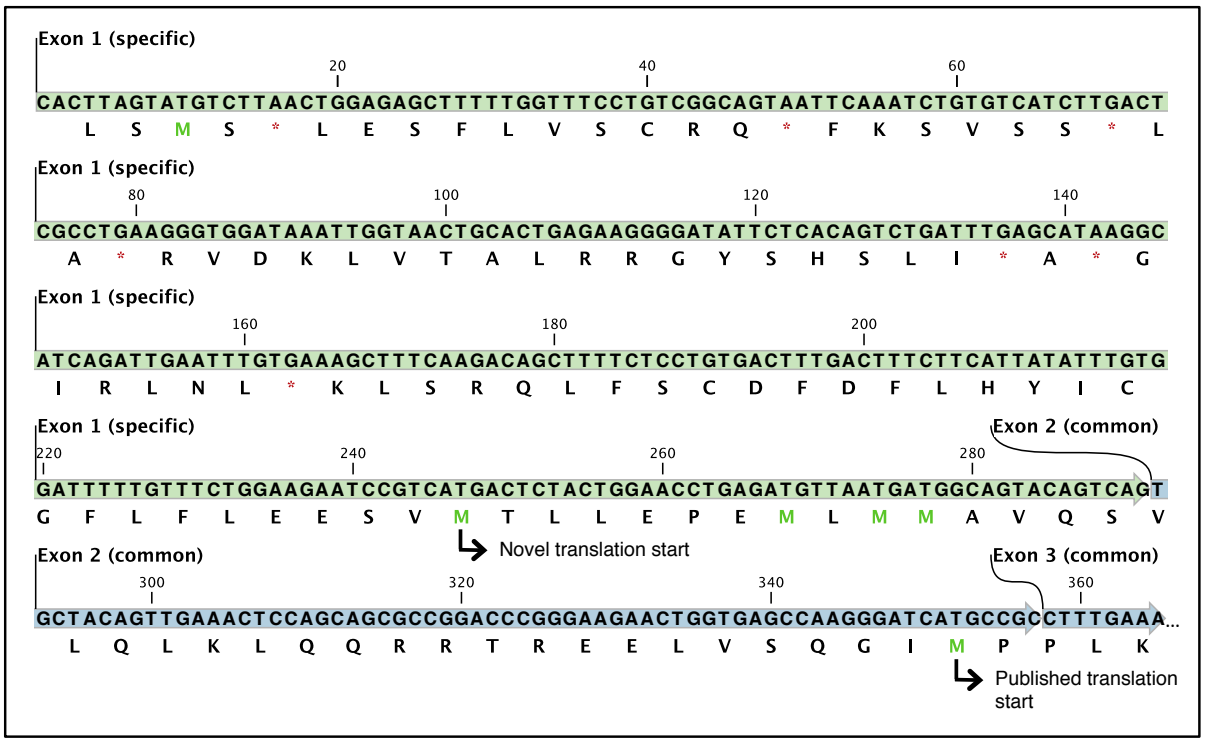

Figure S2. 5' untranslated region (5'UTR) and nucleotide sequence coding for the isoform-specific N-terminal stretch of the novel human MKL1_S isoform.

Sequence obtained in the 5'RACE experiment (Fig. 2A). Green letters: Putative ATG translation initiation codons (coding for Met). Translation is highly probable to start at the first in-frame ATG on the MKL1_S-specific exon1.

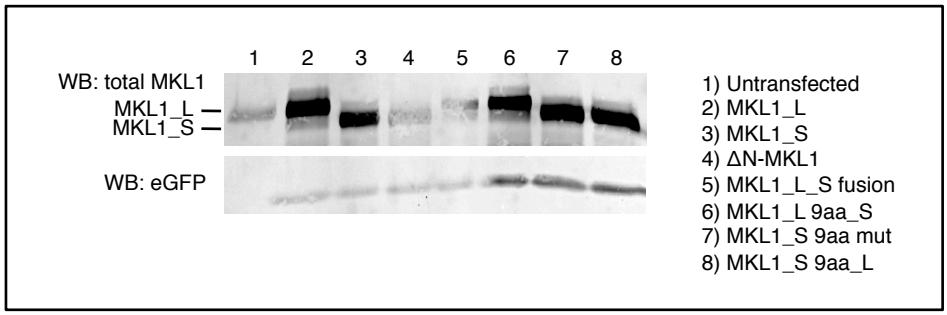

Figure S3. Expression of MKL1 constructs with different N-termini.
The 5'UTR-full length MKL1_L (lane 2) and _S (3) constructs, the construct starting with the published ATG start of MKL1_L (4), or the constructs with alterations or exchange of the predicted 9aa TAD in MKL1_S (5-8) from Fig. 7 were transiently overexpressed in HEK293 cells. Western blot detection with the anti-MKL1 total mAb proves that the constructs 5 and 6, which are expected to start translation at the upstream GTG start codon, indeed migrate at the same size as the MKL1_L isoform (2) and the endogenous MKL1_L isoform (1). Since an eGFP construct in pcDNA3.1 was co-transfected with each of the constructs 2-8, Western Blot detection of eGFP served as control for the successful transfection.

Table S1: Complete list of regulated genes from the gene expression profiling (see Table 1).

Gene name	Description	Fold change [a]	*P* value
Up-regulated with MKL1_S vs. empty vector:			
MMP16	matrix metallopeptidase 16 (membrane-inserted)	**5.86**	1.39E-07
AMBN	ameloblastin (enamel matrix protein)	**5.14**	1.97E-07
SPOCK3	sparc/osteonectin, cwcv and kazal-like domains proteoglycan (testican) 3	**5.04**	8.54E-09
POM121L1P	POM121 membrane glycoprotein-like 1 (rat) pseudogene	**3.89**	2.63E-04
NAP1L3	nucleosome assembly protein 1-like 3	**2.78**	2.44E-06
MKL1	megakaryoblastic leukemia (translocation) 1	**2.41**	3.56E-07
DSEL	dermatan sulfate epimerase-like	**2.33**	1.17E-06
OSTN	osteocrin	**2.23**	3.48E-05
ACTA2	actin, alpha 2, smooth muscle, aorta	**2.02**	2.99E-05
ESRRG	estrogen-related receptor gamma	**1.93**	4.52E-08
MDGA2	MAM domain containing glycosylphosphatidylinositol anchor 2	**1.83**	1.75E-05
DACH2	dachshund homolog 2 (Drosophila)	**1.82**	1.53E-05
TRHDE	thyrotropin-releasing hormone degrading enzyme	**1.79**	3.35E-06
CNN2	calponin 2	**1.67**	6.37E-08
SLC8A1	solute carrier family 8 (sodium/calcium exchanger), member 1	**1.67**	1.71E-05
PDGFD	platelet derived growth factor D	**1.61**	8.28E-06
PGR	progesterone receptor	**1.60**	1.76E-05
RNU5D	RNA, U5D small nuclear	**1.57**	5.53E-04
PPP2R2C	protein phosphatase 2, regulatory subunit B, gamma	**1.52**	3.01E-06
Up-regulated with MKL1_L vs. empty vector:			
POM121L1P	POM121 membrane glycoprotein-like 1 (rat) pseudogene	**5.83**	4.16E-05
MKL1	megakaryoblastic leukemia (translocation) 1	**4.61**	4.29E-09
RPS9	ribosomal protein S9	**4.38**	6.72E-04
AMBN	ameloblastin (enamel matrix protein)	**3.09**	3.65E-06
PCDHA10	Protocadherin alpha-10	**2.58**	2.43E-07
MDGA2	MAM domain containing glycosylphosphatidylinositol anchor 2	**2.43**	9.41E-07
SPOCK3	sparc/osteonectin, cwcv and kazal-like domains proteoglycan (testican) 3	**2.31**	1.61E-06
MMP16	matrix metallopeptidase 16 (membrane-inserted)	**2.30**	4.46E-05
SLC8A1	solute carrier family 8 (sodium/calcium exchanger), member 1	**2.18**	6.58E-07
FABP6	fatty acid binding protein 6, ileal	**2.00**	7.69E-07

ACTA2	actin, alpha 2, smooth muscle, aorta	**1.86**	7.22E-05
NAP1L3	nucleosome assembly protein 1-like 3	**1.86**	1.01E-04
CGB1	chorionic gonadotropin, beta polypeptide 1	**1.78**	7.82E-04
ESRRG	estrogen-related receptor gamma	**1.71**	2.20E-07
NTS	neurotensin	**1.71**	3.39E-05
DACH2	dachshund homolog 2 (Drosophila)	**1.61**	8.04E-05
DSEL	dermatan sulfate epimerase-like	**1.56**	1.45E-04
CGB7	chorionic gonadotropin, beta polypeptide 7	**1.54**	1.84E-07
RORB	RAR-related orphan receptor B	**1.53**	5.71E-05
PDGFD	platelet derived growth factor D	**1.50**	2.62E-05
Down-regulated with MKL1_S vs. empty vector:			
HIST2H2BF	histone cluster 2, H2bf	**-5.11**	1.57E-08
ESRP1	epithelial splicing regulatory protein 1	**-4.20**	2.25E-08
IFI16	interferon, gamma-inducible protein 16	**-2.96**	2.30E-07
MEOX2	mesenchyme homeobox 2	**-2.62**	2.14E-06
PION	pigeon homolog (Drosophila)	**-2.48**	4.25E-05
ZNF730	zinc finger protein 730	**-2.31**	7.67E-06
ZNF737	zinc finger protein 737	**-2.25**	3.18E-07
LGALS8	lectin, galactoside-binding, soluble, 8	**-2.22**	1.14E-04
STS	steroid sulfatase (microsomal), isozyme S	**-2.08**	3.30E-07
MKX	mohawk homeobox	**-2.03**	4.98E-04
ZNF93	zinc finger protein 93	**-2.01**	2.67E-05
HHIP	hedgehog interacting protein	**-2.01**	7.02E-05
DPP4	dipeptidyl-peptidase 4	**-1.97**	5.01E-04
PNPLA4	patatin-like phospholipase domain containing 4	**-1.97**	2.43E-07
SLC6A9	solute carrier family 6 (neurotransmitter transporter, glycine), member 9	**-1.92**	1.02E-04
FAM38B	family with sequence similarity 38, member B	**-1.91**	6.36E-05
PION	pigeon homolog (Drosophila)	**-1.89**	7.68E-04
ODZ1	odz, odd Oz/ten-m homolog 1(Drosophila)	**-1.85**	2.61E-05
ZC3H6	zinc finger CCCH-type containing 6	**-1.85**	2.60E-04
MAP7D2	MAP7 domain containing 2	**-1.77**	3.83E-06
HDHD1A	haloacid dehalogenase-like hydrolase domain containing 1A	**-1.77**	3.21E-07
NMI	N-myc (and STAT) interactor	**-1.76**	2.89E-05
TRPA1	transient receptor potential cation channel, subfamily A, member 1	**-1.75**	2.83E-04

MYOM2	myomesin (M-protein) 2, 165kDa	**-1.74**	1.01E-04
RXRA	retinoid X receptor, alpha	**-1.74**	2.25E-05
DLX5	distal-less homeobox 5	**-1.74**	6.06E-05
HCG8	HLA complex group 8	**-1.73**	1.06E-04
ZNF135	zinc finger protein 135	**-1.72**	3.18E-05
ANKRD7	ankyrin repeat domain 7	**-1.70**	1.98E-04
RERG	RAS-like, estrogen-regulated, growth inhibitor	**-1.69**	5.09E-04
FAM38B	family with sequence similarity 38, member B	**-1.69**	2.34E-04
LAMA2	laminin, alpha 2	**-1.67**	1.82E-05
CPNE7	copine VII	**-1.66**	8.25E-05
ARHGEF9	Cdc42 guanine nucleotide exchange factor (GEF) 9	**-1.66**	1.47E-05
FLJ39632	hypothetical LOC642477	**-1.65**	2.38E-04
ZMAT1	zinc finger, matrin type 1	**-1.65**	4.59E-04
PTPRZ1	protein tyrosine phosphatase, receptor-type, Z polypeptide 1	**-1.64**	1.08E-04
GNG11	guanine nucleotide binding protein (G protein), gamma 11	**-1.64**	1.79E-05
ZNF681	zinc finger protein 681	**-1.64**	6.21E-05
DDR2	discoidin domain receptor tyrosine kinase 2	**-1.63**	1.72E-04
LAMB1	laminin, beta 1	**-1.60**	4.51E-05
PLAC8	placenta-specific 8	**-1.60**	1.33E-04
ASNS	asparagine synthetase (glutamine-hydrolyzing)	**-1.59**	1.26E-05
STYXL1	serine/threonine/tyrosine interacting-like 1	**-1.58**	2.53E-05
TMSL3	thymosin-like 3	**-1.58**	7.47E-06
LOC349196	hypothetical LOC349196	**-1.58**	2.40E-04
DPY19L2P2	dpy-19-like 2 pseudogene 2 (C. elegans)	**-1.58**	4.56E-05
TXLNB	taxilin beta	**-1.58**	4.01E-06
SLC7A11	solute carrier family 7, (cationic amino acid transporter, y+ system) member 11	**-1.57**	3.57E-05
FLRT2	fibronectin leucine rich transmembrane protein 2	**-1.56**	2.20E-04
GRB10	growth factor receptor-bound protein 10	**-1.56**	4.74E-05
RINT1	RAD50 interactor 1	**-1.55**	1.90E-04
SCARNA9	small Cajal body-specific RNA 9	**-1.55**	5.44E-06
NSUN5P2	NOP2/Sun domain family, member 5 pseudogene 2	**-1.54**	4.39E-05
LOC349196	hypothetical LOC349196	**-1.54**	1.83E-04
PPP1R9A	protein phosphatase 1, regulatory (inhibitor) subunit 9A	**-1.54**	3.95E-04
MBNL3	muscleblind-like 3 (Drosophila)	**-1.54**	3.25E-04
ATXN7L1	ataxin 7-like 1	**-1.53**	1.07E-04

CAV1	caveolin 1, caveolae protein, 22kDa	**-1.53**	6.07E-04
ATXN7L1	ataxin 7-like 1	**-1.52**	3.49E-05
MCM3APAS	MCM3AP antisense RNA (non-protein coding)	**-1.52**	8.36E-04
ATXN7L1	ataxin 7-like 1	**-1.52**	2.05E-06
ADAM22	ADAM metallopeptidase domain 22	**-1.51**	4.36E-04
THNSL1	threonine synthase-like 1 (S. cerevisiae)	**-1.51**	7.62E-04
PARVB	parvin, beta	**-1.51**	8.53E-05
SEMA3A	sema domain, immunoglobulin domain (Ig), short basic domain, secreted, (semaphorin) 3A	**-1.50**	3.34E-04
LOC349196	hypothetical LOC349196	**-1.50**	7.57E-05
SLC5A3	solute carrier family 5 (sodium/myo-inositol cotransporter), member 3	**-1.50**	1.59E-04
Down-regulated with MKL1_L vs. empty vector:			
ODZ1	odz, odd Oz/ten-m homolog 1(Drosophila)	**-3.55**	1.00E-07
HIST2H2BF	histone cluster 2, H2bf	**-3.36**	1.68E-07
IFI16	interferon, gamma-inducible protein 16	**-3.35**	9.77E-08
MEOX2	mesenchyme homeobox 2	**-3.15**	5.49E-07
ESRP1	epithelial splicing regulatory protein 1	**-2.88**	2.55E-07
MAP7D2	MAP7 domain containing 2	**-2.77**	4.10E-08
ZNF93	zinc finger protein 93	**-2.61**	2.41E-06
PION	pigeon homolog (Drosophila)	**-2.47**	4.42E-05
LGALS8	lectin, galactoside-binding, soluble, 8	**-2.43**	5.30E-05
FAM38B	family with sequence similarity 38, member B	**-2.24**	1.23E-05
ZNF486	zinc finger protein 486	**-2.20**	7.73E-07
DPP4	dipeptidyl-peptidase 4	**-2.08**	3.06E-04
STS	steroid sulfatase (microsomal), isozyme S	**-2.06**	3.69E-07
MKX	mohawk homeobox	**-2.04**	4.75E-04
RABL2A	RAB, member of RAS oncogene family-like 2A	**-2.03**	4.70E-04
PNPLA4	patatin-like phospholipase domain containing 4	**-1.92**	3.13E-07
SLC7A11	solute carrier family 7, (cationic amino acid transporter, y+ system) member 11	**-1.89**	2.58E-06
ALDH1L2	aldehyde dehydrogenase 1 family, member L2	**-1.88**	1.05E-04
ZNF625	zinc finger protein 625	**-1.88**	3.21E-07
ZNF528	zinc finger protein 528	**-1.85**	4.84E-06
SLC6A9	solute carrier family 6 (neurotransmitter transporter, glycine), member 9	**-1.84**	1.62E-04

ZNF730	zinc finger protein 730	**-1.84**	7.93E-05
STC2	stanniocalcin 2	**-1.82**	7.39E-07
ZNF625	zinc finger protein 625	**-1.82**	1.88E-06
MYOM2	myomesin (M-protein) 2, 165kDa	**-1.80**	6.69E-05
ZNF737	zinc finger protein 737	**-1.78**	4.42E-06
HHIP	hedgehog interacting protein	**-1.74**	3.44E-04
PLAC8	placenta-specific 8	**-1.73**	4.35E-05
TMSL3	thymosin-like 3	**-1.73**	1.90E-06
CNTN4	contactin 4	**-1.72**	1.33E-06
ANKRD7	ankyrin repeat domain 7	**-1.72**	1.62E-04
NRG3	neuregulin 3	**-1.71**	1.48E-05
FLRT2	fibronectin leucine rich transmembrane protein 2	**-1.71**	5.87E-05
RERG	RAS-like, estrogen-regulated, growth inhibitor	**-1.70**	4.59E-04
GPX3	glutathione peroxidase 3 (plasma)	**-1.69**	1.42E-05
TSC22D3	TSC22 domain family, member 3	**-1.69**	3.88E-05
ALDH2	aldehyde dehydrogenase 2 family (mitochondrial)	**-1.68**	1.10E-06
TMSB4X	thymosin beta 4, X-linked	**-1.68**	9.76E-07
TRPA1	transient receptor potential cation channel, subfamily A, member 1	**-1.65**	5.88E-04
ZNF347	zinc finger protein 347	**-1.63**	2.09E-04
TXLNB	taxilin beta	**-1.63**	2.40E-06
SMARCA1	SWI/SNF related, matrix associated, actin dependent regulator of chromatin, subfamily a, member 1	**-1.62**	5.95E-06
HDHD1A	haloacid dehalogenase-like hydrolase domain containing 1A	**-1.60**	1.45E-06
SNORD103A	small nucleolar RNA, C/D box 103A	**-1.59**	2.38E-05
DDR2	discoidin domain receptor tyrosine kinase 2	**-1.58**	2.73E-04
ZNF610	zinc finger protein 610	**-1.58**	9.34E-05
GPR85	G protein-coupled receptor 85	**-1.57**	3.82E-04
ZNF681	zinc finger protein 681	**-1.57**	1.13E-04
ZNF677	zinc finger protein 677	**-1.57**	4.22E-04
FAM38B	family with sequence similarity 38, member B	**-1.56**	6.54E-04
C3orf55	chromosome 3 open reading frame 55	**-1.56**	2.84E-06
GCNT2	glucosaminyl (N-acetyl) transferase 2, I-branching enzyme (I blood group)	**-1.56**	4.10E-04
PRKCH	protein kinase C, eta	**-1.55**	5.86E-04
ID3	inhibitor of DNA binding 3, dominant negative helix-loop-helix protein	**-1.55**	6.06E-07
TAC1	tachykinin, precursor 1	**-1.55**	8.43E-04

PARVB	parvin, beta	**-1.54**	5.61E-05
HSD17B6	hydroxysteroid (17-beta) dehydrogenase 6 homolog (mouse)	**-1.54**	2.79E-05
ZNF135	zinc finger protein 135	**-1.53**	1.72E-04
IFRD1	interferon-related developmental regulator 1	**-1.53**	9.22E-06
ZNF468	zinc finger protein 468	**-1.52**	1.44E-04
LAMB1	laminin, beta 1	**-1.52**	1.13E-04
NMI	N-myc (and STAT) interactor	**-1.51**	2.82E-04
MGC27345	hypothetical protein MGC27345	**-1.50**	1.02E-04
ZNF808	zinc finger protein 808	**-1.50**	5.17E-06
ID1	inhibitor of DNA binding 1, dominant negative helix-loop-helix protein	**-1.50**	8.73E-06
CD99	CD99 molecule	**-1.50**	7.27E-05
Up-regulated with MKL1_S vs. MKL1_L:			
MMP16	matrix metallopeptidase 16 (membrane-inserted)	**-2.54**	1.95E-05
SPOCK3	sparc/osteonectin, cwcv and kazal-like domains proteoglycan (testican) 3	**-2.18**	2.70E-06
OSTN	osteocrin	**-1.92**	1.57E-04
ODZ1	odz, odd Oz/ten-m homolog 1(Drosophila)	**-1.91**	1.79E-05
NRG3	neuregulin 3	**-1.70**	1.53E-05
ADAM21	ADAM metallopeptidase domain 21	**-1.65**	2.95E-05
MAP7D2	MAP7 domain containing 2	**-1.56**	2.49E-05
CNTN4	contactin 4	**-1.54**	8.27E-06
ZNF486	zinc finger protein 486	**-1.51**	1.01E-04
ZNF625	zinc finger protein 625	**-1.50**	9.56E-06
DSEL	dermatan sulfate epimerase-like	**-1.50**	2.87E-04
Up-regulated with MKL1_L vs. MKL1_S:			
MKL1	megakaryoblastic leukemia (translocation) 1	**1.91**	3.79E-06
FABP6	fatty acid binding protein 6, ileal	**1.78**	3.04E-06
HIST2H2BF	histone cluster 2, H2bf	**1.52**	4.70E-04
RXRA	retinoid X receptor, alpha	**1.51**	1.97E-04

[a] Averaged fold-regulations of genes are given with *P*-values in parentheses.

All annotated genes with $P \leq 0.001$ and positive or negative fold change ≥ 1.5 are listed.

Table S2: Sequences of used primers (5' - 3').

Gene name	Forward primer	Reverse primer
Primers for qPCR:		
GAPDH	GGAGTCAACGGATTTGGTC	AAACCATGTAGTTGAGGTC
MKL1_S	TGGCAGTACAGTCAGTGCTACA	GGACTTTTCAAAGGCGGCAT
MKL1_L	ATCCCAATTTGCCTCCACTT	CTTGGCTCACCAGTTCTTCC
MKL1 total	CTCCAGGCCAAGCAGCTG	CCTTCAGGCTGGACTCAAC
MMP-16	GCTACCTTCCACCGACTG	TTCTTCATCCAGTCAATTGTG
SPOCK3	CCCTTCGATCAGGCTTTAG	TGCTTCTTTCATCCTGTGTG
ACTA2/SMA	TGCCTGATGGGCAAGTGA	CTGGGCAGCGGAAACG
CNN1	GCCCAGAAGTATGACCACCA	TGATGAAGTTGCCGATGTTC
Sm22α/transgelin	GGTGGAGTGGATCATAGTGC	ATGTCAGTCTTGATGACCCCA
TNC	CAAGGCAGTGGTGTCTGTGAC	ATCGAGGCCTGTTGTGAAG
Primers for 5'RACE:		
SP1		ACCTGGCCCACAATGATGGCT
SP2		ATGGCTCAGCCGAGGTCTCTT
SP3		GGCTCGAGATAGTCCTCTGTCCTGGC (harboring an XhoI restriction site)

Results

Patent Application

Treating diseases by modulating a specific isoform of MKL1.

Patent Application

Treating diseases by modulating a specific isoform of MKL1.

Scharenberg MA, Sack R, Chiquet-Ehrismann R
Friedrich Miescher Institute for Biomedical Research, Basel, Switzerland

Patent application EP12174531.9, filed on June 29th 2012

Summary of the invention

The present inventors now identified a yet unknown specific isoform of human MKL1, a protein known to be associated with different diseases, e.g., cancer, psoriasis, or fibrosis, in the (de-) differentiation process of muscle cells, such as smooth muscle cells, which are important in the context of coronary artery disease, restenosis, hypertension, and pressure-induced cardiac hypertrophy, and is a part of a mechanosensitive pathway to modulate gene expression, The present inventors found that this specific isoform of human MKL1 is drastically misregulated in diseased tissues as compared to the known, longer isoform of MKL1. The present invention hence provides a method for treating a disease in a subject by modulating an isoform of MKL-1 by administering to said subject a therapeutically effective amount of a modulator of said isoform of MKL1, wherein said isoform of MKL1 comprises the amino acid sequence of SEQ ID NO:1. In some embodiments, said isoform of MKL1 is modulated by an inhibitor. In some embodiments, this inhibitor is an antibody binding to an epitope comprised within SEQ ID NO:2 (the 15 first amino acids of SEQ ID NO:1). In other embodiments, the inhibitor decreases or silences the expression of said isoform of MKL1. In these embodiments, the inhibitor can be a siRNA. In some embodiments of the invention, the subject is a mammal, for instance a human subject. In some embodiments of the invention, the disease to be treated is coronary artery disease, restenosis, hypertension, pressure-induced cardiac hypertrophy. cancer, psoriasis or fibrosis. The present invention also provides a siRNA decreasing or silencing an isoform of MKL1, wherein said isoform of MKL1 comprises the amino acid sequence of SEQ ID NO:1, for use as a medicament to treat cancer, psoriasis or fibrosis.

Furthermore, the present invention also provides an antibody specifically binding to an epitope comprised within SEQ ID NO:2, for use as a medicament to treat cancer, psoriasis or fibrosis. In some embodiments, this antibody inhibits the interaction between said isoform of MKL1 and SRF.

The present invention furthermore provides a method of diagnosing cancer, psoriasis or fibrosis, said method comprising the step of specifically detecting the isoform of MKL1 in a sample obtained from a subject.

In addition, the present invention also provides an isolated nucleic acid comprising (i) a nucleotide sequence coding for the amino acid sequence of SEQ ID NO:1, (ii) or the nucleotide sequence complementary to the nucleotide sequence of (i).

The present invention further provides an isolated nucleic acid comprising (i) a nucleotide sequence coding for the amino acid sequence of SEQ ID NO:2, (ii) or the nucleotide sequence complementary to the nucleotide sequence of (i).

The present invention also provides an isolated amino acid comprising at least 6 contiguous amino acids from SEQ ID NO:2, as well as a recombinant vector comprising a nucleic acid coding for said amino acid sequence.

These and other aspects of the present invention should be apparent to those skilled in the art, from the teachings herein.

SEQ ID NO:1 - Complete amino acid sequence of MKL1_S

SEQ ID NO:2 - Amino acid sequence of the MKL1_S-specific N-terminus

Results

Manuscript II

The SRF coregulator MKL1/MRTF-A interacts with pyruvate kinase M1/M2 in proliferating HEK293 cells.

Manuscript II

The SRF coregulator MKL1/MRTF-A interacts with pyruvate kinase M1/M2 in proliferating HEK293 cells.

Matthias A. Scharenberg, Ismaïl Hendaoui, Ragna Sack, Dominik Zingg, Ruth Chiquet-Ehrismann

Friedrich Miescher Institute for Biomedical Research, Basel, Switzerland

Abstract

Megakaryoblastic leukemia-1 (MKL1/MRTF-A) is a transcriptional coactivator of serum response factor (SRF) and a crucial regulator of actin-mediated motility and the smooth muscle-specific gene transcription program. Recently, MKL1 was shown to be a key player in pathological processes that involve the differentiation into myofibroblast-like cells, such as fibrosis and cancer. Here, we performed a SILAC-based screen for MKL1 interaction partners and identified an interaction with pyruvate kinase M1/M2 (PKM1/2), the rate-limiting enzyme that catalyzes the final pyruvate-producing step of glycolysis. In our experiments we used the HEK293 cell line that almost exclusively expresses the PKM2 isozyme. PKM2 is currently discussed to constitute the major metabolic switch between normal cellular respiration and lactate production found in tumors even in the presence of oxygen, a process known as Warburg effect. The discovered interaction with MKL1 might reveal an unknown link of normal or tumor metabolism to the transcriptional regulation of the actin cytoskeleton and myofibroblast differentiation.

Introduction

Association of the serum response factor (SRF) with members of the myocardin-related transcription factor (MRTF) family has recently been described to regulate the expression of many cytoskeletal, ECM, and contractile genes in a mechano- and growth factor-sensitive manner (Miralles et al., 2003; Wang et al., 2002). The best-studied and most ubiquitously expressed member of this family of SRF coactivators is megakaryoblastic leukemia-1 (MKL1/MRTF-A). Its activity is regulated by the small GTPase Rho and is directly dependent on the polymerization status of the actin cytoskeleton. In quiescent cells, binding to G-actin renders MKL1 inactive, keeping it mainly in the cytosol. Rho-mediated rearrangement of the actin cytoskeleton in response to stimulation from the extracellular environment depletes G-actin and liberates MKL1, which accumulates in the nucleus to activate SRF transcription (reviewed in Posern and Treisman, 2006). The discovery of the Rho-actin-MKL1-SRF pathway established a direct link between changes in the actin cytoskeleton and changes in gene expression, which allows cells to adapt their actin cytoskeleton and motility to signals from their microenvironment (reviewed in Olson and Nordheim, 2010). Although dispensable for embryonic development, MKL1 was shown to have important functions in mechanical stress responses and physiologic and pathologic differentiation processes. Most of these processes relate to the smooth muscle-specific gene program that is controlled by MKL1/SRF, involving the dynamic differentiation and dedifferentiation into myofibroblast-like cells from different precursor cell types (reviewed in Small et al., 2010). One type of myofibroblast-like cells are the cancer-associated fibroblasts (CAFs), which are induced by the tumor cells to differentiate from different precursor cell types, supporting tumor progression (reviewed in Otranto et al., 2012). The Rho-actin-MKL1 pathway emerges as a common pathway that controls myofibroblast/CAF differentiation in response to chemical or mechanical signals from the microenvironment, such as TGF-β or matrix stiffening, respectively (Jeon et al., 2010; Masszi et al., 2010; Minami et al., 2012; Small, 2012). As such, this pathway is of central importance for physiologic tissue repair processes and diseases, such as fibrosis and cancer.

Quiescent cells use glycolysis in the presence of oxygen as the first of 3 steps to fully metabolize glucose and gain more than 30 molecules of ATP, a process called cellular

respiration. The glycolytic process itself is anaerobic and takes place in the cytoplasm. It breaks down a glucose molecule into two pyruvate molecules that can enter the next step of cellular respiration, the citric acid or Krebs cycle in the mitochondria. Here, the carbon framework of the molecules is destroyed to produce CO_2 and high-energy electrons in the form of NADH/$FADH_2$. In the last step, the oxidative phosphorylation, NADH/$FADH_2$ is converted into a proton gradient across the inner mitochondrial membrane by the electron transport chain, which eventually drives ATP production by releasing the energy of the gradient through the ATP synthase transmembrane complex. Oxygen is required as acceptor for the electrons and protons, yielding in water molecules. In the case of an oxygen debt, e.g., during muscle activity, cells switch to anaerobic fermentation, which is a simpler and faster alternative to make ATP. However, in contrast to aerobic respiration, this process only yields two ATP molecules that were produced during glycolysis. The fermentation step that converts pyruvate into lactate is only necessary to recover NAD^+ molecules from NADH for maintaining glycolytic activity. Interestingly, already in the 1920s Otto Warburg described an increased glucose uptake and a shift from cellular respiration to lactic acid fermentation in cancer cells even in the presence of oxygen. This tumor growth-promoting metabolic switch was hence termed the Warburg effect (Koppenol et al., 2011; Warburg, 1956). Till today, the molecular mechanisms that establish the basis for these changes have not been unraveled. Current theories comprise suggestions that mitochondria are damaged in cancer cells, or are left out on purpose, due to their involvement in apoptosis. However, in 2008 Christofk et al. (2008) shed new light on this phenomenon when they found that expression of the M2 isoform of the glycolytic enzyme pyruvate kinase allows the specific switch to higher glucose consumption and increased lactate production in cancer cells. When they replaced the M2 isoform by the highly similar M1 isoform that is hardly expressed in rapidly proliferating cells, tumor cells failed to grow. This and other findings renewed the interest in cancer metabolism in the past years. Pyruvate kinase (PK) catalyzes the last and rate-limiting step of glycolysis, the transfer of a phosphate group from phosphoenolpyruvate (PEP) to ADP, yielding in one molecule of pyruvate and one molecule of ATP. In humans, there are four pyruvate kinase isozymes. In addition to the M1 and M2 isoforms, which only differ in 22 amino acids due to the differential splicing of exons 9 and 10, the L isoform is expressed in the liver and kidney and the R isoform in erythrocytes. The PKM1 isoform is mostly expressed in

differentiated tissues with low proliferation but high energy consumption, such as the brain or the muscles (reviewed in Mazurek, 2012). This isoform was found to be a constitutively active tetramer, which by interacting with other enzymes from the glycolytic enzyme complex guarantees that pyruvate is channeled into the highly efficient cellular respiration process (Mazurek et al., 2001). The PKM2 isoform is expressed as a tetramer in some differentiated tissues (e.g., in the lung). It is also mainly found as a tetramer in normal proliferating cells. However, in tumor cells PKM2 mainly exists in a dimeric form that is not associated with other glycolytic enzymes and channels pyruvate preferably into lactic acid fermentation (Christofk et al., 2008; Gumińska et al., 1997; Imamura et al., 1986). Therefore, pyruvate kinase regulation in cancer cells differs strongly from normal tissues. Importantly, the PKM2 dimer shows only low affinity for the substrate PEP and thus slows down glycolysis, resulting in an accumulation of glycolytic intermediates. These are required in dividing cells to generate nucleotides, amino acids, and lipids, the building blocks of new cells. Thus, expression of the M2 isoform in proliferating cells facilitates a precise regulation of catabolic energy production versus anabolic, biosynthetic processes, and thereby seems to promote tumor growth (reviewed in Mazurek et al., 2005).
Here, we identified an interaction between PKM2 and the transcriptional coactivator MKL1 in proliferating cells by a SILAC-based screen for MKL1 interaction partners. This interaction might represent a novel link between PKM2-mediated cancer metabolism and MKL1-mediated actin motility or myofibroblast/CAF differentiation.

Material and methods

Plasmid constructs

The published human MKL1 cDNA (NM_020831) encoding the MKL1_L isoform and ending with the stop codon was amplified from total RNA of human brain (ams Biotechnology, Bioggio-Lugano, Switzerland) and cloned into the pcDNA3.1 expression vector (Life Technologies, Zug, Switzerland). The translated protein starts at Val-100 of the published protein sequence, as described in the manuscript “The initial phase of TGF-β-induced myofibroblast differentiation involves specific regulation of two MKL1/MRTF-A isoforms”.

Antibodies

A monoclonal antibody against total human MKL1 (recognizing both isoforms, MKL1_L and MKL1_S) was generated as described in the manuscript "The initial phase of TGF-β-induced myofibroblast differentiation involves specific regulation of two MKL1/MRTF-A isoforms". Immunoglobulins were purified from cell culture supernatant of a positive hybridoma clone via ProteinG-Sepharose 4 Fast Flow (GE Healthcare, Otelfingen, Switzerland) following the manufacturer's instructions. Anti-PKM1/2 (C5E6) antibody was purchased from Cell Signaling.

Cell culture and Stable Isotope Labeling with Amino acids in Cell culture (SILAC)

HEK293 cells (EcR293 variant) were obtained from Life Technologies/Invitrogen (Zug, Switzerland). Cells were cultured at 37 °C and 6 % CO_2 in Dulbecco's Modified Eagle Medium (D-MEM; Seromed, Basel, Switzerland) containing 10 % fetal calf serum (FCS; Life Technologies/Gibco, Zug, Switzerland). Cells were transfected with the plasmids using jetPEI™ (Polyplus-transfection SA, Illkirch, France). For generating constitutively expressing cell lines, cells were selected with 800 µg/ml G-418 (Roche, Basel, Switzerland) and pooled clones were cultured in the presence of 200 µg/ml G-418. For SILAC labeling, cells were maintained in either R0K0 (light) or R6K4 (heavy) medium (Dundee Cell Products) supplemented with 10 % dialyzed FCS (Life Technologies/Invitrogen). Cell passaging was performed using trypsin-free cell dissociation buffer (Life Technologies/Invitrogen). After six passages on SILAC medium, full incorporation of the labeled amino acids was confirmed by liquid chromatography-mass spectrometrical (LC-MS) quantification.

Affinity purification for SILAC-based quantification

HEK293 cell lines stably transfected with the empty vector control or the MKL1_L construct were differentially labeled by SILAC. Cells of each cell line were seeded on 6x 15 cm diameter plastic tissue culture dishes (Greiner Bio-One, Kremsmünster, Austria) and grown to a confluency of 80 %. Cells were scraped off and intracellular protein complexes were fixed by resuspending the cells in 0.8 % formaldehyde/PBS for 10 min. To inactivate formaldehyde, cells were pelleted and resuspended in 0.16 M Tris, pH 7.4

for 10 min. The cell lines were lysed separately in RIPA buffer (50 mM Tris pH 8.0, 150 mM NaCl, 1 % NP-40, 0.5 % sodium deoxycholate, 0.1 % SDS, 1 mM EDTA) and the total protein amounts in both lysates were determined by measuring the optical density at 280 nm. Same protein amounts from both cell lines were combined and subjected to affinity purification of MKL1 complexes. For this procedure, purified anti-MKL1 monoclonal antibody had been coupled to $CNBr^{-}$-activated Sepharose beads 4B (GE Healthcare, Otelfingen, Switzerland) according to the manufacturer's instructions and had been poured into a purification column. The column was equilibrated with 3 cycles of elution buffer (0.2 M Glycine-HCl, pH3) and loading buffer (TST buffer = 50 mM Tris, pH 7.6; 150 mM NaCl; 0.05 % Tween20). The combined whole cell extract of the SILAC-labeled cell lines was diluted 1:2 in loading buffer and run over the column for 2 h at room temperature (RT). After washing with RIPA buffer, retained proteins were eluted in 0.5 ml fractions with elution buffer and neutralized immediately with 1 M Tris solution. Protein-containing fractions were pooled, TCA precipitated, and resuspended in Laemmli buffer/100 mM DTT. Cysteine residues were alkylated with 200 mM iodoacetamide for 45 min at RT in the dark. To avoid full reversal of the formaldehyde cross-linking, the proteins in the sample were gently denaturated at 70 °C for 10 min, before separation of the protein complexes via SDS-PAGE (NuPAGE 4-20 % Bis-Tris gels; Life Technologies/Invitrogen). The samples from each experiment, forward and reverse, were separated as single lanes on the gel and subsequently cut into 12 similarly sized slices for the quantitative analysis.

Mass spectrometric quantification

The samples that were excised from the polyacrylamide gels were washed once with 25 mM NH_4HCO_3 and twice with 25 mM NH_4HCO_3/acetonitrile (1:1) each for 30 min at RT, and then digested with 100 ng trypsin (Promega) in 55 µL 25 mM NH_4HCO_3 overnight at 37 °C. Peptides were extracted from the gel pieces with acetonitrile (final concentration 50 %) and analysed by LC-Mass Spectrometry with an LTQ Orbitrap Velos instrument (Thermo Fisher Scientific). Relative quantification was performed using Proteome Discoverer (version 1.3.0.339, Thermo Scientific) with the following parameters:

For peak determination: S/N > 2, 0.75 ppm mass precision within scan
Min. quan value threshold : 10000
Replace missing quan values with min intensity: true
Use single peak quan channels: true
Reject all quan values if not all quan channels are present: true
Mascot score: 15 and higher

The results were transferred into Microsoft Excel for further processing. Non-identical amounts of total protein from the original cell lines that were combined before the affinity purification result in heavy/light ratios that differ from 1, even for proteins that were unspecifically purified ("background" proteins). Therefore, for each experiment the determination of a normalization factor was required, with which all ratios of the experiment were corrected. Keratins, trypsin, and other contaminants were manually excluded and only proteins with at least two quantified heavy/light peptide pairs were considered for the calculation. The median of all ratios of the remaining proteins from an experiment was applied as the normalization factor. Protein ratios determined in a single sample are given as the median of the corresponding peptides ratios. For proteins that were identified in more than one sample, the heavy/light (H/L) ratio was weighted according to the formula

$$\text{H/L ratio} = \frac{\sum_{i=1}^{n} \text{H/L ratio}(i) \times \text{H/L count}(i)}{\sum_{i=1}^{n} \text{H/L count}(i)}$$

with n as the number of bands in which the protein was identified, and H/L count as the number of peptide ratios that were used to calculate a particular protein ratio. Log_2 values of the heavy/light protein ratios were calculated for each, the forward and the reverse experiment, and compiled in a scatter plot. True MKL1 interaction partners are expected in the lower right quadrant of the plot with the forward experiment on the x-axis, showing more than 2-fold enrichment with the MKL1 overexpressing cell line over the empty vector control cell line in each experiment. However, due to the non- or only partly reversed crosslinking, a preservation of intact complexes with MKL1 was assumed. Therefore, proteins were only considered as potential interaction partners if they appeared in at least one of the samples s1-s3, which correspond to the size of MKL1 and above.

Co-immunoprecipitation

HEK293 cells stably overexpressing MKL1_L were lysed in RIPA buffer (50 mM Tris-HCl ph 7.4, 1 % Triton-X-100, 25 mM Hepes, 150 mM NaCl, 0.2 % sodium deoxycholate, 5 mM $MgCl_2$) supplemented with protease inhibitors (Complete EDTA-free, Roche, Basel, Switzerland) and phosphatase inhibitors (PhosSTOP, Roche). 2.5 mg of whole cell extract were pre-cleared with 1.5 mg Protein G Dynabeads (Life Technologies/Invitrogen, Zug, Switzerland) for 1 h at 4 °C. From the precleared extracts, MKL1 was immunoprecipitated by incubating with 2.5 µg of anti-MKL1 total mAb overnight at 4°C. Total mouse IgG2A (Santa Cruz) served as isotoypic negative control. Immunoglobulin complexes were immobilized with 1.5 mg of Protein G Dynabeads for 1 h at 4 °C. After washing with RIPA buffer, the complexes were eluted in denaturing Laemmli sample buffer and separated by 4-15 % gradient SDS-PAGE (Mini-PROTEAN precast gel, Bio-Rad), with 20 µg of whole cell extract as input control. Subsequently, the proteins were transferred to a BioTrace PVDF membrane (PALL LifeSciences, Pensacola, FL, USA) and immunostained with the anti-PKM1/2 or the anti-MKL1 antibody. Visualization of the proteins of interest was achieved by using horseradish peroxidase-coupled secondary antibodies (Life Technologies/Invitrogen). In the case of anti-PKM1/2, Veriblot anti-rabbit (Abcam, Cambridge, UK) substituted the secondary antibody to avoid staining of the immunoglobulin heavy chain from the IP. Stained protein bands were detected on x-ray films (Fujifilm) by incubating with Western Bright Sirius ECL solution (Advansta).

Results

PKM1/2 emerges as a candidate MKL1 interaction partner from a SILAC-based screen

MKL1 is a known transcriptional coactivator of SRF and is inhibited by binding to G-actin. However, apart from these major molecular interactions, MKL1 has been speculated to bind to other transcription factors in the nucleus or to cross-talk with components of other signaling pathways in the cytoplasm. Therefore, we screened for putative MKL1 interaction partners by using Stable Isotope Labeling by Amino Acids in

Cell Culture (SILAC)(Ong et al., 2002). This method is based on the labeling of all cellular proteins with heavy stable isotopes, such ^{13}C or ^{15}N. In contrast to chemical labeling techniques, this is accomplished to 100 %. Essential amino acids that cannot be synthesized by the cells themselves are added to the growth medium, containing either the common light isotopes or the heavy isotopes. Since the cells are dependent on the supplied amino acids for the synthesis of new proteins and to proliferate, the modified amino acids are incorporated to at least 50 % with each cell doubling. We labeled MKL1 overexpressing HEK293 cells and the empty vector-transfected control cells with normal lysine and arginine (R0K0) or a 4 Da heavier lysine and a 6 Da heavier arginine (R6K4)(see Fig. 1). After maintaining the cells in this medium for 6 passages, we confirmed the complete incorporation of these amino acids into cellular proteins by LC-MS quantification of peptides with the physiological masses versus peptides with 4 or 6 Da higher masses. Due to the usage of lysine and arginine labeling, protein digestion with trypsin yields in peptides that each contains a single labeled amino acid. A great advantage of the SILAC system is the possibility to process proteins that originate from different cell lines together, to exclude any bias from the purification process. We fixed protein complexes within the cells by adding 0.8 % formaldehyde, lysed both stably expressing cell lines, and combined same amounts of total protein. We then purified MKL1-containing protein complexes via anti-MKL1 antibody-coupled sepharose beads. Eluted protein complexes were separated according to their size via SDS-PAGE and the resulting gel was divided into 12 slices (s1-s12). After tryptic digest peptides were extracted from the gel slices and subjected to LC-MS quantification.

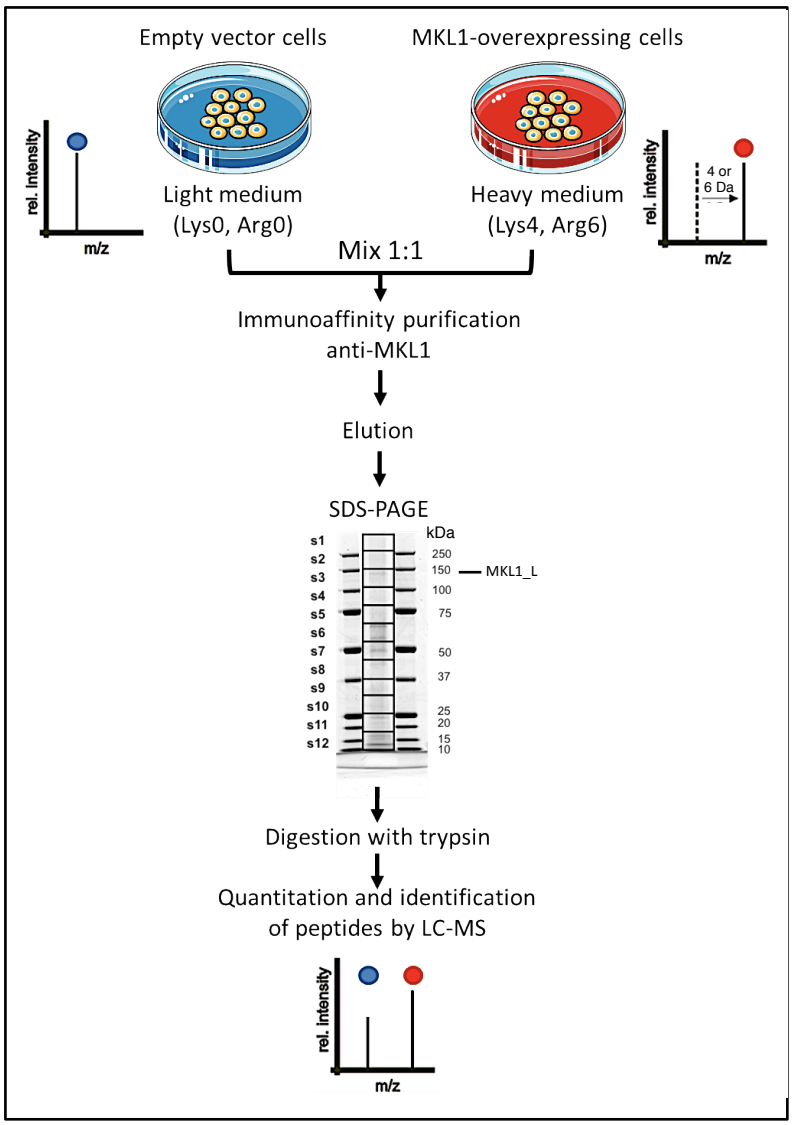

Figure 1. Strategy for the identification of interaction partners of human MKL1.

For the forward experiment, HEK293 cells stably transfected with the empty vector control were grown on SILAC medium containing the 'light' amino acids arginine and lysine (R0K0), whereas cells overexpressing MKL1_L were grown on medium containing 'heavy' isotope-arginine and -lysine (R6K4). Cells were maintained in these media for 6 passages before full incorporation of the labeled amino acids into proteins was confirmed by LC-MS quantification. Equal amounts of total protein from cell lysates of both cell lines were combined and purified via affinity purification using a monoclonal antibody against MKL1. SDS-PAGE-separated proteins were divided into 12 gel fractions (s1-s12) and individually subjected to trypsin digestion and LC-MS quantification. Lysine containing peptide pairs with a mass difference of 4 Da or arginine-containing peptide pairs with a mass difference of 6 Da were quantified for their relative intensity. Quantification yields in a 'heavy'/'light' ratio that represents the relative amounts of co-purified proteins from the original cell lines.

Since the heavy or light labeling of each protein indicated its cell line of origin, the heavy/light ratio allowed the identification of proteins that were preferentially purified together with MKL1. Proteins with a ratio of 1 were unspecifically co-purified with MKL1, e.g., by binding to the beads. Proteins with a ratio clearly different from 1 are candidate interaction partners. To avoid false positive hits, we reversed the experimental setup in a second experiment, in which we labeled the MKL1 overexpressing cells with the 'light' amino acids, and the empty vector cell lines with the 'heavy' amino acids (Fig. 2A). Using the $\log_2$ values of the heavy/light protein ratio, for true MKL1 interaction partners we would expect positive values in the forward experiment and negative values in the reverse experiment, placing them in the lower right quadrant of a scatter plot with the forward experiment on the x-axis (Fig. 2B). Conversely, proteins with negative $\log_2$ heavy/light ratios in the forward experiment and positive values in the reverse experiment would "interact" with the negative control, the empty vector. No proteins located in the corresponding upper left quadrant of the scatter plot, as had been expected since the empty vector does not produce any protein product (Fig. 2C).

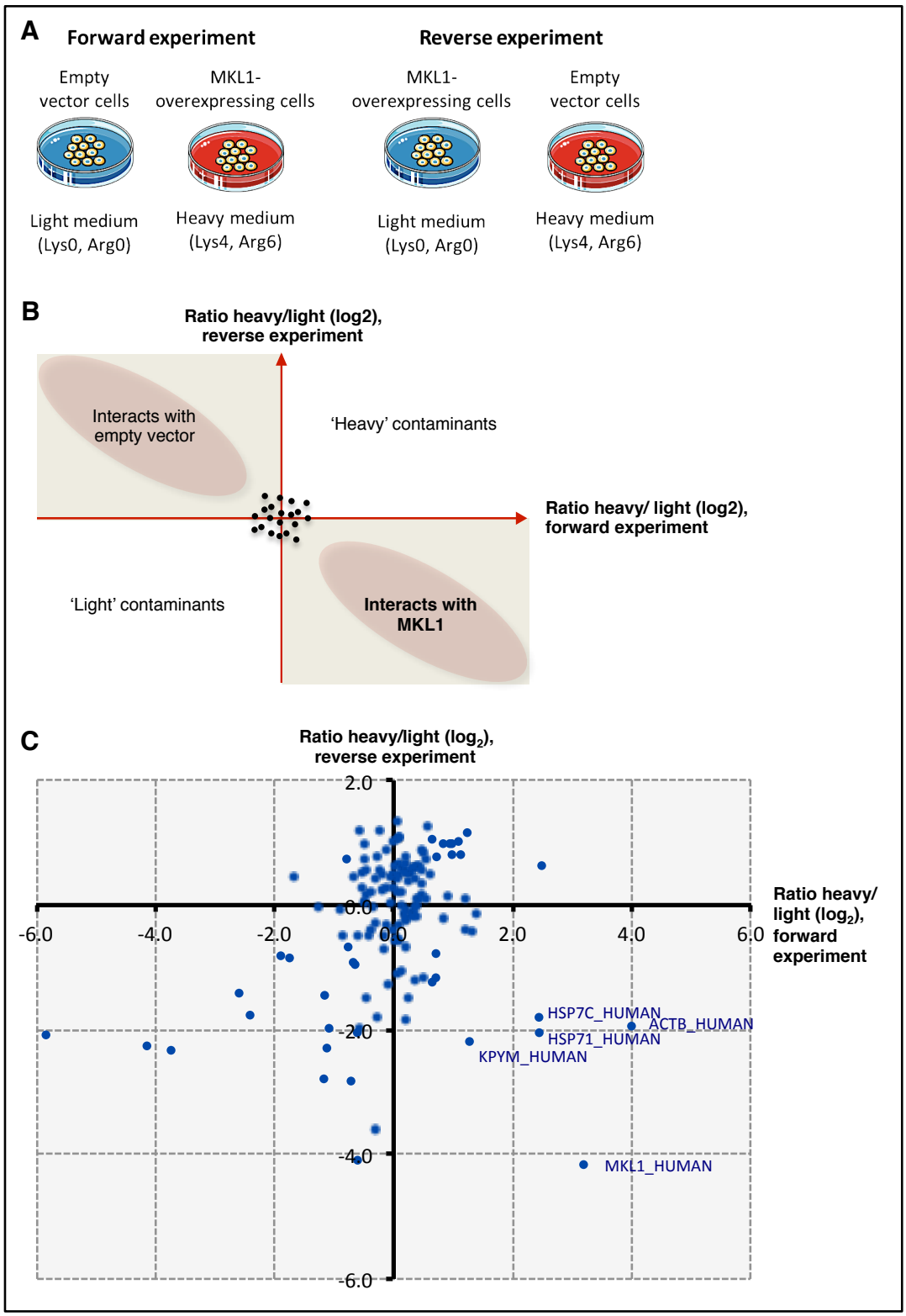

Figure 2. Identification of putative interaction partners of MKL1_L.

A) Experiments were performed as described in Fig. 1. For the reverse experiment, MKL1 overexpressing cells were grown on 'light' medium and empty vector cells were grown on 'heavy' medium. **B)** Calculating the $\log_2$ ratios, interaction partners of MKL1 would yield a positive heavy/light ratio in the forward experiment and a negative heavy/light ratio in the

reverse experiment, localizing in the lower right quadrant of the scatter plot. **C)** Scatter plot summarizing the results of the forward and reverse experiments. All proteins are labeled that were quantified with a heavy/light ratio of ≥ 2 in the forward experiment and a ratio ≤ 0.5 in the reverse experiment, reflecting an enrichment of at least 2-fold in the MKL overexpressing cells over the empty vector control cells.

However, the majority of proteins that clearly deviate from the cloud of identified proteins around ratio 1 located to the lower left quadrant, indicating an enrichment of the light version of a protein, independent of the way of labeling. These proteins are likely to be unspecific, unlabeled contaminations. Conversely, we found no proteins that were strongly enriched in the heavy form in both experiments. MKL1 itself located to the lower right quadrant, proving that both the labeling and the purification of MKL1 worked well in both experiments. Due to the non- or only partly reversed cross-linking, a preservation of intact complexes with MKL1 was assumed. Therefore, proteins were only considered as potential interaction partners if they appeared in samples s1-s3, which correspond to the size of MKL1 and above. Candidate interaction partners that fulfilled these conditions are given in Table 1.

Accession	MW [kDa]	H/L ratio	H/L count	Description
MKL1_HUMAN	98.86	**9.22** ***0.06***	101 *113*	(Q969V6) MKL/myocardin-like protein 1
ACTB_HUMAN	41.71	**15.92** ***0.26***	35 *35*	(P60709) Actin, cytoplasmic 1
KPYM_HUMAN	57.90	**2.43** ***0.22***	8 *7*	(P14618) Pyruvate kinase isozymes M1/M2
HSP71_HUMAN	70.01	**5.44** ***0.24***	23 *25*	(P08107) Heat shock 70 kDa protein 1A/1B
HSP7C_HUMAN	70.85	**5.42** ***0.29***	16 *20*	(P11142) Heat shock cognate 71 kDa protein

Table 1. Summary of the identification of putative MKL1 interaction partners.
SILAC/LC-MS-based quantification of proteins that were co-purified with overexpressed MKL1 in HEK293 cells. All proteins are listed that were quantified with a heavy/light ratio of ≥ 2 in the forward experiment and a ratio ≤ 0.5 in the reverse experiment, reflecting an enrichment of at least 2-fold in the MKL overexpressing cells over the empty vector control cells. H/L ratio = heavy/light ratio, meaning ratio of R6K4 (heavy)-labeled to R0K0 (light)-labeled peptides. H/L count, number of identified heavy-/light-labeled peptide pairs for each protein. Italic numbers represent the results of the reverse experiment.

The heavy/light count for each protein is a hint for the relative abundance of the protein within the sample. Among the candidates is the known MKL1 binding partner β-actin. Novel candidates for MKL1 interaction partners are two proteins of the family of heat shock proteins, heat shock 70 kDa protein 1A/1B and heat shock cognate 71 kDa protein, and the pyruvate kinase isozymes M1/M2. Heat shock proteins are part of the cellular stress response machinery. They act as chaperones, helping other proteins to fold properly and thereby preventing the aggregation of incorrectly folded proteins. In our experiments we compared a cell line that overexpressed the MKL1 protein with a cell line that was transfected with the same plasmid vector, but did not overexpress any protein (empty vector control). It seems probable that the co-purification of the heat shock proteins with MKL1 rather reflects a cellular response to the MKL1 overexpression than specific interactions. Therefore, the pyruvate kinase isozymes M1/M2 emerged as the most promising candidate for a novel MKL1 interaction partner from our screen.

PKM1/2 interacts with MKL1 in HEK293 cells

To confirm the interaction between MKL1 and pyruvate kinase, we performed protein complex immunoprecipitation (Co-IP) experiments. Since endogenous MKL1 in general has a very low abundance in the cell, we used the MKL1_L-overexpressing HEK293 cell line. For the immunoprecipitation of MKL1 from whole cell extracts, we used a monoclonal antibody against a common region of both MKL1 isoforms that was described in the manuscript "The initial phase of TGF-β-induced myofibroblast differentiation involves specific regulation of two MKL1/MRTF-A isoforms."

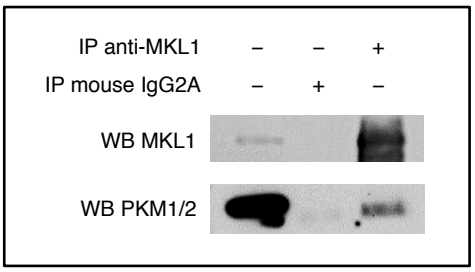

Figure 3. Confirmation of PKM1/2 as an interaction partner of MKL1.
Whole cell lysate from HEK293 cells stably overexpressing MKL1 was either directly applied to Western Blotting (WB) analysis, or after immunoprecipitation (IP) with an isotypic control antibody or a monoclonal antibody against MKL1. Immune staining of the precipitated proteins was performed using the same antibody against MKL1 (WB MKL1), or an antibody targeting the M2 isoform of pyruvate kinase (WB PKM1/2). The exposure time for WB MKL1 was strongly reduced in comparison to WB PKM1/2 to enable visualization of precipitated MKL1 protein. A representative experiment of 3 independent experiments is shown.

Figure 3 shows that only in the case of the immunoprecipitation with anti-MKL1 antibody, but not with the isotypic control antibody, we detected PKM1/2 at the same size as in the input control. This proves that PKM1/2 was specifically purified as part of a complex with MKL1 in the cells. Thus, we confirmed the interaction of MKL1 with pyruvate kinase M1/M2, which we identified as a candidate interaction partner from a two-way SILAC-based screen, in Co-IP experiments.

Discussion

We identified pyruvate kinase (PK) M1/M2 as a novel interaction partner of MKL1. This interaction might reveal a yet unknown connection between actin-mediated gene expression and the glucose metabolism of the cell. We found PKM1/2 in a SILAC-based screen for MKL1 binding partners after formaldehyde cross-linking in proliferating HEK293 cells. In addition to PKM1/2, only few other proteins co-purified with MKL1 in both the forward and the reverse labeled experiment. These proteins comprised β-actin, the major direct inhibitor of MKL1 and two members of the family of heat shock proteins. As indicated before, the binding of the heat shock protein family members could be part of an unspecific cellular stress response to the overexpression of MKL1. Together with β-actin, the heat shock 70-kDa protein 1L and the heat shock cognate 71-kDa protein were also identified as components of the IMP1 ribonucleoprotein granules in HEK293 cells (Jønson et al., 2007), which could also explain their enrichment together with MKL1 and its binding partner β-actin in these cells. Therefore, the identified members of the heat shock family are unlikely to specifically bind to MKL1. Although β-actin is highly abundant in the cell and thus, its ratio in a SILAC-based screen is likely to be "diluted" with unspecifically bound β-actin from both cell lines, we obtained high fold-changes for β-actin in both-way experiments. This was expected due to the specific binding of up to five molecules of the highly abundant globular β-actin to MKL1 (Mouilleron et al., 2011) and therefore justified our screening approach. However, the other well-known binding partner of MKL1, serum response factor (SRF), was not co-purified with our screening approach. This might be due to the low abundance of endogenous SRF, which is likely to be even decreased under cross-linking conditions due to a loss of SRF by cross-linking to the DNA. Moreover, we cross-linked the cellular protein complexes under conditions in which MKL1 was mostly cytosolic, and therefore SRF was not expected to be significantly co-purified with MKL1. For pyruvate kinase M1/2, we detected at least seven peptide pairs in each experiment, with average fold increases of 2.4 (forward) and 4.6 (reverse) compared to the empty vector control. Together with the specific co-purification with MKL1 in our Co-IP experiments, these data establish PKM1/2 as a novel MKL1 interaction partner.

MKL1 exists in two isoforms that differ in their transcriptional activity (see Manuscript 1). Here, we overexpressed MKL1_L, the longer isoform that is made from an upstream

GUG translation start codon (see Manuscript 1). Whether MKL1_S equally binds to PKM1/2 will need to be examined. Moreover, further investigations are required to find out if MKL1 interacts with both PKM isoforms, PKM1 and PKM2, or if this interaction is specific for the M2 isozyme that has specific functions in cancer metabolism. However, a cancer-specific switch from PKM1 to PKM2 expression is still a matter of discussion. Bluemlein et al. (2011) compared tumor-derived with normal tissues and cell lines by mass spectrometry and found no evidence for this shift. In fact, in most tissues and cell lines they found PKM2 to be the major isoform. In the experimentally transformed HEK293 cell line, they determined 96-97 % of total pyruvate kinase were expressed as the M2 isoform. Here, we used the EcR293 cell line, a variant of this embryonic kidney-derived cell line. Therefore, the probability that we identified PKM2 as the interaction partner of MKL1 is high. However, this will need to be confirmed, e.g., by using a PKM2-specific antibody in Co-IP experiments. In case that MKL1 indeed interacts exclusively with PKM2, one important question will be whether MKL1 binds to the glycolytic tetrameric form of PKM2 that is found in normal cells, or to the dimeric form that seems to enable anabolic processes in cancer cells. Several allosteric activators and inhibitors of PKM2 have been identified that regulate the equilibrium between dimeric and tetrameric form and thus PKM2 and glycolytic activity (reviewed in Gupta and Bamezai, 2010). These include metabolic intermediates, such as the allosteric activator fructose-1,6-bisphosphate (Dombrauckas et al., 2005), and oncoproteins and tumor suppressors, such as promyelocytic leukemia (PML) (Shimada et al., 2008). Likewise, the interaction with MKL1 might influence PKM2 activity. MKL1/SRF transcriptional regulation has been implicated in insulin expression and resistance (Jin et al., 2011; Sarkar et al., 2011), but otherwise no direct connection has been reported between the Rho-actin-MKL1-SRF pathway and glucose metabolism. However, altered glucose metabolism has been described in cancer-related processes in which MKL1 plays a role. As mentioned before, MKL1 is a crucial regulator of the myofibroblast/CAF differentiation process, including the epithelial-mesenchymal transition (EMT) that generates myofibroblast-like cells from differentiated epithelial cells. The closely related process of EMT in cancer was recently discovered to alter PK activity and glucose metabolism (Dong et al., 2013). However, the PKM-MKL1 interaction might not only be of importance in cancer cells themselves, but also in stromal precursor cells that are induced to differentiate into CAFs by tumor-derived factors. Recently, the group of Michael Lisanti suggested the

"reverse Warburg effect" model, according to which the CAFs in the tumor stroma are in fact the cells with the high glucose consumption and aerobic glycolysis, not or not only the epithelial tumor cells. By secretion of the energy-rich metabolites lactate and pyruvate CAFs would "feed" the tumor cells and thus promote their growth (Bonuccelli et al., 2010; Pavlides et al., 2009). Considering the vital role of MKL1 for the CAF differentiation process, it seems possible that the PKM-MKL1 interaction is involved in the induction of this effect.

However, it might also be that a non-metabolic function of PKM regulates MKL1 activity in MKL1-dependent processes. As MKL1, PKM2, but not PKM1, was shown to shuttle from the cytoplasm to the nucleus, where it functions as a transcriptional coactivator of transcription factors, such as β-catenin (Yang et al., 2011), Oct-4 (Lee et al., 2008), or HIF-1α (Luo et al., 2011). In addition, not only PKM2 itself is regulated by phosphorylation (reviewed in Gupta and Bamezai, 2010), it also phosphorylates other, non-metabolic proteins on serine/threonine residues (Díaz-Jullien et al., 2011). Since nuclear translocation and activity of MKL1 are dependent on its Ser/Thr phosphorylation status (Muehlich et al., 2008), PKM2 is a candidate upstream regulator of MKL1. In this case, PKM2 would constitute a promising therapeutic target to interfere with MKL1/SRF activity in processes such as fibrosis and cancer.

References

Bluemlein, K., N.-M. Grüning, R. Feichtinger, H. Lehrach, B. Kofler, and M. Ralser. 2011. No evidence for a shift in pyruvate kinase PKM1 to PKM2 expression during tumorigenesis. *Oncotarget*. 2:393-400.

Bonuccelli, G., D. Whitaker-Menezes, R. Castello-Cros, S. Pavlides, R. Pestell, A. Fatatis, A. Witkiewicz, M. Vander Heiden, G. Migneco, B. Chiavarina, P. Frank, F. Capozza, N. Flomenberg, U. Martinez-Outschoorn, F. Sotgia, and M. Lisanti. 2010. The reverse Warburg effect: glycolysis inhibitors prevent the tumor promoting effects of caveolin-1 deficient cancer associated fibroblasts. *Cell cycle (Georgetown, Tex.)*. 9:1960-1971.

Christofk, H., M. Vander Heiden, M. Harris, A. Ramanathan, R. Gerszten, R. Wei, M. Fleming, S. Schreiber, and L. Cantley. 2008. The M2 splice isoform of pyruvate kinase is important for cancer metabolism and tumour growth. *Nature*. 452:230-233.

Díaz-Jullien, C., D. Moreira, C. Sarandeses, G. Covelo, P. Barbeito, and M. Freire. 2011. The M2-type isoenzyme of pyruvate kinase phosphorylates prothymosin α in proliferating lymphocytes. *Biochimica et Biophysica Acta*. 1814:355-365.

Dombrauckas, J., B. Santarsiero, and A. Mesecar. 2005. Structural basis for tumor pyruvate kinase M2 allosteric regulation and catalysis. *Biochemistry*. 44:9417-9429.

Dong, C., T. Yuan, Y. Wu, Y. Wang, T. Fan, S. Miriyala, Y. Lin, J. Yao, J. Shi, T. Kang, P. Lorkiewicz, D. St Clair, M.-C. Hung, B. Evers, and B. Zhou. 2013. Loss of FBP1 by Snail-mediated repression provides metabolic advantages in basal-like breast cancer. *Cancer Cell*. 23:316-331.

Gumińska, M., J. Ignacak, T. Kedryna, and M. Stachurska. 1997. Tumor-specific pyruvate kinase isoenzyme M2 involved in biochemical strategy of energy generation in neoplastic cells. *Acta Biochimica Polonica*. 44:711-724.

Gupta, V., and R. Bamezai. 2010. Human pyruvate kinase M2: a multifunctional protein. *Protein science : a publication of the Protein Society*. 19:2031-2044.

Imamura, K., T. Noguchi, T. Tanaka, G. Staal, and C. van Veelen. 1986. Regulation of isozyme patterns of pyruvate kinase in normal and neoplastic tissues. *Markers of Human Neuroectodermal Tumors, in Staal, GEJ, and van Veelen, CWM,(Eds.), CRC Press, Boca Raton*:191-222.

Jeon, E., S. Heo, I. Lee, Y. Choi, J. Park, K. Choi, D.Y. Park, D. Suh, M. Yoon, and J. Kim. 2010. Ovarian cancer-derived lysophosphatidic acid stimulates secretion of VEGF and stromal cell-derived factor-1 alpha from human mesenchymal stem cells. *Experimental and Molecular Medicine*. 42:280-293.

Jin, W., A. Goldfine, T. Boes, R. Henry, T. Ciaraldi, E.-Y. Kim, M. Emecan, C. Fitzpatrick, A. Sen, A. Shah, E. Mun, V. Vokes, J. Schroeder, E. Tatro, J. Jimenez-Chillaron, and M.-E. Patti. 2011. Increased SRF transcriptional activity in human and mouse skeletal muscle is a signature of insulin resistance. *The Journal of Clinical Investigation*. 121:918-929.

Jønson, L., J. Vikesaa, A. Krogh, L. Nielsen, T. Hansen, R. Borup, A. Johnsen, J. Christiansen, and F. Nielsen. 2007. Molecular composition of IMP1 ribonucleoprotein granules. *Molecular & cellular proteomics : MCP*. 6:798-811.

Koppenol, W., P. Bounds, and C. Dang. 2011. Otto Warburg's contributions to current concepts of cancer metabolism. *Nature Reviews. Cancer*. 11:325-337.

Lee, J., H. Kim, Y.-M. Han, and J. Kim. 2008. Pyruvate kinase isozyme type M2 (PKM2) interacts and cooperates with Oct-4 in regulating transcription. *The international journal of biochemistry & cell biology*. 40:1043-1054.

Luo, W., H. Hu, R. Chang, J. Zhong, M. Knabel, R. O'Meally, R. Cole, A. Pandey, and G. Semenza. 2011. Pyruvate kinase M2 is a PHD3-stimulated coactivator for hypoxia-inducible factor 1. *Cell*. 145:732-744.

Masszi, A., P. Speight, E. Charbonney, M. Lodyga, H. Nakano, K. Szászi, and A. Kapus. 2010. Fate-determining mechanisms in epithelial-myofibroblast transition: major inhibitory role for Smad3. *The Journal of Cell Biology*. 188:383-399.

Mazurek, S. 2012. Pyruvate kinase M2: A key enzyme of the tumor metabolome and its medical relevance. *Biomedical Research (Aligarh)*. 23.

Mazurek, S., C. Boschek, F. Hugo, and E. Eigenbrodt. 2005. Pyruvate kinase type M2 and its role in tumor growth and spreading. *Seminars in Cancer Biology*. 15:300-308.

Mazurek, S., W. Zwerschke, P. Jansen-Dürr, and E. Eigenbrodt. 2001. Effects of the human papilloma virus HPV-16 E7 oncoprotein on glycolysis and glutaminolysis: role of pyruvate kinase type M2 and the glycolytic-enzyme complex. *The Biochemical journal*. 356:247-256.

Minami, T., K. Kuwahara, Y. Nakagawa, M. Takaoka, H. Kinoshita, K. Nakao, Y. Kuwabara, Y. Yamada, C. Yamada, J. Shibata, S. Usami, S. Yasuno, T. Nishikimi, K. Ueshima, M.

Sata, H. Nakano, T. Seno, Y. Kawahito, K. Sobue, A. Kimura, R. Nagai, and K. Nakao. 2012. Reciprocal expression of MRTF-A and myocardin is crucial for pathological vascular remodelling in mice. *The EMBO Journal*. 31:4428-4440.

Miralles, F., G. Posern, A.-I. Zaromytidou, and R. Treisman. 2003. Actin dynamics control SRF activity by regulation of its coactivator MAL. *Cell*. 113:329-342.

Mouilleron, S., C. Langer, S. Guettler, N. McDonald, and R. Treisman. 2011. Structure of a pentavalent G-actin*MRTF-A complex reveals how G-actin controls nucleocytoplasmic shuttling of a transcriptional coactivator. *Science Signaling*. 4.

Muehlich, S., R. Wang, S.-M. Lee, T. Lewis, C. Dai, and R. Prywes. 2008. Serum-induced phosphorylation of the serum response factor coactivator MKL1 by the extracellular signal-regulated kinase 1/2 pathway inhibits its nuclear localization. *Molecular and Cellular Biology*. 28:6302-6313.

Olson, E., and A. Nordheim. 2010. Linking actin dynamics and gene transcription to drive cellular motile functions. *Nature Reviews. Molecular Cell Biology*. 11:353-365.

Ong, S.-E., B. Blagoev, I. Kratchmarova, D. Kristensen, H. Steen, A. Pandey, and M. Mann. 2002. Stable isotope labeling by amino acids in cell culture, SILAC, as a simple and accurate approach to expression proteomics. *Molecular & cellular proteomics : MCP*. 1:376-386.

Otranto, M., V. Sarrazy, F. Bonté, B. Hinz, G. Gabbiani, and A. Desmoulière. 2012. The role of the myofibroblast in tumor stroma remodeling. *Cell adhesion & migration*. 6:203-219.

Pavlides, S., D. Whitaker-Menezes, R. Castello-Cros, N. Flomenberg, A. Witkiewicz, P. Frank, M. Casimiro, C. Wang, P. Fortina, S. Addya, R. Pestell, U. Martinez-Outschoorn, F. Sotgia, and M. Lisanti. 2009. The reverse Warburg effect: aerobic glycolysis in cancer associated fibroblasts and the tumor stroma. *Cell cycle (Georgetown, Tex.)*. 8:3984-4001.

Posern, G., and R. Treisman. 2006. Actin' together: serum response factor, its cofactors and the link to signal transduction. *Trends in Cell Biology*. 16:588-596.

Sarkar, A., M. Zhang, S.-H. Liu, S. Sarkar, F. Brunicardi, D. Berger, and N. Belaguli. 2011. Serum response factor expression is enriched in pancreatic β cells and regulates insulin gene expression. *FASEB journal : official publication of the Federation of American Societies for Experimental Biology*. 25:2592-2603.

Shimada, N., T. Shinagawa, and S. Ishii. 2008. Modulation of M2-type pyruvate kinase activity by the cytoplasmic PML tumor suppressor protein. *Genes to cells : devoted to molecular & cellular mechanisms*. 13:245-254.

Small, E. 2012. The actin-MRTF-SRF gene regulatory axis and myofibroblast differentiation. *Journal of Cardiovascular Translational Research*. 5:794-804.

Small, E., J. Thatcher, L. Sutherland, H. Kinoshita, R. Gerard, J. Richardson, J. Dimaio, H. Sadek, K. Kuwahara, and E. Olson. 2010. Myocardin-related transcription factor-a controls myofibroblast activation and fibrosis in response to myocardial infarction. *Circulation Research*. 107:294-304.

Wang, D.-Z., S. Li, D. Hockemeyer, L. Sutherland, Z. Wang, G. Schratt, J. Richardson, A. Nordheim, and E. Olson. 2002. Potentiation of serum response factor activity by a family of myocardin-related transcription factors. *Proceedings of the National Academy of Sciences of the United States of America*. 99:14855-14860.

Warburg, O. 1956. On the origin of cancer cells. *Science (New York, N.Y.)*. 123:309-314.

Yang, W., Y. Xia, H. Ji, Y. Zheng, J. Liang, W. Huang, X. Gao, K. Aldape, and Z. Lu. 2011. Nuclear PKM2 regulates β-catenin transactivation upon EGFR activation. *Nature*. 480:118-122.

Future Perspectives

Future Perspectives

Since their discovery in the beginning of the 21st century, the members of the MRTF family have been of great interest for our understanding of the transcriptional regulation of actin cytoskeletal and muscle-specific genes. MKL1 with its direct dependence on the actin polymerization status for activity, its function as a mechanosensor, and its ubiquitous expression has attracted particular attention with regard to the regulation of stress-responsive physiological and pathological processes in many tissues. However, only within the past few years it has become clear that MKL1 is an important factor in regulating the differentiation of the major biological effector cell types, the myofibroblast. Regulating the expression of a smooth muscle-specific gene program that includes the main myofibroblast and smooth muscle marker α-smooth muscle actin (SMA), MKL1 triggers the differentiation process in response to extracellular-induced changes in the actin cytoskeleton.

Here, we discovered and characterized for the first time the differential expression of two human MKL1 isoforms. We identified the exact protein sequences of the two isoforms and provide evidence that the novel isoform, MKL1_S, shows a specific transcriptional activity that is not present in the longer isoform MKL1_L. We found that the short isoform MKL1_S is specifically up-regulated during the initial phase of TGF-β-induced differentiation of human adipose tissue-derived stem cells into myofibroblasts/cancer-associated fibroblasts (CAFs). Increasing the ratio of the shorter isoform to the longer MKL1_L isoform might therefore constitute a crucial mechanism to regulate the expression of a group of genes during the maturation process of myofibroblasts/CAFs. When we analyzed different tissues and cell lines regarding their expression of the two isoforms, we found generally lower basal MKL1_S than MKL1_L transcript levels, and only the MKL1_S levels varied strongly between cell types and tissues. This supports our observation that MKL1_S expression can be strongly induced in certain cell types under certain conditions, pointing towards a specific role in dynamic physiological processes. We identified a group of extracellular proteins that were significantly stronger induced by MKL1_S than by MKL1_L in HEK293 cells. We were able to show that expression of MMP-16, the gene with the strongest MKL1_S-specific up-regulation, increased after 96 h of TGF-β-induced differentiation of hASCs, following the MKL1_S up-regulation in this differention model. An analysis of the known

functions of the identified MKL1_S target genes indicates that the regulation of matrix metalloproteinase-2 (MMP-2) activity could be of particular interest with regard to the role of MKL1_S in myofibroblast/CAF differentiation. Interestingly, MMP-16 (also called MT3-MMP) and SPOCK3 (also called testican-3), the genes with the strongest MKL1_S-specific up-regulation, both regulate MMP-2 activity and the two proteins were shown to interact directly (Nakada et al., 2001). The complex formation inhibited the MMP-16-mediated activation of MMP-2. Activated MMP-2 was detected in a variety of tumor tissues (Azzam et al., 1993), where it is thought to support invasiveness by its type IV collagenase activity (reviewed in Stetler-Stevenson et al., 1993). Expression of SPOCK3 was found to be reduced in human glioma tissues compared to normal brain and overexpression of SPOCK3 *in vitro* suppressed the invasive growth of glioma cells (Nakada et al., 2001), making it a candidate tumor suppressor. Moreover, it was reported that expression of pro-MMP-2 is down-regulated by TGF-β as well as in the later phase of myofibroblast differentiation from fibroblasts (Howard et al., 2012). Thus, the MKL1_S-specific concurrent induction of MMP-16 and an inhibitor of MMP-16-mediated MMP-2 activation, SPOCK3, is likely to influence MMP-2 activity and therefore the migratory properties of the differentiating myofibroblast. Alternatively, this simultaneous up-regulation could also constitute a mechanism to promote an MMP-2-independent function of MMP-16 without altering the MMP-2 activity. The preliminary results of our migration assays clearly indicate that MKL1_S overexpressing HEK293 cells migrate slower than MKL1_L overexpressing cells. However, further experiments are required to assess if a high MKL1_S/_L ratio in cells actively inhibits cell migration compared to the empty vector control cells, or if rather a low MKL1_S/_L ratio strongly promotes migration. As the next step, these experiments will need to be performed in myofibroblasts/CAFs after overexpression or knockdown of either of the two MKL1 isoforms. Furthermore, MMP-2 is known to cleave latent TGF-β during the activation process of TGF-β from the ECM (Yu and Stamenkovic, 2000). Thus, MKL1_S might also be involved in the regulation of the feed-forward activation of myofibroblasts via mechanical or chemical release of latent TGF-β from the ECM and its subsequent activation by MMP-2. Such a function would be of immense interest for purposes in Regenerative Medicine and Tissue Engineering, but also for the pharmacological intervention with persistent myofibroblast/CAF differentiation in fibrosis and cancer. Interestingly, the first study that described the MKL1 protein in 2002 discovered the

mouse MKL1 variant that is orthologous to human MKL1_S in a screen for inhibitors of tumor necrosis factor (TNF)-induced cell death in murine embryonic fibroblasts (Sasazuki et al., 2002). This finding indicates a possible function of MKL1_S in protecting the myofibroblast from apoptosis. Currently, many different strategies are tested to interfere with excessive myofibroblast function in fibrosis, some of which are already in clinical trials (reviewed in Hinz et al., 2012). Figure 6 summarizes the current approaches. Targeting MKL1 and maybe specifically MKL1_S adds another promising strategy.

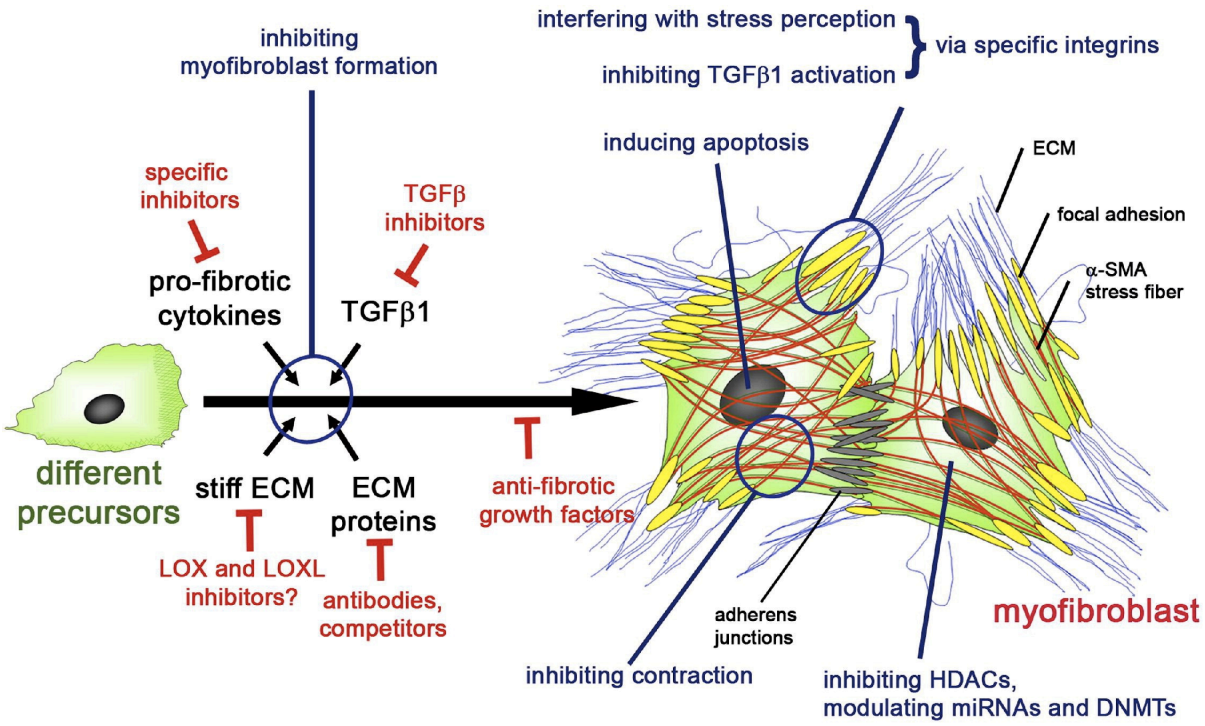

From Hinz et al. (2012)

Figure 6. Current strategies for the pharmacological intervention with myofibroblast differentiation in fibrosis.

The original title of this figure in the review from Hinz et al. (2012) is "The myofibroblast in the center of attention." Different strategies are being followed for the manipulation of myofibroblast activity. Some studies try to intervene at an early stage with the differentiation from the various precursor cell types into the myofibroblast, or at a later stage with specific features of the myofibroblast. Others try to induce apoptosis to resolve the persistent activation of these cells in fibrosis, or prevent their mechanical and chemical feed forward activation. All these approaches may target extracellular proteins, such as the major myofibroblast inducer TGF-β, cell surface receptors, or ECM components, but also intracellular signaling pathways or the nuclear machinery that regulates gene expression, including epigenetic and miRNA-based regulation. Targeting the activity of both MKL1 isoforms or the MKL1_S-specific activity constitutes a novel strategy. HDACs = histone deacetylases; DNMTs = DNA methyl transferases; LOX = lysyl oxidase.

Since MKL1(_S) is an intracellular target, therapeutic antibodies are not a promising option for pharmacological intervention (for a general review see Beck et al., 2010),

although we showed here that the production of an antibody that targets the short MKL1_S-specific N-terminal stretch is possible. Instead, one would have to use small molecule inhibitors, which are still difficult to design to target transcription factors (for a general review see Ghosh and Papavassiliou, 2005). Therefore, finding, e.g., a kinase that acts as a direct upstream regulator of MKL1(_S) could be highly valuable for the pharmacological intervention with MKL1(_S) activity. Already existing inhibitors of Rho, the Rho kinase ROCK, or F-actin, block MKL1 activity (reviewed in Small, 2012), but due to their interference with the integrity of the actin cytoskeleton they are likely to show strong side effects. Notably, because of its specific and strong up-regulation, the MKL1_S isoform also has the potential to become a valuable biomarker for the investigation of TGF-β-induced differentiation into myofibroblasts/CAFs.

However, before targeting MKL1 in diseases such as fibrosis and cancer, detailed studies on the exact functions of the two MKL1 isoforms in these processes will be required. For instance, MKL1_S-specific knockdown studies will reveal whether MKL1_S contributes to the progression from the proto-myofibroblast to the mature myofibroblast and/or to the resolving of the myofibroblast activation by triggering apoptosis or dedifferentiation. The fact that we found SMA among the most strongly up-regulated genes for both MKL1 isoforms argues for an isoform-common regulation of smooth muscle-specific genes and an additional isoform-specific function of MKL1_S in myofibroblast/CAF differentiation. Furthermore, in our gene expression profiling study we identified several genes that were induced by both isoforms that have not yet been described as MKL1 target genes. Remarkably, we found even more genes that were down-regulated by both isoforms than were up-regulated, substantiating the role of MKL1 also as an inhibitor of target gene expression. Future studies will need to address the exact regulation of these novel target genes by both MKL1 isoforms.

As discussed in Manuscript I, assessing the exact function of MKL1_S and MKL1_L in myofibroblast/CAF differentiation will require the identification of putative isoform-specific binding partners and their contribution to isoform-specific activities. As a putative binding site for such factors we identified a functional motif in MKL1_S that mediated the MKL1_S-specific transcriptional activation of MMP-16 and SPOCK-3. Furthermore, performing secondary structure predictions we found a putative motif consisting of four β-strands at the novel N-terminus of MKL1_L that we discovered here. These strands are likely to form a structural domain that influences the folding of the

long N-terminal tail of MKL1_L, and could therefore regulate MKL1_L-specific interactions. As discussed in Additional Finding 3, posttranslational modifications, such as phosphorylation, at isoform-specific N-terminal amino acids constitute a second putative mechanism to regulate MKL1 isoform activity, especially in the case of the longer MKL1_L. A third important factor in regulating the isoform-specific functions might be the heterodimerization between the two isoforms, or with other members of the MRTF family. However, although our understanding of the Rho-actin-MRTF pathway has advanced greatly within the last decade, still little is known about heterodimerization between family members and its relation to MKL1 activity. It will be interesting to see whether heterodimers of the MKL1 isoforms exist, and whether one of the isoforms plays a dominant-positive or -negative role in this interplay.
As explained in section 6.2 of the introduction, MKL1 was named after the MKL1-Rbm15 fusion proto-oncogene that results from a chromosomal translocation in patients with acute megakaryoblastic leukemia (AMKL). The putative tumor-promoting fusion protein is translated from the 5' Rbm15-MKL1 3' transcript, which attaches the Rbm15 protein to the N-terminus of MKL1 at position +3 of the published, but as described earlier non-functional, ATG translation start codon. This results in the putative oncoprotein that lacks the RPEL1 motif, turning it constitutively nuclear and active, but in addition lacks an MKL1_S- or MKL1_L-specific N-terminal stretch. Future studies will have to elucidate whether missing functions of these isoform-specific N-termini contribute to the deregulation of the MKL1 activity in the pathology of AMKL.

As described in Manuscript II, we identified pyruvate kinase M1/M2 as a novel interaction partner of MKL1 in a SILAC- and mass spectrometry-based screen in HEK293 cells. Due to the almost exclusive expression of the PKM2 isozyme in these cells (Bluemlein et al., 2011), we assume that PKM2 was the protein that we found to interact with MKL1, with a final confirmation being required. Considering the crucial role of PKM2 in the cancer-specific glucose metabolism, the crosstalk with MKL1 as a key regulator of actin-mediated cellular motility and myofibroblast/CAF differentiation is of particular interest. To date, no direct connection between the glycolytic activity and the Rho-actin-MKL1 pathway has been reported. As reviewed in Scharenberg et al. (2010) (see introduction), MKL1 has already been implicated to affect several processes in cancer cells that contribute to tumorigenesis and metastasis. However, the MKL1-PKM2

interaction might also be involved in the tumor-induced differentiation of adjacent precursor cells into cancer-associated fibroblasts (CAFs), promoting the progression of the tumor indirectly through the tumor stroma. Besides the question in which cells this potential interaction is of importance, it is of primary interest to find out whether MKL1 interacts with a glycolysis-associated or a non-associated form of PKM2. PKM2 is a multifunctional protein for which several non-glycolytic connections to other pathways have been discovered (reviewed in Gupta and Bamezai, 2010), and therefore it constitutes a putative upstream regulator of MKL1 activity, independent of its glycolytic function. However, it is also possible that MKL1 and its special regulation by the actin cytoskeleton influence the glycolytic activity of PKM2, thus linking actin-mediated transcriptional regulation to glucose metabolism. Via such a connection, extracellular stimulation of a cell with growth factors, cytokines, or mechanical cues could not only trigger a profound adaptation of the actin cytoskeleton or the differentiation into a myofibroblast/CAF, but at the same time induce an adaptation of the cellular energy metabolism to the altered extracellular demands. Either way, unraveling the function of the newly discovered interaction between MKL1 and PKM1/2 is likely to improve our understanding of MKL1-mediated cellular processes.

References

Azzam, H.S., G. Arand, M.E. Lippman, and E.W. Thompson. 1993. Association of MMP-2 Activation Potential With Metastatic Progression in Human Breast Cancer Cell Lines Independent of MMP-2 Production. *Journal of the National Cancer Institute*. 85:1758-1764.

Beck, A., T. Wurch, C. Bailly, and N. Corvaia. 2010. Strategies and challenges for the next generation of therapeutic antibodies. *Nature Reviews. Immunology*. 10:345-352.

Bluemlein, K., N.-M. Grüning, R. Feichtinger, H. Lehrach, B. Kofler, and M. Ralser. 2011. No evidence for a shift in pyruvate kinase PKM1 to PKM2 expression during tumorigenesis. *Oncotarget*. 2:393-400.

Ghosh, D., and A. Papavassiliou. 2005. Transcription factor therapeutics: long-shot or lodestone. *Current Medicinal Chemistry*. 12:691-701.

Gupta, V., and R. Bamezai. 2010. Human pyruvate kinase M2: a multifunctional protein. *Protein science : a publication of the Protein Society*. 19:2031-2044.

Hinz, B., S. Phan, V. Thannickal, M. Prunotto, A. Desmoulière, J. Varga, O. De Wever, M. Mareel, and G. Gabbiani. 2012. Recent developments in myofibroblast biology: paradigms for connective tissue remodeling. *The American Journal of Pathology*. 180:1340-1355.

Howard, E., B. Crider, D. Updike, E. Bullen, E. Parks, C. Haaksma, D. Sherry, and J. Tomasek. 2012. MMP-2 expression by fibroblasts is suppressed by the myofibroblast phenotype. *Experimental Cell Research*. 318:1542-1553.

Nakada, M., A. Yamada, T. Takino, H. Miyamori, T. Takahashi, J. Yamashita, and H. Sato. 2001. Suppression of membrane-type 1 matrix metalloproteinase (MMP)-mediated MMP-2 activation and tumor invasion by testican 3 and its splicing variant gene product, N-Tes. *Cancer Research*. 61:8896-8902.

Sasazuki, T., T. Sawada, S. Sakon, T. Kitamura, T. Kishi, T. Okazaki, M. Katano, M. Tanaka, M. Watanabe, H. Yagita, K. Okumura, and H. Nakano. 2002. Identification of a novel transcriptional activator, BSAC, by a functional cloning to inhibit tumor necrosis factor-induced cell death. *The Journal of Biological Chemistry*. 277:28853-28860.

Scharenberg, M., R. Chiquet-Ehrismann, and M. Asparuhova. 2010. Megakaryoblastic leukemia protein-1 (MKL1): Increasing evidence for an involvement in cancer progression and metastasis. *The international journal of biochemistry & cell biology*. 42:1911-1914.

Small, E. 2012. The actin-MRTF-SRF gene regulatory axis and myofibroblast differentiation. *Journal of Cardiovascular Translational Research*. 5:794-804.

Stetler-Stevenson, W.G., S. Aznavoorian, and L.A. Liotta. 1993. Tumor Cell Interactions with the Extracellular Matrix During Invasion and Metastasis. *Annual Review of Cell Biology*. 9:541-573.

Yu, Q., and I. Stamenkovic. 2000. Cell surface-localized matrix metalloproteinase-9 proteolytically activates TGF-beta and promotes tumor invasion and angiogenesis. *Genes and Development*. 14:163-176.

Appendix

Additional Findings

Additional Findings

Additional experimental procedures

Migration assays

HEK293 cells overexpressing 1) the empty pcDNA3 vector, 2) the 5'UTR-full-length MKL_L construct, or 3) the 5'UTR-full-length MKL_S construct (see Manuscript I for plasmid constructs) were grown in normal growth medium until confluence (see Manuscript I for cell culture). At this time point, a scratch wound in the monolayer was generated with a pipette tip and brightfield pictures were taken at fixed positions (0 h time point). After 24 h in culture the cells were fixed and stained with crystal violet, and brightfield pictures were taken at identical positions. For quantification, the area into which the cells had migrated within 24 h was integrated using an automated segmentation based on Otsu's multithresholding method.

Additional Finding I

MKL1_L expression promotes cell migration (preliminary results).

Results and discussion

Our gene expression profiling after stimulation of the Rho-actin-MKL1 pathway in HEK293 cells overexpressing either the MKL1_L or the MKL1_S isoform revealed several genes that were specifically upregulated with MKL1_S (see Manuscript 1, Table 1). This group comprised genes coding for transmembrane and extracellular proteins, which are likely to contribute to the secretion and modification of the extracellular matrix. Therefore, we wanted to test whether this specific activity of MKL1_S has an effect on the migratory properties of cells. We assessed the ability of HEK293 cells that were stably transfected with 1) the MKL1_L isoform 2) the MKL1_S isoform, or 3) an empty vector control to migrate into a 2-dimensional space by performing scratch wound assays. Until now, we performed and analyzed only two independent experiments, therefore it is not yet possible to determine statistical differences. However, both experiments showed a clear increase in motility of MKL1_L overexpressing cells

compared to MKL1_S overexpressing cells and compared to the empty vector control cells (Fig. A1).

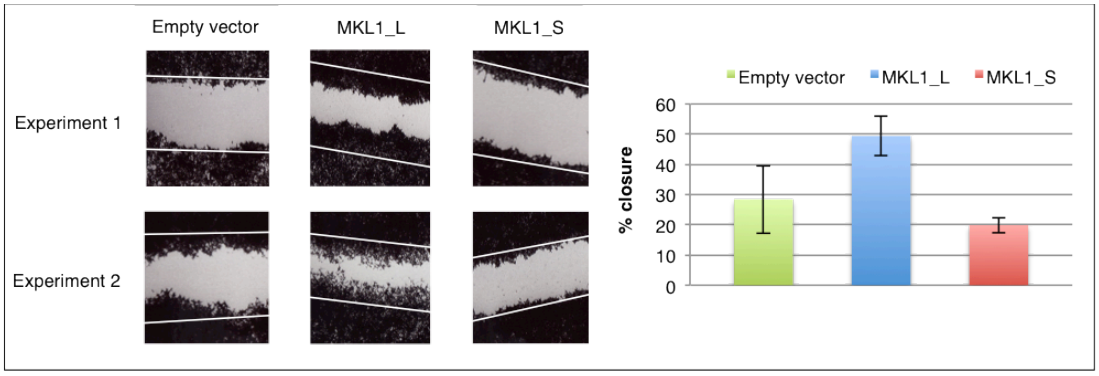

Figure A1. MKL1_L overexpressing cells show increased migration (preliminary data). HEK293 cells that were stably transfected with an empty vector control, the MKL1_L isoform, or the MKL1_S isoform (5'UTR-full length_MKL1 constructs, see Manuscript 1). Migration into a wound within 24 h was quantified. The white lines indicate the approximate boundaries of the original wounds. The average of two independent experiments is displayed, with the upper and lower ends of the error bars indicating the values of the two individual experiments. Further repetitions will be required to assess statistical differences between the cells.

Since the MKL1 isoform overexpressing cells behaved highly similar in both experiments, the probability that MKL1_L overexpression truly ameliorates migration compared to MKL1_S is high. It is important to note that the empty vector control cells behaved differently in both experiments, therefore it is not yet clear whether the MKL1_S overexpressing cells migrate at the speed of the control cells, or if migration is actively inhibited in these cells. In one of the two experiments migration into the wound was almost completely abrogated in the MKL1_S overexpressing cells, pulling the average of both experiments below the average of the control cells. Further repetitions of this experiment will reveal if (1) MKL1_L strongly induces cell migration whereas MKL1_S does not alter it, or (2) MKL1_L induces cell migration whereas MKL1_S inhibits it. Such an active inhibition of migration by MKL1_S would be likely to be linked to the MKL1_S-specific transcriptional activation of the aforementioned group of genes coding for extracellular proteins.

Leitner et al. (2011) found an anti-migratory effect of MKL1 overexpression in strongly-adherent, non-invasive cells (mouse NIH3T3 fibroblast and mammary epithelial EpRas cell lines), whereas in weakly-adherent, invasive carcinoma cells (human breast cancer cell line MDA-MB-231) the overexpression yielded in an activation of migration. The latter finding overlapped with a report that found reduced invasiveness and experimental metastasis after MKL1 knockdown in invasive breast cancer and melanoma cell lines (Medjkane et al., 2009). However, whereas Medjkane and colleagues only targeted total MKL1 levels by RNAi, Leitner and colleagues overexpressed constructs that assumed either the suggested Leu-92 translation start (Miralles et al., 2003) or the published ATG translation start of MKL1_L, none of which constitutes the actual translation start of MKL1_L or MKL1_S according to our findings (see Manuscript 1). Therefore, the individual effects of the two MKL1 isoforms on migration and invasiveness have not yet been inquired. According to the preliminary results presented here, MKL1_L with its long N-terminal tail strongly induces migration, meaning that it is likely to trigger specific cytoskeletal rearrangements or ECM modifications that promote cellular motility. Except for the gene for fatty acid binding protein 6, the genes that we identified to be specifically regulated by MKL1_L were down-regulated compared to MKL1_S. Therefore, if this putative pro-migratory effect of MKL1_L that we propose here is based on its function as a transcriptional regulator, an MKL1_L-mediated down-regulation of genes that inhibit migration is likely. Notably, these migration assays were performed in serum-containing growth medium, but without an extra stimulation of the Rho-actin-MKL1 pathway by lysophosphatidic acid (LPA) as in the gene expression profiling study. It will be interesting to see if such an activation of the pathway and the known migration- and invasiveness-promoting effect of LPA (reviewed in Willier et al., 2013) will further enhance the differential regulation of migration by the two MKL1 isoforms. Moreover, assessing the more physiological 3-dimentional invasion properties of cancer cells or myofibroblasts after overexpression or knockdown of either of the two MKL1 isoforms will provide important information on the role of the isoforms in processes such as tumor invasiveness and myofibroblast activation.

References

Leitner, L., D. Shaposhnikov, A. Mengel, A. Descot, S. Julien, R. Hoffmann, and G. Posern. 2011. MAL/MRTF-A controls migration of non-invasive cells by upregulation of cytoskeleton-associated proteins. *Journal of Cell Science*. 124:4318-4331.

Medjkane, S., C. Perez-Sanchez, C. Gaggioli, E. Sahai, and R. Treisman. 2009. Myocardin-related transcription factors and SRF are required for cytoskeletal dynamics and experimental metastasis. *Nature Cell Biology*. 11:257-268.

Miralles, F., G. Posern, A.-I. Zaromytidou, and R. Treisman. 2003. Actin dynamics control SRF activity by regulation of its coactivator MAL. *Cell*. 113:329-342.

Willier, S., E. Butt, and T. Grunewald. 2013. Lysophosphatidic acid (LPA) signaling in cell migration and cancer invasion: a focused review and analysis of LPA receptor gene expression on the basis of more than 1700 cancer microarrays. *Biology of the cell / under the auspices of the European Cell Biology Organization*.

Additional experimental procedures

Tissue extracts from patients

Brain tumor samples were kindly provided by Maria Maddalena Lino from the University Hospital of Basel in accordance with the guidelines of the ethical committee of the University of Basel. Tumors were diagnosed and graded according to the World Health Organization Classification of Tumors of the Nervous System. Glioblastoma samples were collected from patients aged 39 to 73 (mean age=55 years), as described in Brellier et al. (2011). After weighing of the tissues, samples were thawed on ice, minced and homogenized in RIPA lysis buffer. Normal brain extracts were purchased from BioChain (Newark, CA, USA), including one sample of total brain (P1234035, age 71 Lot No A908046), cerebral cortex (P1234042, age 77, Lot No B107064) and cerebellum (P1234040, age 66, Lot No B109120). 90 µg of each extract were separated on NuPAGE 4-12 % Bis-Tris gels (Life Technologies/Invitrogen) and transferred to a BioTrace PVDF membrane (PALL LifeSciences, Pensacola, FL, USA) for immune staining with anti-total MKL1 mAb (see experimental procedures in Manuscript I) and anti β-actin antibody (Abcam, Cambridge, UK). Visualization of the proteins of interest was achieved by using horseradish peroxidase-coupled secondary antibodies (MP Biomedicals, Illkirch, France) and SuperSignal West DURA Extended Duration Substrate (Thermo Fisher Scientific, Lausanne, Switzerland).

Additional Finding II

Expression of MKL1_S in human brain tumors seems generally reduced.

Results and discussion

MKL1 was shown to play an important role in brain development and neuronal plasticity (reviewed in Kalita et al., 2012). Mokalled et al. (2010) discovered that the brains of mice with only a single allele of either MKL1 or MKL2 developed normally, however, the deletion of both proteins in the brain caused severe abnormalities that resembled the phenotype of brain-specific SRF knockout mice. In Manuscript 1 (Fig. 2D) we compared the relative transcript levels of both MKL1 isoforms in several human cell

lines and tissues. We found total RNA from normal brain as one of the samples with the highest relative transcript levels of MKL1_S. Notably, these levels were approximately 5-fold higher than in a total RNA sample from fetal brain, in which MKL1_L transcript levels were increased instead. We also included 4 astrocytoma cell lines in our transcript analysis and found strongly reduced MKL1_S transcript levels compared to normal brain for 3 of the 4 cell lines, whereas MKL1_L levels were comparable. However, in the *de novo* anaplastic astrocytoma cell line U343MG we found the second highest MKL1_S transcript levels of all tested cell lines and tissues, with an approximately 10^3-fold higher expression than in the other *de novo* anaplastic astrocytoma cell line LN319 and in the *de novo* glioblastoma cell line U373, and an approximately 10^2-fold higher expression than in the glioblastoma cell line T98G (for characterizations of these cell lines see Ishii et al. (1999)). According to the World Health Organization Classification of Tumors of the Nervous System (WHO 2007) anaplastic astrocytomas are classified as grade III and glioblastoma as grade IV astrocytic tumors. *De novo* tumors are primary and highly aggressive tumors. Therefore, the U343MG cell line that showed high transcript levels of MKL1_S is one of two analyzed cell lines that are derived from the lower, grade III tumors. Both grade IV glioblastoma-derived cell lines showed low MKL1_S transcript levels. All four cell lines are derived from male patients between 54 and 67 years of age (Ishii et al., 1999).

To further investigate this reduced MKL1_S expression in glioblastoma cell lines, we analyzed the MKL1 isoform protein levels in extracts from normal human brain as well as in tumor samples from glioblastoma patients. Staining for total MKL1 revealed that MKL1_S was the major isoform in normal total brain extract, but not in extracts from normal cerebellum or cortex (Fig. A2). However, also in these extracts we detected MKL1_S. This was in contrast to four of the five tumor extracts from glioblastoma patients for which we detected MKL1 protein. In these patients MKL1_S was hardly detectable, if at all at much lower levels than MKL1_L. Only in the extract from patient 6 we detected both isoforms, with MKL1_S being even stronger expressed than MKL1_L.

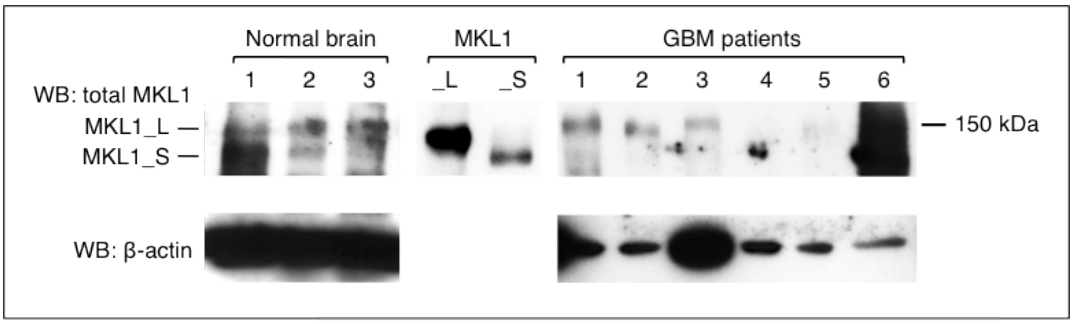

Figure A2. MKL1 isoform expression in healthy brain and glioblastoma.
Extracts from normal human 1) total brain, 2) cerebellum, and 3) cortex as well as from tumors of 6 glioblastoma patients were separated via SDS-PAGE and total MKL1 was detected by Western Blotting (WB). β-actin staining served as loading control. Cell lysates from HEK293 cells overexpressing MKL1_L or MKL1_S were run in parallel as size controls for the MKL1 isoforms. The reduced migration of the isoforms in the brain extracts compared to the isoforms that were overexpressed in HEK293 cells might be caused by brain-specific posttranslational modifications of MKL1, such as phosphorylation.

To summarize, we observed similar reductions of MKL1_S protein levels in tumor extracts from glioblastoma patients compared to normal brain extracts as we did for the transcript levels of glioblastoma cell lines compared to normal brain RNA. Therefore, one could speculate about a putative tumor-suppressing role of the MKL1_S isoform. However, as aforementioned, we also found one cell line and one tumor extract with strong MKL1_S expression. Moreover, for truly assessing such a function of MKL1_S more patient samples and controls from matched brain areas would be required. To our knowledge, no correlation of SRF/MKL1 expression or activity with the appearance and grade of brain tumors has yet been described in the literature.

References

Brellier, F., S. Ruggiero, D. Zwolanek, E. Martina, D. Hess, M. Brown-Luedi, U. Hartmann, M. Koch, A. Merlo, M. Lino, and R. Chiquet-Ehrismann. 2011. SMOC1 is a tenascin-C interacting protein over-expressed in brain tumors. *Matrix biology : journal of the International Society for Matrix Biology*. 30:225-233.

Ishii, N., D. Maier, A. Merlo, M. Tada, Y. Sawamura, A. Diserens, and E. Van Meir. 1999. Frequent co-alterations of TP53, p16/CDKN2A, p14ARF, PTEN tumor suppressor genes in human glioma cell lines. *Brain pathology (Zurich, Switzerland)*. 9:469-479.

Kalita, K., B. Kuzniewska, and L. Kaczmarek. 2012. MKLs: co-factors of serum response factor (SRF) in neuronal responses. *The international journal of biochemistry & cell biology*. 44:1444-1447.

Mokalled, M., A. Johnson, Y. Kim, J. Oh, and E. Olson. 2010. Myocardin-related transcription factors regulate the Cdk5/Pctaire1 kinase cascade to control neurite outgrowth, neuronal migration and brain development. *Development (Cambridge, England)*. 137:2365-2374.

Additional experimental procedures

Identification of phosphorylation sites

The affinity purification of MKL1_L from HEK293 cells overexpressing the 5'UTR-full-length MKL_L construct and the mass spectrometrical detection of peptides from the corresponding SDS-PAGE gel slice is described in Manuscript I. Here, in addition to the detection from the gel we identified peptides after in-solution digest of the purified protein. Therefore, purified proteins were precipitated with TCA (trichloro acetic acid) and dissolved in 100 mM NH_4HCO_3. After reduction with TCEP (*tris*(2-carboxyethyl)phosphine), alkylation with iodoacetamide, and addition of acetonitrile to a final concentration of 2.5 % the proteins were digested with endoproteinase AspN (Roche, Basel, Switzerland) at 37 °C overnight. Searches for phosphate modifications were performed against a database containing the human MKL1_L sequence that starts at the identified GTG translation start (as described in Manuscript 1) using Mascot 2.3.

Additional Finding III

Identification of novel MKL1 phosphorylation sites and of MKL1_L-specific phosphorylation.

Results and discussion

MKL1 activity was shown to depend on the phosphorylation of certain serine/threonine residues. Miralles et al. (2003) described a serum-induced size increase of overexpressed MKL1 (with the published human ATG start, which we termed ΔN-MKL1 in our experiments) that was sensitive to phosphatase treatment. Since phosphotyrosine-specific antibodies did not detect MKL1, the authors concluded that MKL1 was phosphorylated at serine/threonine residues. Using Rho- and MEK/ERK-inhibitors in fibroblasts, each reduced MKL1 phosphorylation and a combination of both abolished it, indicating that these two pathways are responsible for the regulation of this posttranslational modification. In their experiments, constructs truncated C-terminally of position 471 in ΔN-MKL1 (corresponding to position 571 in MKL1_L) were only minimally phosphorylated, indicating that the major phosphorylation sites are located at

the C-terminus. Kalita et al. (2006) were able to show that a constitutive activation of the ERK1/2 pathway in neurons resulted in MKL1 phosphorylation, as did an *in vitro* incubation of immunoprecipitated MKL1 with active ERK2. These results proved that the ERK1/2 pathway is required and sufficient for MKL1 phosphorylation. Muehlich et al. (2008) mapped one of these serum-inducible and ERK1/2-dependent phosphorylation sites to serine 454 (of ΔN-MKL1, corresponding to position 554 in MKL1_L). Although serum also stimulates the nuclear accumulation of MKL1 within a few minutes, the authors found that prevention of serum-stimulated phosphorylation at S454 by mutation of this residue induced a constitutively nuclear localization of MKL1. In addition, they found that phosphorylation at S454 was required for the interaction of MKL1 with G-actin. They concluded that serum treatment initially induces nuclear accumulation of MKL1 via activation of the Rho-actin-MKL1 pathway, but then promotes MKL1 binding to G-actin via phosphorylation at S454 and thus nuclear export of MKL1. In addition to S454, three more validated serine/threonine phosphorylation sites of MKL1 can be found in the UniProt, NCBI, and Phosida databases (accession numbers Q969V6, NP_065882.1, and IPI00163729, respectively), namely pS6, pT305, and pT450, which correspond to pS106, pT405, and pT550 in MKL1_L.

Knowing of the crucial regulation of MKL1 activity by phosphorylation, we purified the MKL1_L isoform, which starts at a GTG codon upstream of the RPEL1 motif as explained in Manuscript 1, from HEK293 cells that were stably transfected with the 5'UTR-full length MKL1_L construct. We digested the proteins with endoproteinase AspN, a zinc metalloendopeptidase that selectively cleaves peptide bonds N-terminal to aspartic acid residues, either in solution or in the excised gel band from SDS-PAGE. Liquid chromatography-mass spectrometrical (LC-MS) analysis of the resulting peptides yielded in several putative serine phosphorylation sites (see Table A1).

Peptide position		Peptide Sequence	Phosphorylation site with the highest probability		
(GTG start) MKL1_L	Publ. ATG (ΔN)-MKL1		(GTG start) MKL1_L	Publ. ATG (ΔN)-MKL1	Best ion score
29-52		DEPVLVSLSAAP**s**PQSEAVANELQ	S41		63.1
242-268	142-168	EARVSEPLLSATSA**s**PTQVVSQLPmGR	S256	S156	68.4
777-804	677-704	DSPGLSSGSPQQPSSQPG**s**PAPAPSAQM	S795	S695	43.9
864-895	764-795	DFKEPPSLPGKEKPSPKTVcG**s**PLAAQPSPSA	S885	S785	44.1
896-915	796-815	ELPQAAPPPPG**s**PSLPGRLE	S905	S805	67.3
955-961	855-861	DHPP**s**Pm	S959	S859	32.8

Table A1: Putative MKL1 phosphorylation sites detected in MKL1_L.
The analysis was performed in solution. For each peptide the best Mascot ion score against a database containing the human MKL1_L sequence that starts at the identified GTG translation start (as described in Manuscript 1) is provided. For peptides containing more than one serine or threonine an unambiguous alignment of the phosphorylation site within the peptide is not possible. The sites with the highest scores are marked bold, but the difference to the next best-fit score is small in some cases. Most of the identified phosphorylation sites are in the C-terminal third of MKL1. None of the sites identified in this analysis is included in the UniProt, NCBI, or Phosida databases, which contain the published ATG start (ΔN)-MKL1 protein. s = phosphorylated serine, m = oxidized methionine.

None of the identified sites matched the ones found in the common databases. Interestingly, whereas the four phosphorylation sites from the databases all locate within the N-terminal half of MKL1, four of the six putative sites that we found locate between residues 795-959, meaning in the proline-rich C-terminal third of MKL1. As aforementioned, Miralles et al. (2003) found the major phosphorylation sites to be located C-terminally of position 571 of MKL1_L. Furthermore, the predicted C-terminal 9aa TAD that is common to both MKL1 isoforms (see Manuscript 1) lies embedded within these 4 sites. Therefore, the phosphorylation sites that we identified here have the potential to be major MKL1 phosphorylation sites regulating MKL1 activity. Future experiments will have to prove a functional importance of these MKL1 modifications. The same applies for the other two sites that we identified in the N-terminal third of MKL1_L. Notably, the S41 site is located in the isoform-specific, long N-terminal stretch of MKL1_L, and therefore phosphorylation at this site constitutes a putative mechanism of regulating MKL1_L-specific functions. Future studies will reveal if this phosphorylation site is involved in, e.g., the suppression of the MKL1_S-specific

transcriptional activity in MKL1_L (see Manuscript 1), or in the putative migration-promoting function of MKL1_L (see Additional Finding 1).

References

Kalita, K., G. Kharebava, J.-J. Zheng, and M. Hetman. 2006. Role of megakaryoblastic acute leukemia-1 in ERK1/2-dependent stimulation of serum response factor-driven transcription by BDNF or increased synaptic activity. *The Journal of neuroscience : the official journal of the Society for Neuroscience*. 26:10020-10032.

Miralles, F., G. Posern, A.-I. Zaromytidou, and R. Treisman. 2003. Actin dynamics control SRF activity by regulation of its coactivator MAL. *Cell*. 113:329-342.

Muehlich, S., R. Wang, S.-M. Lee, T. Lewis, C. Dai, and R. Prywes. 2008. Serum-induced phosphorylation of the serum response factor coactivator MKL1 by the extracellular signal-regulated kinase 1/2 pathway inhibits its nuclear localization. *Molecular and Cellular Biology*. 28:6302-6313.

Acknowledgements

I would like to thank you, Ruth, that you took me over as a “PhD orphan” after the Hofsteenge lab had closed down - I am deeply grateful for that. I would also like to thank you that you were always there for me with great scientific support and that you gave me the freedom to follow my own ideas.

I would like to thank Gerhard Christofori for being the co-advisor of my thesis.
I would like to thank Matthias Chiquet and Patrick Matthias for being members of my Thesis Committee.

I would like to thank Jan Hofsteenge for an exciting year in his lab, and for being a great teacher and an honest person.
I would also like to thank Constanze, Carsten, Chun-I, Daniel, Ragna, and Dominique for a warm welcome at the FMI and for a nice atmosphere in the Hofsteenge lab.

I would like to thank all former and present members of the Chiquet lab (Roman, Ulrike, Sabrina, Jay, Enrico, Florence, Jan, Dominik, Maria, Irem, Francesca, Ismaïl, Jacqueline, Rahel, Jonas, and our “guest scientist” Richard) for a nice atmosphere in the lab and for many unforgettable lunch discussions.

I would like to thank Ismaïl for taking over the PKM project, for being so enthusiastic about it, and for some really good scientific discussions. And of course for his tolerance towards the “German Mafia”.

I would like to thank Jan and Jonas for countless half-past-two-coffee-breaks and for all the fun and the very familiar atmosphere in our office.

I would like to thank Jacqueline for all her support in the lab over the years and for doing many, many SEAP assays for me. I am really sorry that not more of them made it into my thesis.

I would like to thank Gwen MacDonald for all the advice and the reagents I got from her over the past years.

I would like to thank Ragna for spending all that time on the project, for teaching me a lot, and for creating a great atmosphere in our collaboration.

I would like to thank Ben Pippenger for not hesitating a second when I overran him with the idea for the collaboration and for making the last year of my PhD a great adventure. Let's keep on saving the world.

Special thanks go to Jonas and Dominik for their extremely unselfish help in times when I had more ideas than I could execute myself. You two are really creative and I think we make a great team. I had lots of fun and a fantastic time with you guys.

I would like to thank Toni for being a great friend and for his highly motivating mentality to reach for the stars, while being totally down-to-earth.

I would like to thank Meikes parents for always being there for us and for their unlimited support over the past years.
I would also like to thank my dad and my sister for their support.
I would like to thank my mom for always being positive and supportive, and for cheering me up whenever she gets the chance. And simply for being a great mom.

And last, but definitely not least, I would like to thank you, Meike. For your help, for your love, for everything. To have something as beautiful as you in my life gives me this warm happiness and gratefulness deep inside, which has made my life so far a highly enjoyable walk. I hope you will accompany me on this walk until the end of the path.

Curriculum Vitae

Name	**Matthias A. Scharenberg** née Schmidt
Date and place of birth	7 December 1980 Haan, Germany
Current address	Schneckenbergweg 5, 79639 Grenzach-Wyhlen, Germany
Email	**Matthias.Scharenberg@Novartis.com**

WORK EXPERIENCE

2009 - 2013	**PhD Thesis** **Friedrich Miescher Institute for Biomedical Research**, Novartis Research Foundation, Basel, Switzerland, Mechanisms of Cancer department Supervisor: Prof. Dr. Ruth Chiquet-Ehrismann "Identification and Characterization of Two Isoforms of Human Megakaryoblastic Leukemia-1 and their specific regulation in Myofibroblast Differentiation."
Jan. – Dec. 2008	Research Associate in the laboratory of Prof. Dr. Jan Hofsteenge, **Friedrich Miescher Institute for Biomedical Research**, Basel, Switzerland

EDUCATION

2001 - 2007	**Diploma studies in Biochemistry** Leibniz University of Hannover/Hannover Medical School, Germany Major subjects: Biochemistry, Immunology, Biophysical Chemistry
Feb. – Sept. 2007	**Diploma thesis** Hannover Medical School, Institute for Cellular Chemistry, Hannover, Germany, Supervisor: Prof. Dr. Herbert Hildebrandt *"Interactions of Polysialic Acid and NCAM with FGF Receptors "*
July – Sept. 2006	**Internship in New Zealand (accredited as part of diploma studies)** University of Canterbury, Centre of Integrated Research in Biosafety, Christchurch, New Zealand, Supervisor: Assoc. Prof. Dr. Jack Heinemann *"Molecular Cloning of the oriT into a URA3- Plasmid Vector for the Investigation of Bacterial Recombination Frequencies"*
2000 - 2001	**Civilian service** Office for the Environment, Solingen, Germany Responsibilities included, e.g., collection and analysis of wastewater samples.
June 2000	**Abitur/A-levels** August-Dicke Gymnasium, Solingen, Germany

POSITIONS OF RESPONSIBILITY

2010 - 2013 — **Student Representative of the Friedrich Miescher Institute**
(4 to 5 students representing almost 100 PhD students at the FMI)

2008 - 2013 — **Responsible person within the Friedrich Miescher Institute**

- for the near-infrared imaging system Odyssey, LI-COR
- for the fluorescence imaging system Typhoon 9400, GE Healthcare

PROFESSIONAL SKILLS AND DIPLOMA

Cell culture
- Primary (Adipose tissue-derived stem) cell culture and differentiation, SILAC

Molecular Biology
- DNA Microarrays (sample preparation, analysis), quantitative RT-PCR, 5'RACE, siRNA knockdown, molecular cloning, promoter-reporter assays

Imaging
- Immunofluorescence microscopy, Fluorescent Imaging Systems Typhoon 9400
(GE Healthcare) and Odyssey (LI-COR)

Protein Science
- Mass Spectrometry (sample preparation and parts of analysis), Co-IP, monoclonal antibody production (e.g., screening clones by ELISA and Western Blot), protein purification (bacterial and mammalian expression systems)

2012 — **Workshop "Team Work & Leadership Competencies for PhD Students"**
by Golin Wissenschaftsmanagement, Friedrich Miescher Institute, Basel

2011 — **Graduate course "Key Issues in Drug Discovery & Development"**
Department of Pharmaceutical Sciences, University of Basel, Switzerland

LANGUAGE SKILLS

German — Native speaker
English — Fluent
French — Basic school level (4 years)

OTHER INTERESTS

Tennis, Trail Running — I truly enjoy doing sports, and beyond that it creates a perfect balance to my professional career. I have played tennis in a team since I was a child. During my studies I gave beginners and advanced tennis courses at the university.

Cycling — I go to work by bike every day (15 km). This keeps me fit and I can arrange my ideas.

Publication list

PUBLICATIONS

2013 "The initial phase of TGF-β-induced myofibroblast differentiation involves specific regulation of two MKL1/MRTF-A isoforms."
Scharenberg MA, Pippenger BE, Sack R, Zingg D, Schenk S, Ferralli J, Martin I, Chiquet-Ehrismann R
Manuscript under review (Journal of Cell Science)

2013 "The SRF coregulator MKL1/MRTF-A interacts with pyruvate kinase in proliferating HEK293 cells."
Scharenberg MA, Hendaoui I, Sack R, Zingg D, Chiquet-Ehrismann R
Manuscript in preparation

2011 "Polysialic Acid Controls NCAM Signals at Cell-Cell Contacts to Regulate Focal Adhesion Independent from FGF Receptor Activity"
Eggers K, Werneburg S, Schertzinger A, Abeln M, Schiff M, Scharenberg MA, Burkhardt H, Mühlenhoff M, Hildebrandt H
Journal of Cell Science 124 (2011), 3279–3291

2010 "Megakaryoblastic Leukemia Protein-1 (MKL1): Increasing Evidence for an Involvement in Cancer Progression and Metastasis"
Scharenberg MA, Chiquet-Ehrismann R, Asparuhova MB
The International Journal of Biochemistry & Cell Biology 42 (2010) 1911–1914

PATENT APPLICATIONS

2012 Patent application EP12174531.9, filed 29.06.12
"Treating diseases by modulating a specific isoform of MKL1."
Scharenberg MA, Sack R, Chiquet-Ehrismann R

POSTER PRESENTATIONS

2012 "A Novel Isoform of Human MKL1/MRTF-A is a Potent Transcriptional Activator of a Group of Extracellular Proteins in HEK293 Cells."
Scharenberg MA, Ferralli J, Chiquet-Ehrismann R
Gordon Conference and Gordon Research Seminar
"Signal Transduction by Engineered Extracellular Matrices"
Biddeford, ME, USA

2011 "Human Tenascin-C Promoter Reporter Constructs are Induced by the Transcription Factor MEF2A and the Cofactor MKL1"
Scharenberg MA, Ferralli J, Chiquet-Ehrismann R
FMI-CRG Joint PhD Meeting
Pyrenees, Spain

2012, 2011, 2010 Various posters (titles not listed)
FMI Annual Research Meetings
Changing locations within Switzerland